ABSTRACT

Title of Document: MITIGATION OF DELAYED ETTRINGITE FORMATION IN LABORATORY SPECIMENS.

Hafizulrehman Shaikh,
Master of Science, 2007

Directed By: Professor Amde M. Amde,
Department of Civil and Environmental Engineering

The objective of this study was to determine if the growth of delayed ettringite formation (DEF) in existing concrete can be reduced or even prevented with commercial products. Additionally, the objectives were to determine if externally treating concrete specimens with water repellents and crystal growth inhibitors will decrease DEF-related expansion. The research required casting laboratory specimens for expansion and weight measurements, for strength testing, and for scanning electron microscope (SEM). Three of the four products, ChimneySaver, Dequest 2060S, and Good-Rite K752, reduced concrete expansion and weight change when compared to the control set. The study indicates that ettringite may have to be identified and mitigated early to prevent deleterious effects.

MITIGATION OF DELAYED ETTRINGITE FORMATION IN LABORATORY SPECIMENS

By

Hafizulrehman Shaikh

Thesis submitted to the Faculty of the Graduate School of the
University of Maryland, College Park, in partial fulfillment
of the requirements for the degree of
Master of Science
2007

Advisory Committee:
Professor Amde M. Amde, Chair
Professor M. Sherif Aggour
Research Professor, Chung C. Fu

Acknowledgements

The research reported herein was sponsored by the Maryland State Highway Administration (MDSHA). Sincere thanks are due to Mr. Earle S. Freedman, Deputy Chief Engineer of Bridge Development, MDSHA; Mr. Peter Stephanos, Director of Materials and Technology, MDSHA; and Mr. Jeffrey H. Smith, Chief, Research Division, MDSHA, for their guidance and support. The authors are very grateful to Mr. Paul Finnerty, Office of Materials and Technology, Precast/Prestressed Concrete Division, MDSHA, for his technical advice and support throughout the project and for coordinating and administrating support from the state of Maryland. The authors also appreciate the support provided by Ms. Barbara Adkins, MDSHA; and by Ms. Vicki Stewart, MDSHA.

The project is very grateful to Dr. W. Clayton Ormsby, Research Chemist, Salut, Inc., for the help and expertise provided on the Scanning Electron Microscope work; Dr. Richard Livingston, Senior Physical Scientist, Office of Infrastructure R&D, Federal Highway Administration in McLean, Virginia for his knowledge and advice during the course of the research.

Appreciations are due to Mr. Haejin Kim, Lab Manager, and Mr. Solomin Ben-Barka, Laboratory Technician, at the National Ready Mix Concrete Association (NRMCA) Laboratory in Greenbelt, MD for helping with testing and storage of concrete samples.

Special thanks to fellow graduate students Mr. Micah Ceary and Mr. Jorgomai Ceesay for providing technical information and assistance in sample preparation and testing.

Table of Contents

List of Tables

List of Figures

Chapter 1: Introduction

1.1 Statement of Problem

Over the past few decades delayed ettringite formation has caused deleterious expansion and premature concrete deterioration particularly in transportation structures such as bridges and roadway pavements. The premature deterioration of in-service structures costs state and local governments millions of dollars in rehabilitation or replacement of these structures. As part of a cost saving procedure, a delayed ettringite formation mitigation program maybe needed for existing in-service structures to curb the growth of ettringite and to decrease the associated costs. Treating existing concrete with water repellents or crystal inhibitors may help slow the expansion of concrete and thus reduce premature deterioration due to delayed ettringite formation.

1.2 Background

This report is part of a project conducted by the University of Maryland on delayed ettringite formation (DEF) for the Maryland State Highway Administration (MDSHA). The research was divided into two phases. Phase I was completed in July 2004 and yielded two reports. This report forms the second volume of the Phase II report.

Phase I reports included "Pilot Field Survey of Maryland Bridges for Delayed Ettringite Formation Damage" (Amde et al. 2004a) and "Influence of Fine Aggregate Lithology on Delayed Ettringite Formation in High Early Strength Concrete" (Amde

et al. 2004b). The first report investigated the possible presence of DEF in cast-in-place concrete bridges in the MDSHA Bridge Inventory (Amde et al. 2004a, 2004b, 2005c, 2005d) . Non-destructive tests, including potassium autoradiography, were performed on bridge abutments, piers and wingwalls with visible map cracking (Livingston et.al 2001a, 2004, 2005). In addition, cores were drilled and analyzed with a scanning electron microscope (SEM). The study concluded that DEF is present in Maryland bridges with and without visible map cracking. The study also concluded that visible map cracking, most commonly associated with ASR, was not a definitive indicator of ASR. The second report investigated the influence of fine aggregates on delayed ettringite formation (Amde et al. 2004c, 2005e). Concrete specimens were prepared and tested with varying types of fine aggregates. The research concluded that the type of fine aggregate can significantly affect DEF-related expansion. Fine aggregate with high MDSHA ASR rating and stored under water experienced the greatest expansion.

Phase II reports build upon Phase I research and consists of laboratory testing and a continuation of the field study. Phase II laboratory research concentrates on mitigation of DEF. The field study investigates the differences in morphology and apparent quantities of DEF in the cores drilled from Maryland bridges. Several parameters were investigated including the degree of moist map cracking and the usage of an air entrainment agent in order to establish a correlation with DEF in the concrete. If a correlation is established, mitigation or prevention methods can be developed or refined.

Other related studies by University of Maryland include investigation of the effect of several parameters on concrete expansion and deterioration (Livingston et. al 2001b, 2001c). These parameters were identified through an exhaustive literature review and included the effects of potassium and magnesium. The effect of water or steam curing and accelerated test methods were also investigated. The research concluded that subjecting concrete specimens to a heat cycle has a primary role in accelerating expansion. The concrete specimens subjected to a heat cycle after 7 days experienced much more expansion compared to specimens subjected to a heat cycle months after curing. The dimension of the concrete specimens also affects the rate of expansion. Concrete members with smaller dimensions (cores) experienced larger expansion rates compared to members with large dimensions (prisms). Increasing the potassium content has a deleterious effect on concrete expansion. However, increasing magnesium content has a minor effect on concrete expansion. Studies at University of Maryland have also shown that class F fly ash and mix water conditioners have mitigating effects on DEF (Amde et. al. 2003, 2005a, 2006).

A 2002 study investigated the influence of several parameters on delayed ettringite formation (Azzam 2002). The parameters included varying fine aggregates, potassium content, curing conditions and exposure conditions. Admixtures such as Class F fly ash and mix water conditioner were also studied. Results of the study concluded that concrete made with natural and reactive sand exhibited extremely large expansion while crushed sand exhibited small expansion. Steam cured concrete experienced larger expansion than water cured concrete. Although, the fine aggregate played a more critical role than the curing condition. Increasing potassium content

and moist environment negatively affects the expansion. On a positive note, fly ash and mix water condition decreased expansion and ettringite formation. Lastly, the research concluded that calcium hydroxide and calcium silicate hydrate gel are involved in the expansion and formation of ettringite.

1.3 Objective and Scope of Work

The primary objective of this study is to determine if externally treating concrete specimens with water repellents and crystal growth inhibitors will reduce or even prevent the growth of DEF and therefore stop or slow concrete expansion. Another objective was to correlate expansion and weight change data with mitigation effectiveness of a particular product on laboratory specimens. The mitigation effectiveness of particular product on laboratory specimens was investigated by collecting expansion and weight change data on the laboratory specimens. The following scope of work describes what was necessary to achieve the primary objective:

1. Perform a literature review to investigate delayed ettringite mitigation techniques.
2. Research and identify water repellent and crystal growth inhibitor products for concrete application. Products were selected based on literature review and previous research performed at other universities.
3. Prepare a treatment method. An ASTM standard does not exist for applying and testing external treatments to concrete, so a treatment method was developed for each product.

4. Prepare a test method. Concrete mix design, curing conditions, storage conditions, and heat cycle were selected to accelerate ettringite growth.
5. Perform quantitative tests on concrete specimens including expansion measurements, weight change measurements, compression test and SEM analysis.
6. Analyze results and discuss the effectiveness of mitigation treatment and the testing methods.

1.4 Outline of Report

The thesis consists of seven chapters as follows:

- Chapter 2 presents the critical literature review on delayed ettringite formation and mitigation technique. A literature review of ASR and ASR mitigation techniques are also included in this chapter.
- Chapter 3 describes experimental approach and treatment methodology.
- Chapter 4 describes the products selected for this research project. The products include two commercial water repellents and two crystal growth inhibitors and treatment application procedure.
- Chapter 5 describes concrete specimen preparation and the various tests performed on these specimens. The chapter describes the procedures from concrete mix design to testing of the specimens at various laboratories.

- Chapter 6 presents results of the various tests with graphs and tables. The chapter concludes with discussion of the test results.
- Chapter 7 summarizes the thesis and presents conclusions.

Chapter 2: Literature Review

2.1 Delayed Ettringite Formation (DEF)

The mechanisms of delayed ettringite formation have been the subject of many controversies over the past few decades. Even the term "delayed ettringite formation" or DEF is the subject of numerous debates. A literature review conducted by Day in 1992 suggests that the term DEF implies that conditions may be suitable for ettringite growth but does not form. This implication is not true. Additionally, the term DEF implies that the primary ettringite that forms early in the cement hydration forms as delayed ettringite formation at a "delayed" or later point in time, which is also untrue. Day concludes that the term "secondary ettringite" is a more accurate term because it distinguishes between primary ettringite and ettringite that forms under different conditions and point in time. For this research the term "Delayed Ettringite Formation" is used because it was more prevalent in research papers than "Secondary Ettringite."

Ettringite growth is customary in the cement hydration process and is formed by a reaction between gypsum and calcium aluminate. This primary ettringite or early form of ettringite does cause damage to concrete. Ettringite crystals continue to grow for days but eventually decompose. However, ettringite may persistently grow afterwards due to environmental conditions or chemical reactions within the cement. This persistent growth of ettringite is known as delayed ettringite formation and has led to the deterioration of cast-in-place concrete as well as pre-cast concrete since the 1980s. Taylor (1990) indicates that the conditions for damage to occur include an

internal temperature of 65-70°C and a constantly saturated atmosphere. Cements with high contents of SO_3, alkalis and MgO are prone to excessive concrete expansion. The common chemical formula for ettringite is $3CaO{\cdot}Al_2O{\cdot}3CaSO_4{\cdot}32H_2O$ or, in chemists notation, is $C_6A\hat{S}_3H_{32}$.

Table 2.1 - Cement Chemists' Notation

Notation	Compound
C	CaO
S	SiO_2
$\hat{S}$	SO_3
A	Al_2O_3
H	H_2O
$\hat{C}$	CO_2
M	MgO
T	TiO_2
N	Na_2O
F	Fe_2O_3
P	P_2O_5
K	K_2O

2.2 Mechanism of Delayed Ettringite Formation

There are two controversial hypotheses to explain the mechanism of delayed ettringite formation. The two hypotheses are the Uniform Paste Expansion Theory and the Crystal Growth Pressure Theory. The main controversy between these two has been whether the gaps between the paste-aggregate interfaces are the cause of expansion or the result of expansion. These gaps are typically filled with ettringite crystals. The crystal growth hypothesis (Heinz and Ludwig 1986) suggests that

expansion is caused by the growth of ettringite crystals on the surface of some cement particles through a solution mechanism or a topochemical reaction. A topochemical reaction is a solid state hydration mechanism where the product forms at the surface of the solid interface and grows in a direction perpendicular to the solid interface (Ceesay 2004). Alternatively, the uniform paste expansion theory attributes the expansion to water absorption. The ettringite crystals form inside the gaps or cracks after the initial expansion has occurred. The gaps are produced when the hardened cement paste expands and separates from the aggregate. Both theories lack conclusive research and Day (1992) suggests that both mechanisms are possible depending on the environmental condition.

2.3 Damage Due to Delayed Ettringite Formation

According to Day (1992), the earliest possible reported damage to cast-in-place concrete by DEF was observed by Kennerley in 1965. Kennerley investigated a deteriorated cold-joint in the Roxburgh Dam in Otago, New Zealand and noticed a white deposit, ettringite. In 1980, Pettifer and Nixon recorded several cases of concrete deterioration possibly by ettringite. These cases included concrete bases of substations in the English midlands and the Pirow Street Bridge in Cape Town, South Africa. The pores and voids of the substation concrete were filled with ettringite even though there was minimal amount of sulphates in the soil. The Pirow Street Bridge showed cracking only four years after completion and required repairs after nine years. The concrete was composed of reactive aggregates with low alkali cement. Also in the early 1980s, Volkwein was examining 12 to 80-year old concrete bridges for carbonation, chloride penetration, deterioration and corrosion. Volkwein (1980)

found needle shaped crystals in cracks and around aggregates in concrete contaminated by CI ions. He concluded that, since the sulphate content did not change in the concrete, the chloride ions caused the formation of the ettringite. This conclusion is contradictory to laboratory results of Attiogbe (1990) who found that DEF would not form in concrete prisms soaked in sodium-chloride solution.

Premature cracking was first noticed in pre-cast concrete in railway ties and cladding panels in Germany and Scandinavia during the 1960s and 70s. The cracking initiated at the corners and edges of the panels and migrated into the interior. Studies indicate the cracking occurred due to frost, loads, and premature or improper heating. These migrating cracks caused a separation of the aggregates and cement matrix. Petrographic examination confirmed the existence of ettringite crystals in the cracks. Heat-treatment was the likely cause of failure of the ties in Germany. A Research Institute (1990) report noted that heat treatment had two major impacts: (1) inadequate pre-treatment allowed internal damage through debonding of the aggregate and cement matrix, and (2) heat treatment interrupted the normal formation of ettringite which eventually continued when the concrete hardened. The Scandinavian ties were fabricated with high early strength cement and cured at 75-85°C. A report by Tepponen (1987) noted visible damage after 15 years and thin section analysis revealed ettringite in the cracks. Subsequent studies however concluded that poor frost resistance and not ettringite was the main reason for the deterioration. Furthermore, publications and experiments by Hienz and Ludwig (1987) noted damage to pre-cast units manufactured with high-early-strength cement and heat treatment during production. They noticed that damage always occurred on

units exposed to the weather and subjected to moisture saturation. They concluded that the damage was caused by the reformation of ettringite in hardened concrete following heat-treatment.

In recent years Departments of Transportation (DOTs) across the United States have begun to identify in-service structures with premature concrete deterioration. In 1995, Texas DOT found damage to pre-stressed beams, abutments, columns, and bents requiring remedial repair or removal from service only after a few years (Lawrence 1999). The damage was revealed in the form of map cracking produced by alkali-silica reaction (ASR), delayed ettringite formation (DEF) or both. The 1995 investigation was prompted when fifty-six of sixty-nine box girders fabricated in San Marcos, Texas were damaged by ASR, DEF, or both. Sixteen other structures were found to have similar damage. Petrographic analysis on the damaged structures confirmed DEF in the cement paste and cracks of the pre-cast box girders. The field investigation found four high mast illumination pole foundations along U.S. 59 with DEF related cracking. Additionally, thirty percent of the pre-stressed Type IV beams on IH 45 were found to be deteriorated after only six years of service. DEF related cracking was also found on two adjacent cast-in-place bent caps and columns on IH 37 (Folliard 2006).

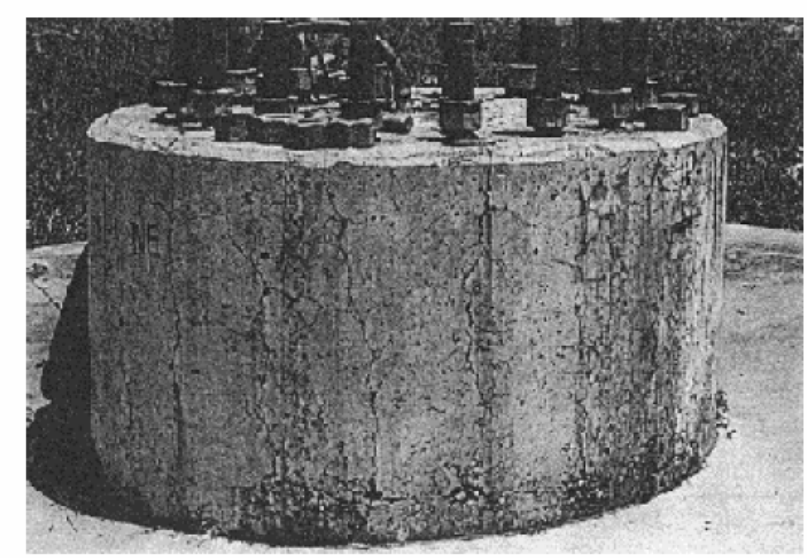

Figure 2.1 - High Mast Illumination Pole Foundations with DEF-Related Map Cracking along U.S. 59 in Texas (Lawrence 1999)

Similarly, Iowa DOT initiated field and laboratory studies to determine the cause of premature concrete pavement deterioration (Scholarholtz 2002). The study tested cores taken from seventeen concrete pavements in Iowa. Laboratory experiments were also conducted to evaluate the effect of cement composition, mixing time, and admixtures on the premature deterioration. The report concluded that construction practices such as poor mixing and poor aggregate grading played key roles in the premature deterioration. The report also concluded that the deteriorated pavements contained poor to marginal entrained-air voids systems. Petrographic analysis revealed that the entrained air void system was filled with ettringite.

In 2004, the University of Maryland conducted a pilot study to investigate the extent of delayed ettringite formation damage in existing cast-in-place concrete bridges for the Maryland State Highway Administration (Amde et al. 2004a, 2005b,

Livingston et. al. 2002, 2006b). Twenty-nine cores were taken from sixteen bridges with various degrees of map cracking utilizing the state's PONTIS Bridge Management System. See Figures 2.2 and 2.3 for sample core results. The study also included non-destructive testing of in-service bridges utilizing potassium autoradiography and impact echo (Livingston et. al. 2006c and 2006d, McMorris et. al 2006, Newman et. al. 2006). The research revealed that Maryland concrete, much like that in Texas and Iowa, has DEF in its in-service structures. DEF was present in twenty-six of the twenty-nine cores. Two cores that tested positive for DEF were from a bridge with no visible signs of map cracking. The two non-destructive tests did not yield any correlations to delayed ettringite formation.

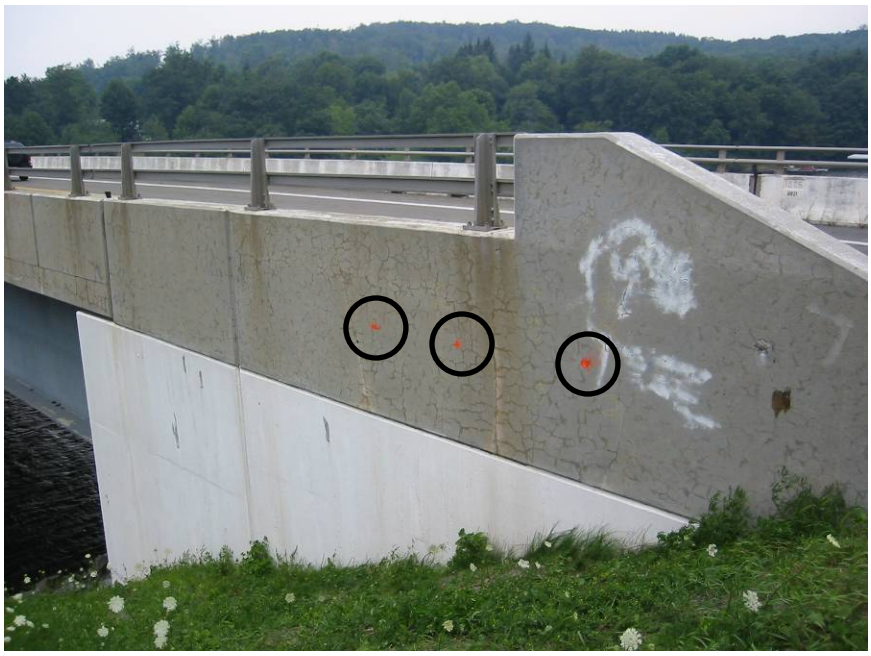

Figure 2.2 - Coring Locations on Bridge No. 1102100
(U.S. 219 over Deep Creek Lake) (Amde et al. 2004a)

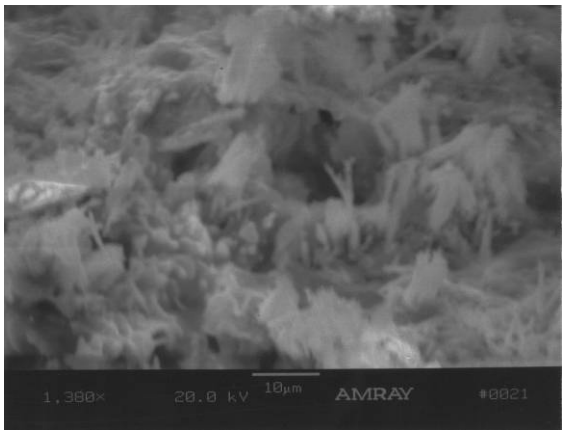

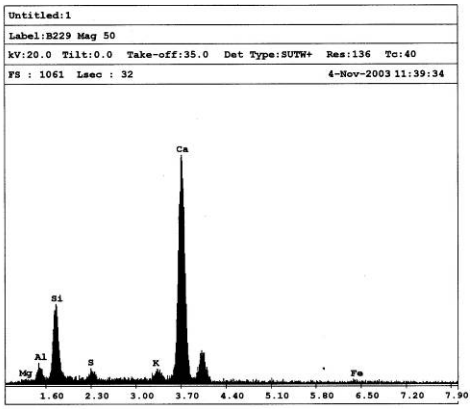

EDAX ZAF Quantification (Standardless)
Element Normalized
SEC Table : Default

Element	Wt %	At %	K-Ratio	Z	A	F
MgK	0.44	0.67	0.0021	1.0240	0.4604	1.0061
AlK	3.51	4.78	0.0212	0.9936	0.6028	1.0107
SiK	16.17	21.20	0.1164	1.0223	0.6976	1.0097
S K	2.36	2.72	0.0189	1.0179	0.7652	1.0265
K K	2.95	2.78	0.0297	0.9753	0.9229	1.1161
CaK	72.01	66.16	0.6746	0.9975	0.9385	1.0007
FeK	2.56	1.69	0.0214	0.9091	0.9200	1.0000
Total	100.00	100.00				

(a) Ettringite on the Surface **(b) Analysis of Whole Picture (a)**

Figure 2.3 – Ettringite Image and EDAX Table for Core From Bridge No. 1102100 (U.S.219 over Deep Creek Lake) (Amde et al. 2004a)

2.4 DEF and Alkali Silica Reaction (ASR)

ASR was discovered first and there is considerably more research on the topic than DEF. Alkali-silica reaction occurs between the alkalis (Na_2O and K_2O) in the cement and reactive silica (quartz and tridymite) in aggregates to form a gel product. The gel reacts with moisture to produce expansion stresses in the concrete which eventually yields cracking. Expansion can occur in relative humidity above 80 percent. On the concrete surface ASR produces fine random cracks known as "map cracking." In reinforced concrete the cracks are parallel to the reinforcing steel. Two test methods have been developed to measure the potential reactivity of aggregates: ASTM C1260 and ASTM C1293. There is no standard ASTM test method to assess

the potential for DEF. However, the Duggan Test is extensively used to accelerate the growth of ettringite.

There is much confusion and controversy over the influence of DEF and ASR on concrete since both cause expansion and are easily identifiable by map cracking. Shimada (2005) reports numerous researchers claim that ASR, accelerated by heat curing, is the primary cause of expansion and cracking. The DEF forms afterwards in the cracks and gaps of the aggregate interface to produce a minimal amount of expansion. Diamond and Ong (1994) also concluded that the large expansion that occurred during and after steam curing was due to ASR not DEF. They observed that DEF formed in cracks preceded by ASR and, when non-reactive aggregates were used, there was no expansion. On the other hand, Johansen (1993) reported that ASR may cause cracks inside the aggregates and the surrounding paste but not at the paste-aggregate interface which contradicts the previous researcher's claims. The gap formation at the paste-aggregate interface is a common characteristic of DEF-related expansion. Still, other researchers have proven that ASR is not a prerequisite for DEF through observed DEF-related expansion in laboratory specimens with non-reactive aggregates (Shimada 2005).

2.5 Mitigating Delayed Ettringite Formation

Research on the topic of mitigating delayed ettringite formation is scarce and the majority of the research has been focused on detailing the mechanisms of ettringite growth and the factors related to expansion. However, research has been under way to test if external chemical treatments, such as sealers, have the ability to limit or even prevent ettringite growth. Research projects conducted by the Iowa and

Texas Departments of Transportation (TxDOT) within the past few years have tested external treatments in the form of sealers and crystal growth inhibitors in reducing DEF-related expansion. Additionally, a stricter quality control criterion is being developed in the selection of concrete materials and curing temperatures.

Cody et al. (2001) experimented with commercial crystal inhibitors commonly used to prevent crystallization in industrial processes such as water treatment plants and boilers. Laboratory specimens as well as cores from in-service bridges were treated with various concentrations of four different crystal inhibitors and subjected to different storage conditions. The working theory was that if the amount of ettringite is reduced there will be a corresponding reduction in concrete expansion and cracking. If both ettringite and expansion are reduced simultaneously than the case for ettringite and expansion interaction is strengthened. The researchers found that two phosphonate inhibitors, Dequest 2060S and Dequest 2010, were the most effective in reducing ettringite growth. Good-Rite K752 and Wayhib S were less effective than the two phosphonates. Cody et al. (2001) concluded that there is a direct link between ettringite growth and concrete expansion because the only known effect of the commercial inhibitors is to reduce crystal growth.

Klingner et al. (2004a-c) experimented with surface treatments impermeable to water but permeable to water vapor for mitigating concrete deterioration for TxDOT. In the pilot tests researchers tested twenty-three different combinations of mitigation techniques composed of solutions based on silane, siloxane, linseed oil, polyurethane, and high-molecular-weight methacrylate (HMWM). Afterwards, two confirmatory tests (A & B) were performed with refined test methods and a reduced

number of mitigation techniques including six silane treatments and one epoxy treatment. Laboratory specimens consisted of 3" x 3" x 11.25" prisms cured at 23°C and 95% relative humidity. Gage studs were installed in some of the specimens to measure length change measurements. Two plastic sleeves were either cast or drilled into some specimens for moisture measurements. The treated specimens were subjected to three different storage conditions. The wet/dry condition consisted of periodically varying the humidity between 10% (dry) and 100% (wet). The indoor specimens were subjected to accelerated aging by heat treatment and the outdoor specimens were placed in actual field conditions. Data collected from an acoustic emission monitor was used to calculate the Felicity ratio. The study concluded that Silane combined with either TxDOT's Appearance Coat Paint or Opaque Concrete Sealer were the most effective in mitigating concrete deterioration caused by delayed ettringite formation or alkali-silica reaction.

The types of cement and aggregates used in the concrete mix plays a crucial role in the development of ettringite growth. Numerous researchers (Hienz, Kelham, Fu et al.) have linked an increased content of C_3A, C_3S, MgO, Na_2O_{eq} and SO_3 in cement to an increased amount of DEF. However, reducing the content of these elements in cement would be challenging if not impossible. Fu (1996) analyzed the effect of mineral additives on the expansion of cement mortars. He concluded that Class F fly ash and ground granulated blast furnace slag (GGBFS) were the most effective mineral additives in reducing DEF related expansion in Portland cement mortar. Similarly, Heinz (1989) reported mortars containing blends of fly ash or GGBFS with known expansive cements did not expand after curing at 90°C.

Collepardi (1999) acknowledged that an important factor in reducing DEF-related deterioration is related to cement composition. High early strength cement (Type III) with high C_3S and C_3A content has an increased susceptibility to DEF. Furthermore, Collepardi (1999) declares that pozzolanic material such as silica fume can be effective in reducing DEF-related damage.

High curing temperatures have also played a harmful role in the premature deterioration of concrete due to DEF. Famy (2002) concluded that the risk of DEF-related expansion cannot be reliably avoided by placing restrictions on cement composition but can be eliminated by limiting the internal concrete temperature. Numerous international and U.S. agencies have enacted temperature guidelines to help prevent delayed ettringite formation. Table 2.2 summarizes some international accelerated curing temperatures (Folliard 2006).

Table 2.2 - International Heat Curing Specifications (Folliard 2006)

Country	Agency/ Specification	Max Temp.
U.S.A.	PCI	70°C (158°F) *
Canada	CSA / A23.4-94	70°C (158°F)
Denmark	DS482	70°C (158°F)
England	Manual of Contract Documents for Highway Works	70°C (158°F)
Germany	Committee for Reinforced Concrete	60°C (140°F)
South Africa	SABS/0100-2:1992	60°C (140°F)
Spain	UNE/83-301-91	70°C (158°F)

* - 80°C if potential for DEF is minor

2.6 Mitigating Alkali Silica Reaction

Extensive mitigation and test methods are available for preventing ASR-related concrete deterioration. Most mitigation methods center on limiting the amount of alkali in the cement and the use of reactive aggregates. Agencies such as AASHTO, PCA, and ASTM have developed cement and aggregate specifications for preventing ASR. The use of low-alkali cements may seem an obvious solution to preventing ASR, however, there are controversies about its availability and effectiveness. Duchesne and Berube (1994) suggest limiting alkali content to 5 lb per cubic yard. Leming and Nguyen (2000) disagree, pointing out that deleterious effects of ASR occurred at 3.4 lb per cubic yard. Rogers (1993) contends that low alkali content cements are not practical in Canada where the climate dictates the use of durable concrete with low cement to water ratio and air-entrainment.

Admixtures such as fly-ash, slag, and silica fume have been proven to reduce ASR related expansion; however, there is no general consensus on the minimum percentage that should be used. Furthermore, improper proportioning may actually result in an increase of ASR. Despite differences of opinions, admixtures seem to be the preferred method for mitigating ASR. Table 2.3 summarizes admixture requirements of some U.S. agencies.

Table 2.3 - Admixture Requirements for Selected Agencies (Folliard 2006)

	Cementitious Material Percentage (By Mass)			
Mineral Admixtures	AASHTO (minimum)	TxDOT	PCA/ACPA	USACE
Fly Ash Class F	15%	20% - 35%	Must meet ASTM C1260 or C441 expansion limits	Must meet ASTM C1260 or C441 expansion limits
Fly Ash Class C	30%	Must meet ASTM C1260 or C441 expansion limits	"	"
GGBF Slag	25%	35%-50%	"	"
Silica Fume	5%	<10%	"	"

Limiting the use of reactive aggregates is the second method for reducing ASR; however, one ideal test method to quantify the reactiveness of aggregates does not exist (ACI 1998). Federal and state agencies specify different test methods to determine aggregate reactivity including ASTM Standards C227, C289, C295 and C1293. USACE (2000) reports that none of these standard tests, independently or in combination, provides a definitive answer as to whether a particular aggregate is reactive. Organizations such as CSA, PCA and AASHTO have developed flowcharts to aid in the analysis of an aggregate. The flow charts have similar paths and suggest the same test methods. Figure 2.4 shows the Flowchart developed by AASHTO (Folliard 2006).

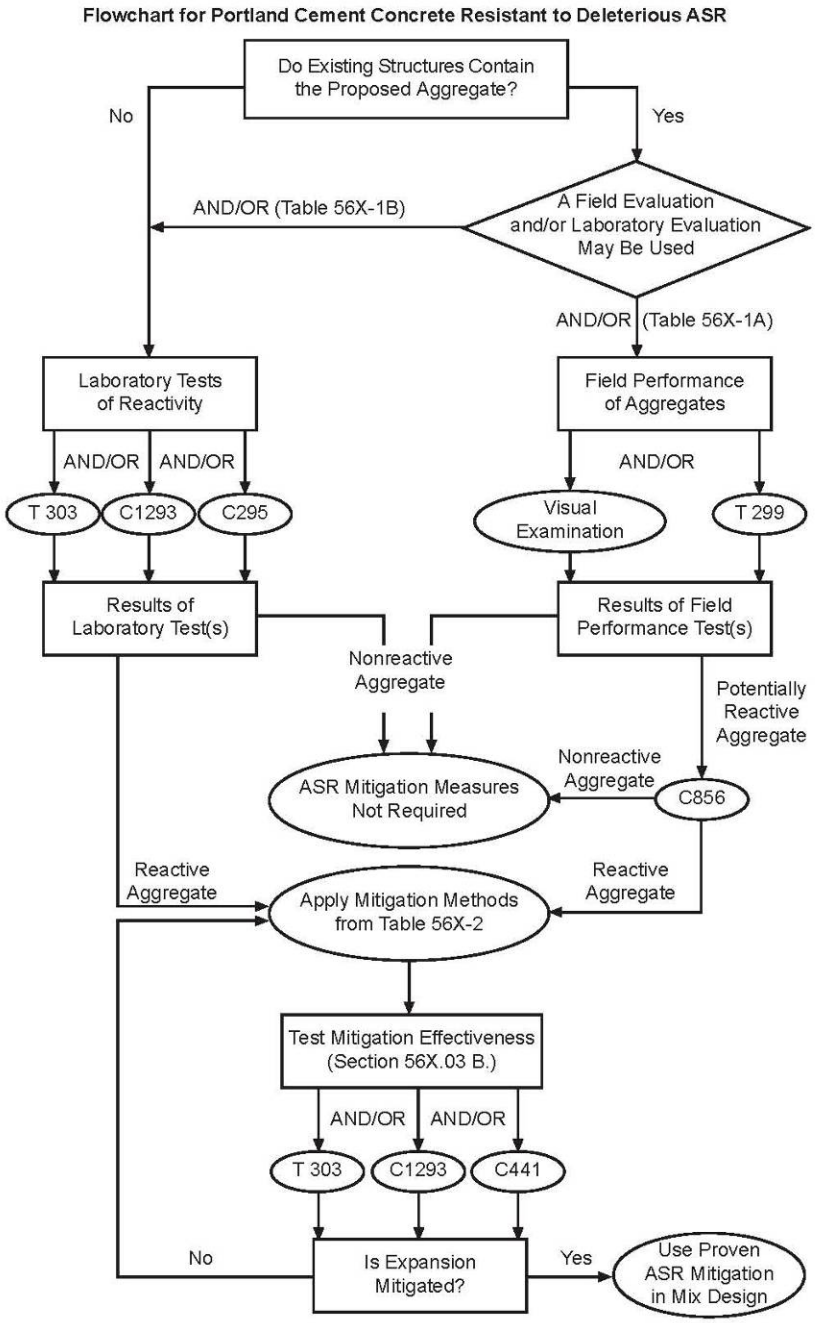

Figure 2.4 - AASHTO Flowchart to Mitigate ASR in Portland Cement Concrete (Folliard 2006)

Chapter 3: Experimental Approach

This chapter describes the reasoning behind the testing methodology for this study. An ASTM standard does not exist to test the mitigating effectiveness of the water repellents or crystal inhibitors on DEF. A primary objective and a series of boundary conditions had to be established in order to have a well defined study. This chapter only summarizes the experimental approach. More detailed explanations of the concepts are provided in Chapters 4 and 5.

The primary objective of this study is to determine if externally treating concrete specimens with water repellents and crystal growth inhibitors will decrease DEF-related expansion in laboratory specimens. The study is geared toward mitigating DEF in existing concrete such as bridge decks, parapets, abutments, etc. The focus of the study is not towards mitigating DEF in newly cast concrete. Therefore, mitigating DEF through the use of admixtures in the concrete mix or varying curing conditions is not considered in this study. The most practical technique to mitigate DEF in existing and in-service concrete structures appears to be with chemical treatment.

The mitigating products are tested on concrete specimens prepared in the laboratory. Since ettringite crystals take years to develop, an accelerated ettringite growth method was needed. Research at the University of Maryland and literature reviews aided in developing a concrete mix design, curing conditions, and storage conditions suitable for accelerated ettringite growth. Type III cement and a potassium admixture were utilized in the concrete mix design. The specimens were

steam cured at 85 degrees Celsius for twenty-four hours. A heat treatment known as the UMD/FHWA Modified Duggan cycle was applied to the concrete specimens eight days after water curing. Finally they were permanently stored under water which is known to accelerate the expansion.

Sample preparation was not as challenging as selecting and applying the products for this study. The water repellents and crystal inhibitors are being utilized to test two different hypotheses for mitigating DEF. The first hypothesis for reducing ettringite growth involves limiting the amount of water molecules into the concrete (Merrill 2004). This particular hypothesis was tested utilizing the two water repellents, ChimneySaver and Radcon Formula #7. The two water repellents were identified through search of commercial websites that manufacture or distribute such chemicals. The second method for mitigating ettringite growth attacks the ettringite molecules at their core (Cody et al. 2001). Crystal inhibitors are designed either to reduce precipitation or modify the precipitation morphology. The two crystal growth inhibitors were identified and selected through a literature review. Dequest 2060S and Good-Rite K-752 were previously tested by Cody et al. for Iowa Department of Transportation in 2001.

After the sample preparation was established and mitigation products were identified the next challenge was to determine the application procedure. The application had to incorporate how the product would be applied to the concrete specimens, how much was to be used, and at what concrete age it should be applied. It was decided to apply mitigation products only once and at full concentration. Other researchers, particularly Cody et al. (2001) at Iowa State University, diluted the

crystal inhibitors with distilled water and applied the diluted solution at weekly or monthly intervals. One application at full concentration would seem more economically reasonable for field application. The water repellents were applied with pressurized hand sprayers. The crystal inhibitors were applied with paint rollers because the products were too viscous for the hand sprayers. Researchers realize that brushing inhibitors on a bridge deck or abutment is not reasonable. In order to test the full capability of the inhibitor the decision was made not to dilute the products.

The age at which the concrete samples were treated with the mitigation products would impact the effectiveness of the product. If the product was applied too early there was a possibility that no ettringite would develop in the concrete specimens and effectiveness of the product would not be realized. If the product was applied too late the accelerated growth of ettringite would deteriorate the concrete specimen to a point that no amount of treatment would prove effective. Previous research by the University of Maryland indicated that the expansion increases between thirty and fifty days after completion of heat treatment (Amde et al. 2004b, Ceesay 2004, Ramadan 2000). The increased expansion was observed around forty days for the concrete specimens in this particular study. At forty days the specimens were removed from the storage, dried, and treated with a mitigation product. The water repellents were applied per manufacturer's directions. Manufacturer's directions for the two crystal inhibitors were not available since the products are not applied to concrete. Directions were developed by the researchers and are described in detail in Chapter 4. After application the concrete specimens were returned to storage and testing measurements were continued for 300 days.

Four tests were selected to monitor the effectiveness of the mitigation products. Ettringite causes expansion of the concrete leading to deleterious consequences. Expansion and weight change measurements were recorded at 3 to 5-day intervals for the first 180 days and once a week thereafter. Previous research indicated that the majority of expansion occurs within the first six months and thus more measurements were recorded in the first 180 days. Compression test was utilized to determine if the strength of the concrete was affected by the mitigation products. A Scanning Electron Microscope (SEM) was utilized to verify the existence of ettringite and to categorize the various morphologies of the ettringite.

Chapter 4: Mitigation Products

4.1 Introduction

Four products were selected for this research including two water repellents and two crystal growth inhibitors. The water repellents and crystal growth inhibitors were selected to test two hypotheses of reducing ettringite related damage to concrete. The first hypothesis is aimed at reducing a vital ingredient, water, in the formation of ettringite crystals. The second hypothesis is aimed at reducing the growth of ettringite crystals at an early period of existence in the concrete. If any of the products are successful there would be appreciable reduction in the expansion of the concrete specimens.

The first hypothesis for reducing ettringite growth involves limiting the amount of water molecules into the concrete (Merrill 2004). This particular hypothesis is tested utilizing the two water repellents, ChimneySaver and Radcon Formula #7. It is hypothesized that limiting the amount of water penetration into the concrete will limit a key ingredient in the growth of ettringite crystals. Water repellents create hydrophobic zones just under the concrete surface and this hydrophobic zone repels water molecules but allows water vapor to travel freely into the concrete. It is essential that water vapor move freely in order to reduce pressures caused by the freeze-thaw cycle. Without the necessary amount of water the ettringite formation should be reduced thus leading to much longer lasting concrete.

The second method for mitigating ettringite growth attacks the ettringite molecules at their core (Cody et al. 2001). Crystal inhibitors are designed either to reduce precipitation or modify the precipitation morphology. Essentially, crystal growth inhibitors prevent the growth of crystallite at the "pre-critical nuclei" stage. At the "pre-critical nuclei" stage the ettringite crystals are at their infancy and therefore unable to fully develop into crystals. Subsequently the crystals dissolve and never fully precipitate. Crystal inhibitors are widely used in various industrial processes but not as an external application on concrete.

4.2 Water Repellents

Sealers, water repellents and waterproof coatings are similar solutions and generally fall into two categories: penetrants and film formers. Penetrating sealers, such as silanes, siloxanes, and silicates, react chemically within the concrete to create a hydrophobic zone to shield against water penetration and deicing chemicals. Film forming sealers are the type most often used for decorative concrete and they form a protective film on the surface of the concrete. There are three primary types of film formers: acrylics, epoxies and polyurethanes. This research is concentrated towards silicone based penetrants.

When applied, silane and siloxane repellants penetrate into the concrete and react chemically with silicate material to form a resin. The resin that forms is designed to make the capillaries of the concrete smaller than that of a water molecule and at the same time allow water vapor to flow freely (see Figure 4.1). Silane molecules have one silicone atom and have smaller molecular structure than siloxane molecules which have multiple silicone atoms. Accordingly, silanes are able to

penetrate deeper into the concrete and are typically used on denser surfaces such as horizontal slabs and cast-in-place smooth faced concrete. A comparison of silanes and siloxanes is provided by Dow Corning Corporation in Figure 4.2.

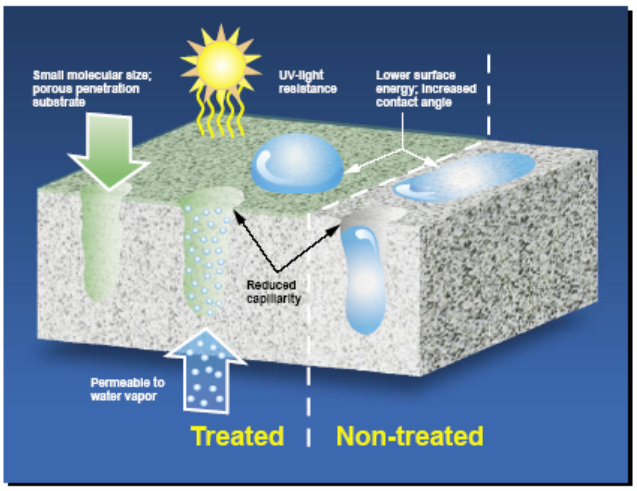

Figure 4.1 – Silicone-Based Sealers Penetrate Deep Into the Concrete To Form a Hydrophobic Zone (Dow Corning 2006)

Silicones for water repellency

SILANES	SILOXANES
Smallest silicone molecules	Linear polymers
Low surface tension and low viscosity – excellent spreading and penetration on most substrates	Low surface tension – excellent spreading on most substrates
Depth of penetration and water exclusion, but allows water vapor to pass	Helical siloxane structure repels (beads) liquid water, but allows water vapor to pass
Alkoxy silanes used for water repellency react with themselves and any OH-functional to form silicone resin network	Different chemistries enable reactivity with substrate or other siloxanes
Penetration along with UV/heat and oxidation stability combine for excellent durability	Highly resistant to degradation from UV, heat, oxidation
Silicones are present in many forms and functionalities and are often used in combination to yield the desired properties.	

Figure 4.2 - Properties of Silicones for Water Repellency (Dow Corning 2006)

4.2.1 ChimneySaver

ChimneySaver® is a siloxane based water repellent which reacts with minerals in concrete or masonry and ultraviolet light to form a hydrophobic zone 1/16" to 1/4" below the surface. This hydrophobic zone prevents water molecules from penetrating the concrete optimistically resulting in the slower growth of ettringite. It has a milky white color and does not leave a glossy finish after application. After the application of ChimneySaver® the concrete specimens are allowed to dry in ultraviolet light for 4-6 hours (See Figure 4.3). ChimneySaver® is designed to protect adobe; architectural, precast, or cast-in-place concrete; and brick

and stone masonry (SaverSystems 2005). It was purchased from a chimney supply warehouse store in a 3-gallon container (see Figure 4.4a)

.

PHYSICAL PROPERTIES

COLOR. . . . . Milky white

SOLVENT. . . . . .Water

SPECIFIC GRAVITY, AT 25° C 1.00

WEIGHT. . . . . 8.34 #/gallon

FLASH POINT . . . . . None

PENETRATION . . . . . 1/16" - 1/4" (depending on substrate)

VOC CONTENT (EPA METHOD 24). . . . . .50.6 gr/ltr (.422 #/gallon)

SHELF LIFE. . . . . .18-24 months in original sealed container

YELLOWING . . . . . None

SURFACE APPEARANCE AFTER APPLICATION . . . . . Unchanged

TECHNICAL DATA

TEST	DESCRIPTION	RESULTS
ASTM C 67-91 Section 7	% reduction in absorption on brick during immersion in water for 24 hrs.	96.9%
ASTM C 140-91	% reduction in absorption on 3000 psi concrete during immersion in water for 24 hrs.	91.29%
ASTM C 97-90	% reduction in absorption on Indiana limestone during immersion in water for 48 hrs.	81.7%
Federal Specification SS-W-110-C-3.5	Treated mortar cubes shall have less than 1% absorption after immersion in water for 72 hrs.	92%
OHD-L-35	Water vapor transmission	100%
ASTM C 67-91 Section 10	Resistance to efflorescence	Excellent, no efflorescence on treated specimens
ASTM G 53-88	Accelerated weathering (QUV) 3000 hrs.	No loss in water repellency
ASTM 514-86	% reduction of leakage through masonry walls,	99.9%

Figure 4.3 - ChimneySaver Physical Properties and Technical Data (SaverSystems 2005)

4.2.2 Radcon Formula #7

Radcon® Formula #7 is a sodium silicate solution that reacts with calcium and water in the concrete to form a gel like substance in pores and cracks (See Table 4.1). This gel creates a sub-surface hydrophobic zone which prevents water molecules and chloride ions from entering the concrete. Radcon® Formula #7 can seal existing cracks up to 2.0 mm (3/32") wide. It is applied on rooftops, decks, parking garages, runways, and other concrete structures. After application, the

specimens are dried 4-6 hours then generously washed with water. Further washing of specimens is required 24 hours and 48 hours after application. Radcon® Formula #7 is a clear solution which leaves a glossy and somewhat slippery finish after initial washings. The glossy finish dissolved after several days in the lime water bath (Radcrete Pacific Pty. Ltd. 2005). Radcon® Formula #7 was purchased from the product distributor in Dallas, Texas (see Figure 4.4b).

Table 4.1 - Radcon Formula #7 Physical Properties and Performance Characteristics (Radcrete Pacific Pty. Ltd. 2005)

Radcon Formula #7 – Physical Properties	
Color	Clear to slightly opaque
Specific Gravity at 25^{o} C	1.225
Flash Point	None
Viscosity	14.3 cps or 0.1172 Stokes
pH	11.7
Radcon Formula #7 – Performance Characteristics	
Reduction of chloride diffusion coefficient by 89%	
Water permeability reduced by 70%	
Reduces scaling in freeze-thaw environments by 89%	
Allows 84.1% moisture permeability	

4.3 Crystal Growth Inhibitor

Crystallization inhibitors are used in a wide-ranging spectrum of applications including industrial water treatment, household & industrial detergents, industrial cleaners and enhanced oil recovery operations. They are most commonly used as antiscalants, dispersants, and corrosion inhibitors. Cody (1991) states that there are

three major groups of commercial organic inhibitors: organic phosphate esters, phosphonates, and polyelectrolytes. One phosphonate and one polyelectrolyte were chosen for this research. Almost all commercial inhibitors are organic chemicals (polycarboxylates and phosphonates) and are effective in preventing the precipitation of various minerals including calcite, gypsum, and barite (Cody 1991). According to Cody (1991) the most effective inhibitors have molecules which are negatively charged by deprotonation under alkaline condition and have a moderate to high pH. Furthermore, the effectiveness of the inhibitor increases with concentration. The two major effects of inhibitors are the prevention or reduction of undesired precipitation and modification of precipitate morphologies. Inhibitors prevent crystallization by preventing the growth of "pre-critical nuclei" or crystal nuclei that are too small to be stable. These small crystal nuclei are prevented from growing and stabilizing into crystallites and consequently dissolve.

4.3.1 Dequest 2060S

Dequest 2060S is a phosphonic acid based solution with exceptional scale inhibition ($CaCO_3$) capability. Dequest 2060S is a highly viscous solution with a honey like quality and a pH < 2 (see Table 4.2). Due to the high viscosity, a 3"-wide paint roller was used for application. After application a thin layer of foam formed on the surface of the concrete. This foamy film was easily removable with the touch of a finger. Dequest 2060S uses include cooling water treatment, peroxide bleach stabilization and scale control in oil fields (Solutia Inc. 2005). Dequest 2060S was obtained from Solutia Inc. based out of St. Louis, Missouri (see Figure 4.4c).

Table 4.2 - Dequest 2060S Physical Properties and Performance Characteristics (Solutia Inc. 2005)

Dequest 2060S – Physical Properties	
Color	Amber
Specific Gravity at 20^{o} C	1.42
Odor	Pungent
Viscosity	~1000 cP
pH	<2.0
Dequest 2060S – Composition	
Methylene Phosphonic Acid	48% - 52%
Hydrogen Chloride	15% - 17%
Phosphonic Acid	3%
Formaldehyde: <100 PPM	< 100 PPM

4.3.2 Good-Rite K-752

Good-Rite® K-752 is a water soluble acrylic acid polymer (See Table 4.3). It is composed 47% by polyacrylic acid and has a pH between 2.2 and 3.0. Good-Rite® K-752 has a clear color and viscosity of 950 centa-poise at 25^{o}C. Due to the high viscosity, a 3"-wide paint roller was used for application. Suggested applications include scale control agents in water treatment applications and soil removal and antiredeposition aids in detergents and cleaners (Noveon Inc. 2005). Good-Rite® K-752 was obtained from Noveon Inc. based out of Cleveland, Ohio (see Figure 4.4d)

Table 4.3 - Good-Rite K-752 Physical Properties and Performance Characteristics (Noveon Inc. 2005)

Good-Rite® K-752 – Physical Properties	
Color	Clear/Amber
Specific Gravity at 25^{o} C	1.2
Odor	Slightly Acidic
Viscosity 25^{o} C	950 cP
pH	2.2 – 3.3
Good-Rite® K-752 – Composition	
Polyacrylic Acid	47%
Water	37%
Sodium Polyacrylate	16%

(a) ChimneySaver®

(b) Radcon® Formula #7

(c) Dequest® 2060S

(d) Good-Rite® K-752

Figure 4.4 – Mitigation Products Including Two Water Repellents (a & b) and Two Crystal Growth Inhibitors (c & d)

4.4 Mitigation Product Application Procedure

Water repellents were applied to concrete specimens with pressurized hand sprayers. Crystal inhibitors products were applied with a paint roller due to their high viscosity. A total of nine sets of concrete cylinders and prisms were cast. Each set consisted of nine 3" x 3" x 11.25" prisms and thirteen 4" diameter x 8" tall cylinders. One set was the control and no product was applied. Four sets were applied with individual products (Set Nos. 2, 3, 4, 7) and the four remaining sets were applied with cross combinations of water repellent and crystal growth inhibitors (Set Nos. 5, 6, 8, 9). Within each set 10 of 13 cylinders and 8 of 9 prisms were treated. See Tables 4.4 and 4.5 for Treatment Summary. The one prism was utilized to verify the existence of ettringite through SEM analysis at 30 days. The first three cylinders were used to determine the compressive strength at 30 days after the completion of the Duggan Cycle. All products were applied only after the existence of ettringite was verified with SEM and an increase in the expansion curves was established which occurred approximately 40 days after completion of Duggan cycle.

Table 4.4 - Concrete Specimen Treatment Schedule

Set 1	Control	Control
Set 2	Water Repellent A	ChimneySaver
Set 3	Water Repellent B	Radcon Formula #7
Set 4	Crystal Inhibitor A	Dequest 2060S
Set 5	Crystal Inhibitor A + Water Repellent A	Dequest 2060S + ChimneySaver
Set 6	Crystal Inhibitor A + Water Repellent B	Dequest 2060S + Radcon #7
Set 7	Crystal Inhibitor B	Noveon K752
Set 8	Crystal Inhibitor B + Water Repellent A	Noveon K752 + ChimneySaver
Set 9	Crystal Inhibitor B + Water Repellent B	Noveon K752 + Radcon #7

Table 4.5 - Concrete Specimen Treatment Schedule per Set

CYLINDERS	
1	No Treatment
2	No Treatment
3	No Treatment
4	Treated
5	Treated
6	Treated
7	Treated
8	Treated
9	Treated
10	Treated
11	Treated
12	Treated
13	Treated

PRISMS	
1	Treated
2	Treated
3	Treated
4	Treated
5	Treated
6	No Treatment
7	Treated
8	Treated
9	Treated

4.4.1 Water Repellent Application Procedure

Concrete specimens were treated with water repellents utilizing pressurized hand sprayers commonly used in lawn and garden application. The sprayers consisted of a two-gallon polyethylene tank, a hand pump and a two-foot long extension wand with an adjustable nozzle (See Figure 4.5). The tank was filled with approximately 1 to 2 liters of product and than the hand pump was twisted into place. The tank was pressurized until the handle yielded stiff resistance (approximately 50 strokes). After the tank was pressurized the nozzle was held approximately 2" from the face of the concrete which is sprayed in a vertical motion from the top down. Two coats of treatment were applied to each prism and cylinder with a 5-minute break between sprayings.

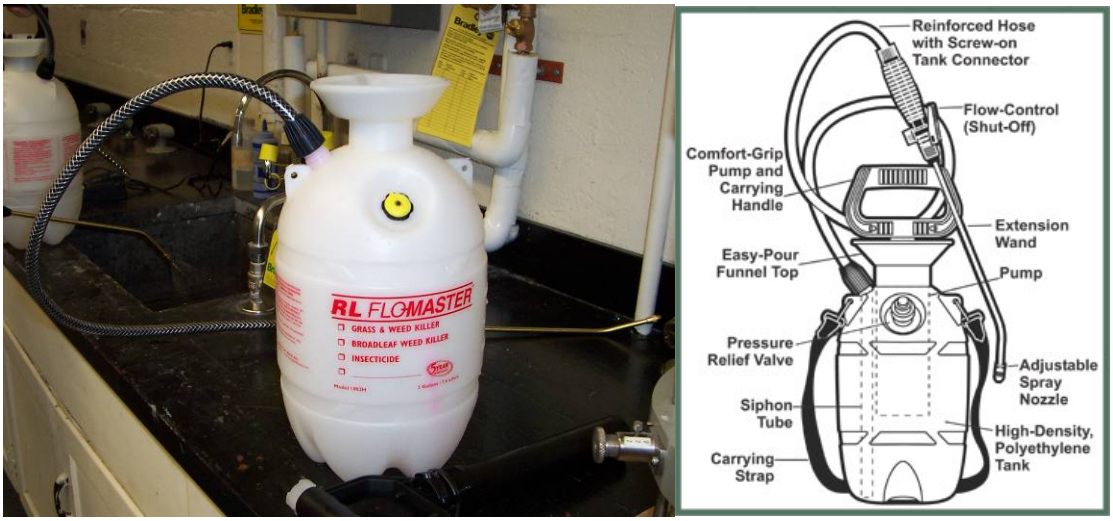

Figure 4.5 – Pressurized Polyethylene Hand Sprayers

Before applying the treatment products all specimens were cleaned with tap water to remove any excess lime and limewater from the surface then dried at room temperature for approximately 30 minutes (no visible moist locations). Once dried, a set of concrete prisms and cylinders were placed vertically standing on plastic lids to catch excess runoff. One set was sprayed with either ChimneySaver® (Set No. 2) or Radcon Formula #7® (Set No. 3). All specimens were left out in the sunlight for approximately 4 to 6 hours to dry and were periodically rotated for even sunlight exposure. Once the products were dried, the specimens were moved into dry storage buckets located inside the laboratory. The concrete specimens treated with the Radcon Formula #7 were washed with regular tap water before being placed in dry storage. The specimens were washed again 24 hours and 48 hours after application per manufacturer's direction. After the final washing, both the ChimneySaver (Set No. 2) and Radcon Formula # 7 (Set No. 3) prisms and cylinders were returned to the

lime-water bath storage condition. See Outlined Procedures in Table 4.6 and Figures 4.6 and 4.7 for application photographs.

Table 4.6 - Water Repellent Treatment Procedure

	ChimneySaver (Set #2)	Radcon Formula #7 (Set #3)
Day 1	Clean and Spray Specimens Dried in sunlight for 4-6 hours Placed in dry storage tubs	Clean and Spray Specimens Dried in sunlight for 4-6 hours Washed with tap water Placed in dry storage tubs
Day 2	-	Washed with tap water Placed in dry storage tubs
Day 3	Returned to storage conditions	Washed with tap water Returned to storage conditions

Figure 4.6 - Water Repellent Treatment of Concrete Specimens Utilizing Pressurized Hand Sprayers

Figure 4.7 - Specimens Treated with Radcon Formula #7 were Washed After 4-6 Hours of Drying and 24 Hours and 48 Hours After Application

4.4.2 Crystal Inhibitor Application Procedure

Specimens are cleaned with tap water and dried at room temperature (no visible moist locations). Crystal growth inhibitors Dequest® 2060S and Good-Rite® K-752 were applied to three sets each (6 sets total) with separate three-inch wide paint rollers (See Figure 4.8). Specimens were allowed to dry for 4 to 6 six hours in direct sunlight and each specimen was rotated periodically to make sure all surfaces were dried evenly. After the specimens were dried they were stored for 7 days in dry plastic bins inside the laboratory. The seven-day period would allow the viscous inhibitors to penetrate the concrete. On the seventh day the inhibitors had formed a hard dry shell coating on the surface of the concrete.

The Good-Rite K-752 coating had a hardened egg shell feel and was easily scraped off the surface of the concrete with a plastic brush. On the other hand the Dequest 2060S had adhered to the concrete and required the use of a metal tipped spatula to be removed from the surfaces of the specimen. It was necessary to remove the excess material to allow the ChimneySaver and Radcon Formula #7 to penetrate the concrete in the cross combination sets (See Section 4.4.3). The specimens were wiped with a damp cloth to remove any dust particles and allowed to dry at room temperature. Two sets of the Dequest 2060S and Good-Rite K-752 prisms and cylinders (4 sets total) were sprayed with either ChimneySaver® or Radcon Formula #7®. Crystal inhibitor application procedure is described in Table 4.7.

Figure 4.8 - Crystal Inhibitor Being Applied with 3" Wide Roller

Table 4.7 - Crystal Inhibitor and Cross Combination Treatment Procedure

	Dequest 2060S (Sets #4, 5, 6)	**Good-Rite® K-752 (Sets #7, 8, 9)**
Day 1	Clean and treat specimens with rollers Dried in sunlight for 4-6 hours Placed in dry storage tubs	Clean and Spray Specimens Dried in sunlight for 4-6 hours Placed in dry storage tubs
Days 2-6	Stored in dry tubs	Stored in dry tubs
Day 7	Excess product scraped off surface *(For Cross Combination Follow Water Repellent Procedure in Table 4.6.)* Sprayed Set #5 with Chimney Saver Sprayed Set #6 with Radcon Formula 7	Excess product scraped off surface *(For Cross Combination Follow Water Repellent Procedure in Table 4.6.)* Sprayed Set #8 with Chimney Saver Sprayed Set #9 with Radcon Formula 7
Day 8	-	Washed with tap water Placed in dry storage tubs
Day 9	Returned to storage conditions	Washed with tap water Returned to storage conditions

4.4.3 Cross Combination Application Procedure

Four sets of the concrete specimens were applied with a combination of crystal growth inhibitor and water repellent. The inhibitor was applied first and allowed to dry for seven days. On the seventh day the excess material was scraped off as described in Section 4.4.2. The ChimneySaver and RadconFormula #7 were applied using the same procedure described in Section 4.4.1. The cross combination product treatment is described in Table 4.7.

Chapter 5: Concrete Sample Preparation and Test Methods

5.1 Introduction

This chapter describes the procedures followed in the preparation of concrete specimens and the subsequent testing regimen. All nine sets of concrete specimens were prepared using the same materials, mix design, and curing conditions. Additionally, all specimens were subjected to the UMD/FHWA Modified Duggan Cycle to accelerate the growth of the ettringite crystals. The purpose of the research is to test the mitigating capabilities of the products described in Chapter 4. For this reason it was essential to have a consistent set of specimens. Any variance in the preparation of samples would lead to incoherent results.

The chapter concludes with an explanation of the four tests conducted on prisms and cylinders. It is important to note that the testing regimen was conducted relative to the completion of the UMD/FHWA Modified Duggan Cycle and not the casting/curing of the specimens. For instance, the 30-day compression tests were conducted 30 days after completing the Duggan Cycle or about 47 days after casting. Initial weight and length measurements were also conducted after the completion of the Duggan Cycle. Figure 5.1 describes the tasks and the required time necessary to complete the preparation of the specimens.

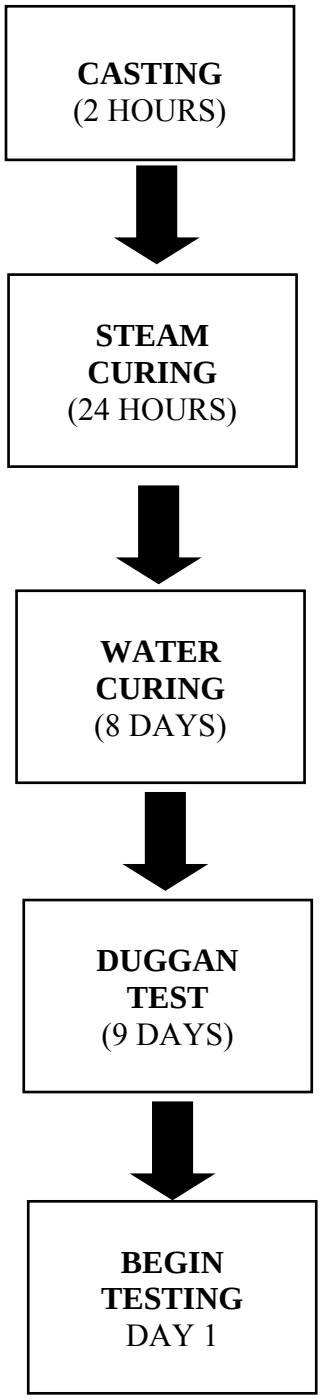

Figure 5.1 - Sample Preparation Sequence. All Testing Was Conducted Relative to the Completion of the Duggan Cycle

5.1.1 Research Laboratories

Three research facilities were used throughout the course of this project and they are described as follows:

1) University of Maryland (UMD) – College Park, MD.

   UMD structural lab was the primary location for the mixing, casting, and curing of all concrete specimens. The facility was also used to run the Duggan Cycle and to permanently store concrete cylinders in plastic tubs filled with lime water. This facility was chosen for its open work space with a retractable bay door and its two large ovens with the capacity to hold seventy concrete specimens.

2) National Ready Mix Concrete Association (NRMCA) – Greenbelt, MD.

   NRMCA lab was primarily used to conduct length change measurements, weight change measurements, and compression tests. The lab was also used to permanently store all concrete prisms in plastic tubs filled with lime water.

3) Turner-Fairbank Highway Research Center (TFHRC) – Mclean, VA.

   TFHRC is federally owned and operated by the Federal Highway Administration (FHWA). TFHRC conducts research and develops new technologies for the highway industry. The facility was used to investigate the mechanism of delayed ettringite formation through the use of a Scanning Electron Microscope (SEM) with Energy Dispersive Analysis X-ray (EDAX).

5.2 Concrete Mix Design

In order to test the mitigating potential of the water repellents and crystal inhibitors a highly expansive concrete mix design was necessary for this research. The ability of the ettringite to form in the concrete in a short period of time (~6 months) was the most crucial element of the mix. Previous research performed at the University of Maryland and the literature review indicated that the use of quick hardening Type III cement, steam curing and high potassium content increases concrete expansion and growth of ettringite crystals (Ceesay 2004).

The concrete mix for this research was proportioned using the Absolute Volume Method with water to cement ratio of 0.5 and a slump of 4 inches without the potassium carbonate admixture. Potassium carbonate admixture was added to the mix to increase the potassium content of the cement to 1.5% by weight. The addition of the potassium carbonate reduced the slump by 1.5". Furthermore, the workability of the concrete mix and the set time of the concrete were also reduced.

The materials were mixed in a 3.0 cubic foot capacity rotating mixer in accordance with ASTM C192M. A total of 9 batches, representing nine sets of prisms and cylinders, were prepared over a course of three days (i.e., 3 sets per day). All 9 batches were proportioned and mixed in the same manner. Each set consisted of thirteen - 4"-diameter x 8"-tall cylinders and nine-3" x 3" x 11.25" prisms. One set required approximately 1.8 cubic feet of concrete and approximately 16.2 cubic feet of concrete was used for all nine sets. See Table 5.1 for breakdown of the concrete materials per batch.

Table 5.1 - Mix Design for One Set (13 Cylinders and 9 Prisms)

Mix Design per Set
13 cylinders & 9 prisms ~1.8 cu.ft. of Concrete

	Specimen Concrete Mix Weight	%
Water =	27.9 lb	10.4%
Cement =	55.8 lb	20.9%
Coarse Aggregate =	109.9 lb	41.1%
Fine Aggregate =	73.6 lb	27.5%
Total =	267.2 lb	100.0%
K_2CO_3 Required =	295.4 gram	

5.3 Materials

Materials for the mix were purchased from local suppliers and quarries. The aggregates were found using the 2005 Maryland State Highway Administration (SHA) Aggregate Bulletin. The fine aggregate was selected based on its expansive quality. SHA requires quarries to perform ASTM-C1260 (MSMT 212) every three years to determine the alkali reactivity of fine and coarse aggregates. According to ASTM, the ASR ratings are as follows: Low (0 – 0.09%), Medium (0.10% – 0.19%), and High (> 0.20%).

The fine and coarse aggregates purchased from quarries were very moist and had to be dried. The aggregates were placed in a thin layer on plastic bags on the laboratory floor and it took approximately 48 hours to dry at room temperature of about 22^{o}C (See Figure 5.2).

Figure 5.2 - Drying of Fine Aggregates at Room Temperature

5.3.1 Fine Aggregate

Fine aggregate was orange colored siliceous sand with a relatively high ASR Rating of 0.23. The 1/2 ton of sand was purchased from an Aggregate Industries quarry in Brandywine, Maryland which is located in the southern part of Prince George's County. Sieve Analysis and Physical Properties are shown in Figures 5.3 and 5.4. Williams concludes that fine aggregates with higher ASR ratings are more susceptible to DEF related expansion (Amde et al. 2004b).

ASTM C-33 CONCRETE SAND SIEVE ANALYSIS

Sieve Size (INCHES)	Sieve Size (metric)	% Passing	Specification A.S.T.M. C33	MARYLAND TABLE 901-A
3 / 8"	9.5 mm	100 %	100 %	100%
#4	4.75 mm	99 %	95 – 100 %	95-100%
#8	2.36 mm	83 %	80 – 100 %	-
#16	1.18 mm	64%	50 – 85 %	45-80
#30	600 micro	44 %	25 – 60 %	-
#50	300 micro	17 %	5 – 30 %	10-30
#100	150 micro	3 %	0 – 10 %	2-10
#200	75 micro	0.9 %	0 – 3 %	

LOOSE WEIGHT-98.6 LBS/CU.FOOT
RODDED WEIGHT-105.9 LBS/CU.FOOT

Figure 5.3 - Fine Aggregate Sieve Analysis

DELETERIOUS SUBSTANCES

Test	Result	Specification
Clay Lumps / Friable Particles	0.2 %	0 – 0.5 %
Coal and Lignite	0.02	0 – 0.5 %
Organic Impurities	Plate #1	Plates #1 - #3

PHYSICAL PROPERTY REQUIREMENTS

Test	Result	Specification
Fineness Modulus	2.90	2.3 – 3.1
Bulk Specific Gravity (SSD)AASHTO T 84	2.63	N / A
Soundness AASHTO T 104	0.8 %	0 – 10 %
Absorption	0.5 %	N / A
ASTM D-2487	Identification	SW

RESULTS OF TEST METHOD FOR POTENTIAL ALKALI REACTIVITY OF AGGREGATES

Recent Test Results------November 16, 2002 o

Mortar bar Expansion
MSMT 212 ----ASTM C 1260
NewCem Slag

Source of sand	Type I/II Cement %	New Cem %	7-Day Expansion --------- %				14-Day Expansion ------- %			
			A	B	C	Avg.	A	B	C	Avg. +
Brandywine	70	30	0.041	0.038	0.037	0.04	0.080	0.074	0.070	0.08
	50	50	0.006	0.006	0.007	0.01	0.015	0.017	0.016	0.02

+ Concrete Sand is innocuous with 30% and 50% Cement replacement with Slag

Figure 5.4 - Fine Aggregate Physical Properties and Alkali Reactivity of Aggregate

5.3.2 Coarse Aggregate

Coarse aggregate consisted of No. 57 limestone with a low ASR Rating of 0.07 and maximum aggregate size of 1". Approximately 3/4 ton of aggregate was purchased from a Lafarge quarry in Frederick, Maryland. Sieve Analysis and Physical Properties are shown in Figure 5.5.

SIEVE SIZE	1 1/2"	1"	3/4"	1/2"	3/8"	#4	#8
Frederick #57 Stone % Passing	100.0	100.0	93.5	39.1	15.3	3.7	1.2
MSHA/ASTM/AASHTO Specifications	100	95-100	--	25-60	--	0-10	0-5

ASTM C 127 Specific Gravity, BSSD	-	2.75
ASTM C 127 Absorption Percent	-	0.3
ASTM C 29 Void Content	-	44.1%
ASTM C 29 Unit Wt., Dry Rodded	-	95.7#/C.F., 1.29(tons/cy)
AASHTO T104 Soundness, % Loss	-	1.8%
ASTM C 131 Los Angeles Abrasion	-	19% wear
ASTM C 289 Potential Reactivity	-	Innocuous
ASTM C 227 Alkali Reactivity	-	0.019 @ 6 Months (Innocuous)
ASTM C 586 Alkali Carbonate Reactivity	-	-0.03% @ 16 Weeks (Innocuous)
MSMT 212 Alkali Reactivity, rapid test	-	0.07% expansion (Innocuous)by MD SHA
ASTM C142 Clay Lumps & Friable Particles		0%
ASTM C117 -200 by Wash	-	1.5%
MSMT 203 Flat and Elongated Pieces	-	4.2% (5 to 1 Ratio)
ASTM C123 Light Weight Pieces	-	None
AASHTO T 260 Total Chloride	-	1 ppm

ASTM C33 Type 5S
MOHs Hardness = 4.0

Figure 5.5 - Coarse Aggregate Sieve Analysis & Physical Properties

5.3.3 Type III Cement

Eight 94-lb bags of Lehigh Type III Cement were purchased from a local supplier. All bags were from the same batch produced in Allentown, Pennsylvania. A small sample of the cement was sent to CTL Group in Skokie, Illinois for an x-ray fluorescence (XRF) spectroscopy. A spectroscopy result indicated the potassium

content of the cement to be 0.57% (K_2O) and was eventually increased to 1.5% by the use of potassium carbonate admixture. See Table 5.2 for XRF Spectroscopy Results.

Table 5.2 - X-Ray Fluorescence Spectroscopy Results for Type III Cement

Report of Chemical Analysis Type III Cement	
Analyte	Weight %
SiO_2	19.09
Al_2O_3	4.71
Fe_2O_3	3.34
CaO	61.97
MgO	3.47
SO_3	3.42
Na_2O	0.14
K_2O	0.57
TiO_2	0.27
P_2O_5	0.12
Mn_2O_3	0.32
SrO	0.04
Cr_2O_3	0.03
ZnO	0.11
L.O.I. (950^oC)	2.44
Total	100.04
Compounds per ASTM C150-04a	
C_3S	61
C_2S	9
C_3A	7
C_4AF	10

5.3.4 Potassium Carbonate

Ramadan (2000) and Ceesay (2004) concluded that increasing the potassium content has a detrimental effect on concrete expansion resulting in premature loss of compressive strength and concrete deterioration. Anhydrous granular reagent grade potassium carbonate (K_2CO_3) was dissolved in the mixing water of the concrete mix to raise the potassium content of the concrete mixture from 0.57% to 1.5% by weight of cement. The K_2CO_3 was dissolved in the batch water prior to the water being poured into the mixer. It was calculated that 1.167 grams of K_2CO_3 per 100 grams of cement was necessary to increase the potassium content to 1.5% (See Figure 5.6).

5.3.5 Molds

PVC cylinder molds with lids were 4" diameter by 8" tall and complied with ASTM C192 and ASTM C470. A total of 117 single-use molds were used in the project (9 sets x 13 cylinders per set = 117 total molds). Cylinders were used to determine the compressive strength of the concrete at set intervals.

Reusable steel molds measuring 3" x 3" x 11.25" were used to cast the concrete prisms. The end plates of the molds had inserts for steel gauge studs used for length change measurements per ASTM C490-86. The gage studs were placed in the molds using a 10" long steel gage bar per ASTM C490 (see Figure 5.7) and the molds were lightly coated with form release prior to casting. A total of 27 molds were used three times to cast 81 prisms (9 sets x 9 cylinders per set = 81 total molds). Prisms were used to monitor weight and length changes and for SEM analysis.

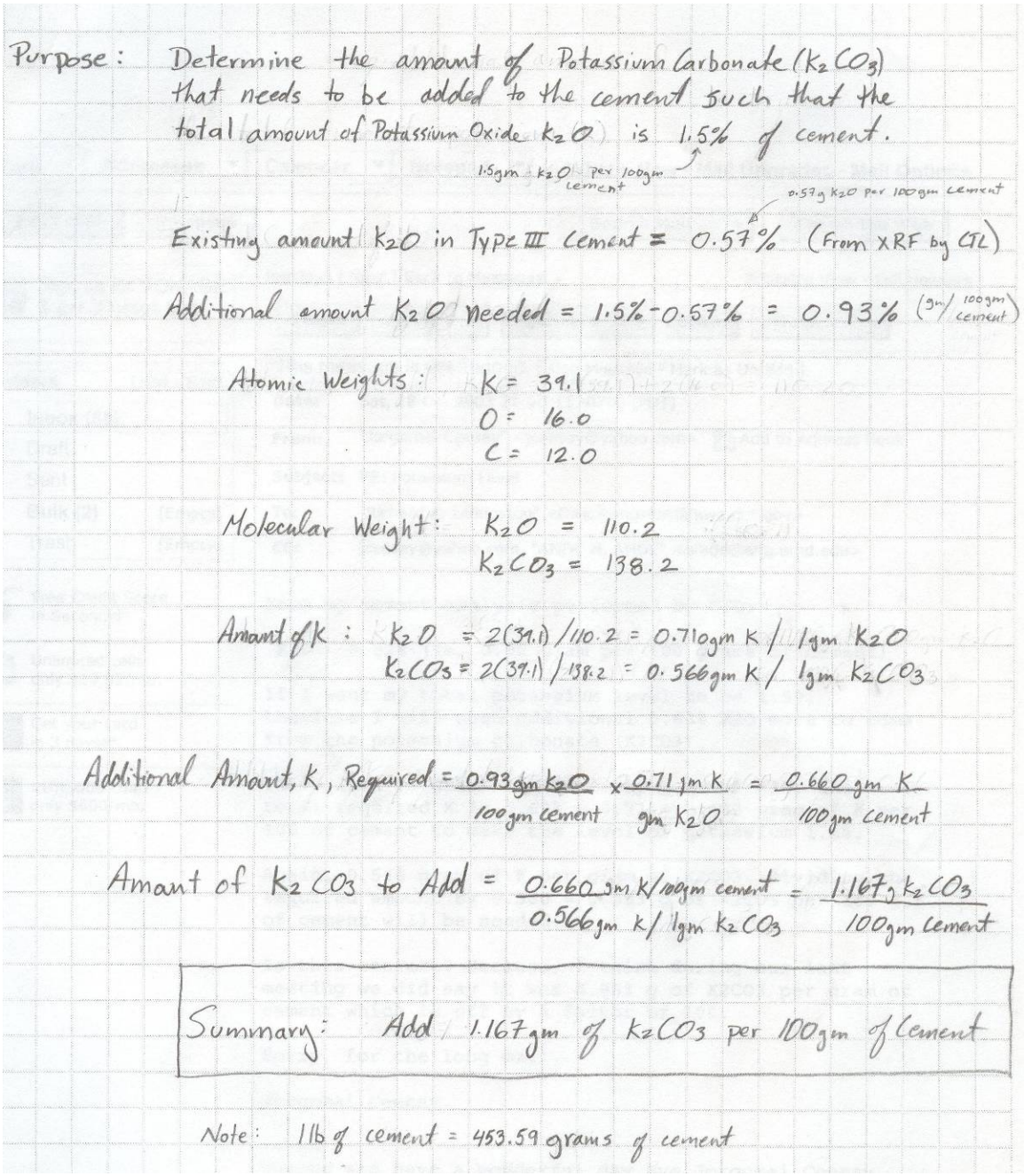

Figure 5.6 - Potassium Carbonate Addition Calculation

Figure 5.7 - Steel Prism Mold with Studs and 10" Long Steel Gage

5.4 Casting

Nine sets of prisms and cylinders were cast over a course of three days (i.e., 3 sets per day) following ASTM C192. See Figure 5.8 for casting schedule. A total of 81 prisms and 127 cylinders were cast and cured for this research project utilizing the mix design described in Section 5.2. Casting began with the proportioning of aggregates, cement, and water in 5-gallon plastic buckets on a 200-lb capacity mechanical scale (see Figure 5.9). The potassium carbonate was measured on digital metric scale and dissolved in the water. One set of prism and cylinder molds were arranged on the floor along with 3/8" diameter steel tamping rods and rubber mallets (see Figure 5.10). Vibrators were not used in casting of the prisms and cylinders. The materials were mixed in a 3.0 cubic foot capacity rotating mixer in accordance

with machine mixing procedure outlined in ASTM C192M. A digital stop watch was used to keep track of the mixing and resting cycles (See Figure 5.11).

Once the batch was mixed it was poured into a moistened wheel barrow and rolled into lab. The cylinder molds were prepared in two layers with rodding and tapping after each layer. Each layer was rodded 25 times and tapped lightly with rubber mallet 15 times. The prisms were also prepared in two layers except they were rodded 34 times (See Figure 5.12). ASTM requires prism molds to be rodded one time for each square inch of surface area (i.e., 3" x 11.25" = 33.75 sq. in. = 34 strokes). After the specimens were filled, the tops of the molds were struck off with a trowel. PVC lids were placed on the cylinder molds and the steel molds were wrapped in aluminum foil to prevent shrinkage.

Since three sets were cast on the same day the cylinder molds and aluminum foils were marked 1, 2, or 3. The markings not only prevented the prisms and cylinders from being mixed together but also made certain the testing would not be compromised. Although the same mix design was used for all nine sets there is still some variability due to moisture content of the aggregates and the amount of water in the mixer.

	Sets #1, 2, & 3	Sets #4, 5, & 6	Sets #7, 8, & 9
Saturday, September 10, 2005	Cast specimens & cure in oven		
Sunday, September 11, 2005	Demold & place in bath		
Monday, September 12, 2005	Bath Day 1		
Tuesday, September 13, 2005	Bath Day 2		
Wednesday, September 14, 2005	Bath Day 3		
Thursday, September 15, 2005	Bath Day 4		
Friday, September 16, 2005	Bath Day 5		
Saturday, September 17, 2005	Bath Day 6	Cast specimens & cure in oven	
Sunday, September 18, 2005	Bath Day 7	Demold & place in bath	
Monday, September 19, 2005	Bath Day 8 & Start Duggan Day 1	Bath Day 1	
Tuesday, September 20, 2005	Duggan Day 2	Bath Day 2	
Wednesday, September 21, 2005	Duggan Day 3	Bath Day 3	
Thursday, September 22, 2005	Duggan Day 4	Bath Day 4	
Friday, September 23, 2005	Duggan Day 5	Bath Day 5	
Saturday, September 24, 2005	Duggan Day 6	Bath Day 6	
Sunday, September 25, 2005	Duggan Day 7	Bath Day 7	
Monday, September 26, 2005	Cooling Day 1	Bath Day 8 & Start Duggan Day 1	
Tuesday, September 27, 2005	Cooling Day 2	Duggan Day 2	Cast specimens & cure in oven
Wednesday, September 28, 2005	*Transfer to NRMCA*	Duggan Day 3	Demold & place in bath
Thursday, September 29, 2005		Duggan Day 4	Bath Day 1
Friday, September 30, 2005		Duggan Day 5	Bath Day 2
Saturday, October 01, 2005		Duggan Day 6	Bath Day 3
Sunday, October 02, 2005		Duggan Day 7	Bath Day 4
Monday, October 03, 2005		Cooling Day 1	Bath Day 5
Tuesday, October 04, 2005		Cooling Day 2	Bath Day 6
Wednesday, October 05, 2005		*Transfer to NRMCA*	Bath Day 7
Thursday, October 06, 2005			Bath Day 8 & Start Duggan Day 1
Friday, October 07, 2005			Duggan Day 2
Saturday, October 08, 2005			Duggan Day 3
Sunday, October 09, 2005			Duggan Day 4
Monday, October 10, 2005			Duggan Day 5
Tuesday, October 11, 2005			Duggan Day 6
Wednesday, October 12, 2005			Duggan Day 7
Thursday, October 13, 2005			Cooling Day 1
Friday, October 14, 2005			Cooling Day 2
Saturday, October 15, 2005			*Transfer to NRMCA*

Figure 5.8 - Casting, Curing, and Duggan Cycle Schedule

Figure 5.9 - Proportioned Mix Design for One Set in 5-Gallon Buckets

Figure 5.10 - Cylinder and Prism Molds with Tamping Rods and Rubber Mallets Arranged on the Floor in Preparation for Casting

Figure 5.11 - Concrete Mixer with Wheel Barrel at UMD Structural Lab

Figure 5.12 - Casting of Concrete Prisms with Tamping Rod and Rubber Mallet

5.5 Curing

All nine sets of concrete were steam cured immediately following casting in one of two ovens. The 27-prisms were cured in a conventional oven and the 39-cylinders were cured in a temperature chamber. Due to the limited space, the cylinders and prisms were cured in different ovens (see Figures 5.13 & 5.14). Steam curing was simulated by setting each oven to a temperature of 85^{o}C and placing bowls of water on the racks. The steam curing lasted for 24 hours $\pm$ 4 hours, then the specimens were removed from the ovens and demolded. After demolding the specimens were allowed to cool for two hours before being stored in a lime water bath for eight days of water curing.

Figure 5.13 - Steam Curing of Cylinder Molds at 85^{o}C in Temperature Chamber

Figure 5.14 - Steam Curing of Prism Molds at 85^{o}C in Conventional Oven

5.6 Storage Conditions

All specimens were permanently stored (i.e., fully submerged) in lime water after the completion of the Duggan Cycle. Lime water bath was also used for the eight days of water curing and during the Duggan Cycle (see Figure 5.15). Hydrated lime, purchased from a local nursery, was dissolved with plain water in large 39-gallon tubs to produce a high pH solution. Hydrated lime is known chemically as calcium hydroxide or $Ca(OH)_2$ and comes in the form of a white powder. ASTM C511 dictates the use of lime water instead of plain water to prevent leaching of calcium hydroxide from the specimens.

Figure 5.15 - Concrete Specimens Stored in 39-Gallon Tubs Filled with a Mixture of Plain Water and Calcium Hydroxide

5.7 UMD/FHWA Modified Duggan Cycle

The UMD/FHWA Modified Duggan Cycle was applied to all nine sets of specimens after curing in a lime water bath for eight days. The main objective of the UMD/FHWA Duggan Cycle is to accelerate subsequent expansion of the concrete and the growth of ettringite.

The Duggan Cycle was originally developed to measure the potential for alkali-silica susceptibility of concrete. Later research performed at UMD/FHWA transformed the test into a method to relate concrete expansion to ettringite growth. The original test consisted of measuring the expansion of cores over a course of 20 days. Prior to the expansion measurements the cores were put through a 10-day heating and cooling cycle. Duggan suggested that any expansion over 0.05% in the first 20 twenty days should be of concern and the concrete mix design should be altered (Duggan 1987 & 1989).

5.7.1 Duggan Cycle Sample Preparation

Duggan suggested that test samples consist of cylindrical cores, approximately 1" diameter x 2" long, drilled from larger concrete specimens. The ends of the cores should be polished smooth and parallel. After the cores are placed through a heating and cooling cycle, expansion measurements are made. Initial length readings are recorded prior to the heating and cooling cycle.

For this project the UMD/FHWA modified Duggan Sample Preparation method was utilized. The 1" x 2" cylindrical cores were substituted with 3" x 3" x 11.25" concrete prisms with gage studs. The studs were used to measure the length change specified under ASTM C490. The initial length reading was performed after

the completion of the Duggan cycle and prior to permanent storage. This was done because the expansion measurements for this project were to be recorded over several months instead of the 20 days suggested by Duggan.

5.7.2 UMD/FHWA Modified Duggan Cycle

The UMD/FHWA Modified Duggan Cycle is a nine-day heating and cooling regimen performed on concrete specimens after curing in a lime water bath. The regimen consists of three cycles with a heating temperature of eighty-two degrees Celsius and a cooling temperature of twenty-two degrees Celsius (room temperature). The first two cycles are similar and subject the specimens to 24 hours (1 day) of heating, 2 hours of air cooling and 22 hours of water cooling. The third cycle subjects the specimens to 72 hours (3 days) of heating followed by 48 hours (2 days) of air cooling (See Figure 5.16). After the second day of air cooling, initial length measurements are taken and the specimens are permanently stored in a lime water bath. Subsequent length change measurements are recorded at 3 to 5-day intervals for the first 180 days and once a week thereafter.

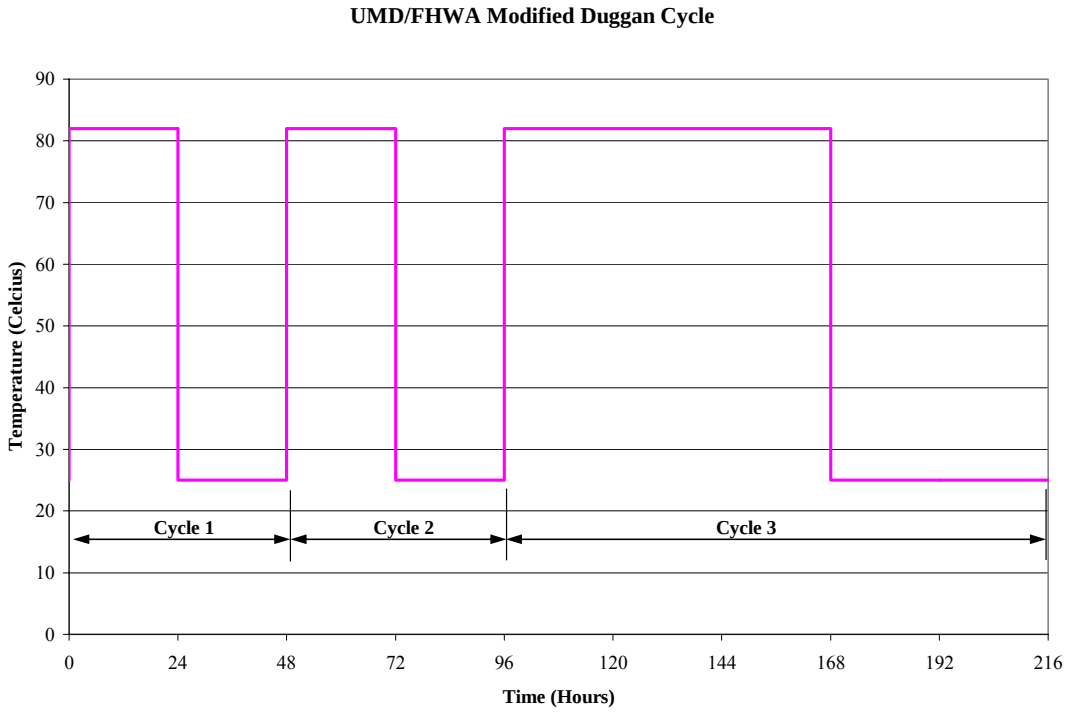

Figure 5.16 - UMD/FHWA Modified Duggan Cycle

5.8 Tests and Test Frequency

Four tests were performed on all concrete specimens during this research to chart the effectiveness of the mitigation products. The fours tests included (1) length change measurements, (2) weight change measurements, (3) compressive strength tests, and (4) Scanning Electron Microscope (SEM) Spectrometry tests. The first three tests were performed at the National Ready Mix Concrete Association (NRMCA) Laboratory in Greenbelt, Maryland. The SEM Spectrometry was performed at the Federal Highway (FHWA) Turner-Fairbank Highway Research Center (TFHRC) located in McLean, Virginia. Length and weight change measurements were performed simultaneously. Similarly, compressive test and SEM spectrometry were performed concurrently.

5.8.1 Expansion Test

Expansion or length change measurements were performed in accordance to ASTM C490 utilizing a comparator with a digital display accurate to $\pm$ 0.0001 inches. (see Figure 5.17). Initial length measurements were made after the completion of the Duggan Cycle and prior to permanent storage in lime water. Measurements for five of the nine prisms in each set were recorded at 3 to 5-day intervals for the first 180 days and once a week thereafter. The remaining four prisms were used for SEM analysis (see Table 5.3). Length change measurements were made relative to a 10" long invar bar and concrete specimens were surface dried with paper towels prior to placing in the comparator. For statistical precision the average of the five measurements was calculated and used in the graphs. Length change was calculated as follows:

$$\text{Length Change (\%)} = [(La - Li)/G] \times 100\%$$

Where:

La = comparator reading of specimen at the age of measurement (in)

Li = initial comparator reading after completion of Duggan Cycle (in)

G = gage length = 10 inches

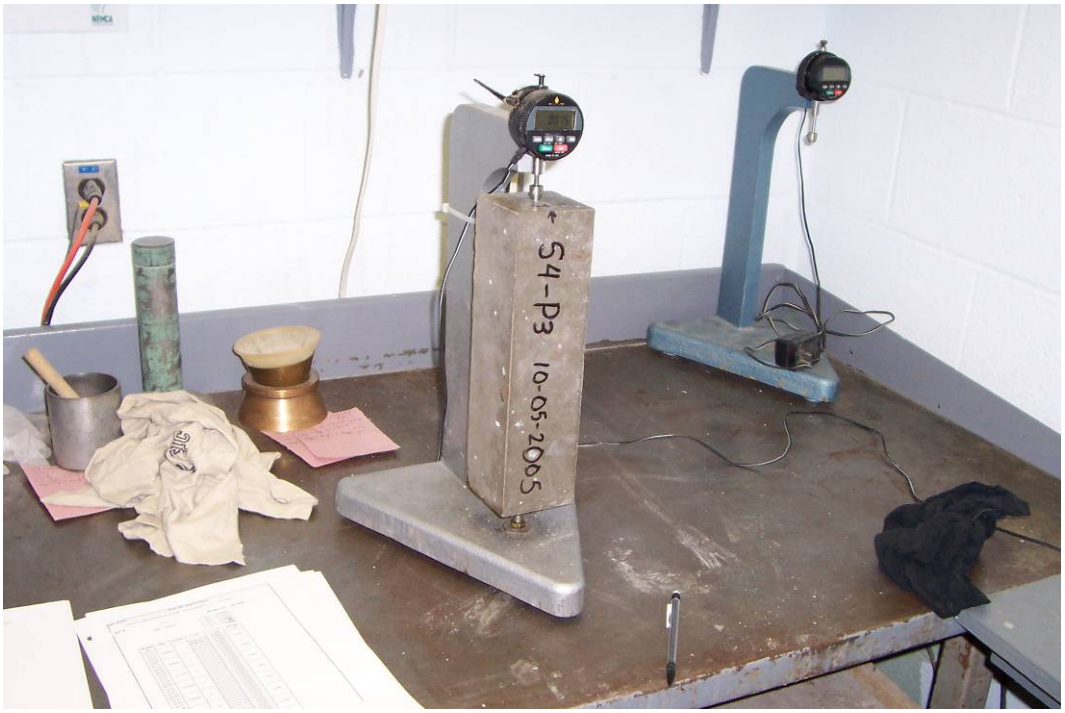

Figure 5.17 - Length Change Measurement Device (Comparator)

Table 5.3 - Concrete Specimens Stored in Lime Water

PRISMS		
1	Weight and Expansion	Treated
2	Weight and Expansion	Treated
3	Weight and Expansion	Treated
4	Weight and Expansion	Treated
5	Weight and Expansion	Treated
6	30 day SEM	No Treatment
7	90 day SEM	Treated
8	240 day SEM	Treated
9	2 year SEM	Treated

5.8.2 Weight Change Measurements

Ceesay (2004) and Ramadan (2000) concluded that an increase in expansion is linearly correlated to an increase in the weight of the specimens. The specimens in this research were also weighed on a digital scale with ± 0.1 gram accuracy (See Figure 5.18). Weight change measurements were performed concurrently with length measurements and on the same five prisms. Likewise, the initial weight was recorded after the completion of the Duggan Cycle and just prior to permanent storage in lime water. The average weight change of the five prisms was calculated and plotted in the graphs. Weight change was calculated as follows:

$$\text{Weight Change (\%)} = [(W - Wi)/Wi] \times 100\%$$

Where: W = weight of specimen at the age of measurement

Wi = initial weight after completion of Duggan Cycle

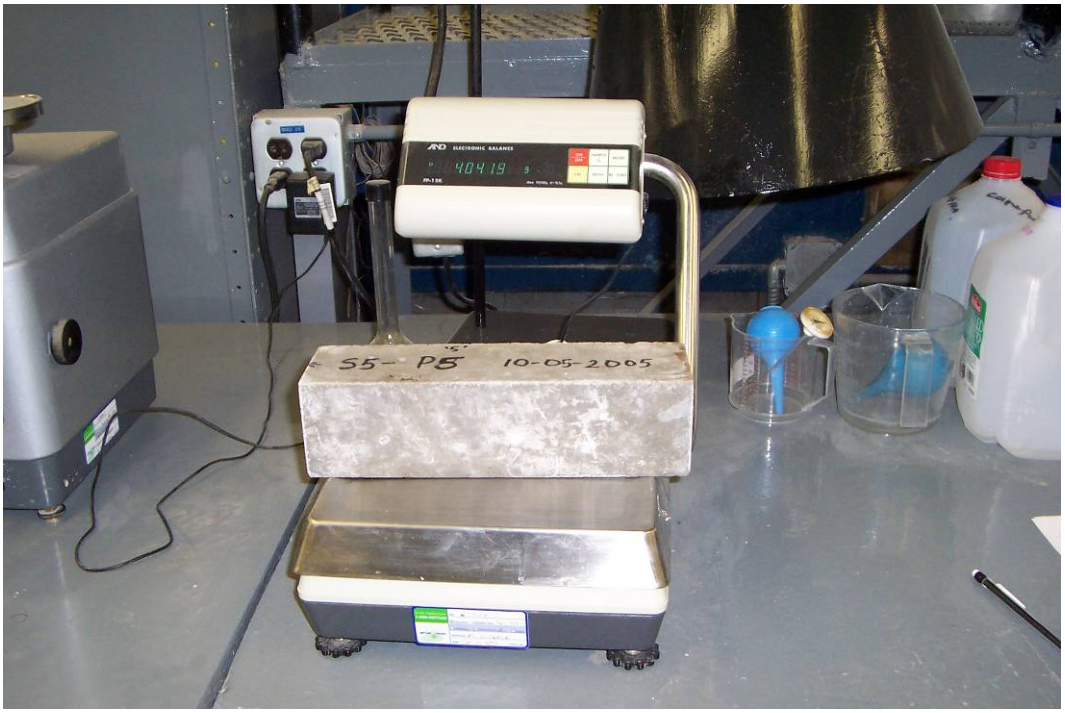

Figure 5.18 - Weight Change Measurement Scale

5.8.3 Compression Test

Compressive strength was performed in accordance with ASTM C39 (4" x 8" cylinders) utilizing a 300,000-pound capacity hydraulic machine with digital controls (see Figure 5.19). Specimens were initially surface dried with paper towels and tested at a load rate of 25,000 lb/min. Three specimens per set were tested at 30 days (± 2 days), 90 days (± 2 days), and 240 days (± 2 days). The remaining four specimens can be tested in the future (see Table 5.4). The average compressive strength of the three cylinders was calculated and plotted in the graphs.

Figure 5.19 - Compression Strength Test Machine

Table 5.4 - Cylinder Testing per Set

CYLINDERS		
1	30-day compression	No Treatment
2	30-day compression	No Treatment
3	30-day compression	No Treatment
4	90-day compression	Treated
5	90-day compression	Treated
6	90-day compression	Treated
7	240-day compression	Treated
8	240-day compression	Treated
9	240-day compression	Treated
10	2-year compression	Treated
11	2-year compression	Treated
12	2-year compression	Treated
13	Extra	Treated

5.8.4 Scanning Electron Microscope (SEM) Spectrometry

The existence of ettringite was verified with the use of a scanning electron microscope with an energy dispersive analysis x-ray (EDAX) (see Figure 5.20). The electron microscope works by directing a beam of accelerated electrons with 10 to 20 kilovolt of energy at the concrete sample. After striking the sample the electrons scatter into three distinct signals known as secondary electrons, backscattered electrons, and x-rays. The secondary and back scattered electrons are used to create a three-dimensional image of the sample. The images produced by the SEM can be small as 100nm. The x-ray analyzer (EDAX) is used to determine the energy spectrum of the scattered x-rays. Each element emits a distinct energy spectrum which is compared to a database of known elements allowing for positive

identification of ettringite. Furthermore, the identified elements are quantified by percentage of weight and printed in a table by the EDAX ZAF database.

Figure 5.20 - Scanning Electron Microscope at TFHRC

The identification and quantification of ettringite is solely dependent on the quality of the concrete sample. In 1995, Stella Marusin published a paper comparing various methods of SEM sample preparation methods. These methods included thin sections, sawn polished sections, sawn unpolished sections, and fractured sections. Marusin (1995) concluded that fractured surfaces work best for investigating DEF.

For this research project fractured samples were produced from 3" x 3" x 11.25" concrete prisms at given intervals and from all nine sets (see Table 5.3). The prisms were wrapped in plastic and fractured with a hammer to produce samples

approximately 1 to 1.5 cm in diameter. A high-quality sample is flat, rough and preferably dislodged from an aggregate and cement paste interface. Two samples were produced from each prism: (1) Exterior section of the prism and (2) interior section of the prism. The samples are glued to carbon stubs with carbon paint and dried in a vacuum oven at 55^{o}C for approximately fifteen minutes (see Figure 5.21). Once dried, the carbon stubs placed in a carbon coating machine. The carbon coating is applied with a Hummer 10.2 Sputtering System with a CEA 2.2 carbon evaporation accessory (see Figure 5.22). The purpose of the carbon coating is to insure electrical conductivity and to prevent charging effects in the microscope. After carbon coating, the sample, is ready to be analyzed in the scanning electron microscope.

Figure 5.21 - Vacuum Oven Used to Dry Concrete Samples Carbon Glued To Carbon Stubs Placed Inside Corks

Figure 5.22 - Carbon Coating Machine

Chapter 6: Test Data Presentation

6.1 Expansion Results

Five 3" x 3" x 11.25" concrete prisms per set were used for expansion and weight change measurements. Each point on the graphs represents the average of the five expansion measurements. The standard deviation of the five measurements was calculated for each data point and plotted as the vertical error bars. Measurements were recorded 3-5 day intervals for the first 180 days then once a week thereafter for a total of 300 days. Linear regression analysis was performed on the expansion measurements and plotted on a graph. The rate of expansion (first derivative) was calculated and curves were developed. A linear relationship was developed between the standard deviation and average expansion to determine the coefficient of variance (COV). A total of four graphs were developed for each set and are described as follows:

- Graph 1 – Expansion versus Time with Error Bars (Standard Deviation)
- Graph 2 – Rate of Expansion versus Time (First Derivative)
- Graph 3 – Linear Regression Analysis Graph (Best Fit Lines)
- Graph 4 – Standard Deviation versus Expansion (COV)

Expansion test results are described per groups of three sets in Sections 6.1.1 to 6.1.3. Results of all nine sets are summarized in Section 6.1.4. Overall, five sets experienced smaller expansion than the Control prisms (Set No. 1). Three of the five sets were treated with Good-Rite K752 alone and in combination with ChimneySaver or Radcon Formula #7 (Set Nos. 7, 8, & 9). The remaining two were treated with ChimneySaver (Set No. 2) and Dequest 2060S (Set No. 4). However, the standard

deviation was high in these sets due to variation in the expansion measurements. Linear regression analysis or best-fit-lines were developed for the expansion graphs. Each graph had three best-fit-lines: 1) initial expansion (~100 days), 2) middle portion with heavy expansion (~150 days), 3) plateau of the expansion (~50 days). Though not true for all sets, the general trend between the slope of the middle section and the maximum expansion seems to indicate that the steeper the slope of the middle section results in greater expansion. This trend can be seen in Table 6.4 by comparing the rankings of the maximum expansion and the slope of the middle section best-fit-line. The maximum expansion was reached in the third section or the plateau.

Livingston (2006) has proposed that correlation between the standard deviation and the expansion data indicates heterscedascity and a sign of uniform volumetric expansion. The slope of the best-fit-line on the standard deviation versus expansion graph is the ratio of the standard deviation to the mean which is known as the coefficient of variation (COV).

6.1.1 Control & Water Repellents (Set Nos. 1 – 3)

Expansion graphs for Set Nos. 1, 2, and 3 are shown in Figures 6.1 to 6.12. The Control prisms (Set No. 1) experienced a maximum average expansion of 2.18% with a maximum rate of expansion of 0.0161 %/day on day 127. The ChimneySaver (Set No. 2) reached a maximum average expansion of 1.68% with a maximum rate of expansion of 0.0152 %/day on day 127. Radcon Formula #7 (Set No. 3) reached a maximum expansion of 2.27% on Day 236 and a maximum expansion rate of 0.0192 %/day on Day 127. Radcon Formula #7 expansion measurements were discontinued

after 236 days because two of the five prisms expanded so much that they could no longer be measured in the length measurement device (comparator). The average of the three remaining prisms skewed the expansion results lower and thus were ignored. Length change measurements were taken for the remaining eight sets for all 300 days. The rate of expansion for all three sets never reached a true asymptote. However, the last rate of expansion (Day 300) for Set Nos. 1 and 3 were 0.0005 in/day and 0.0003 in/day respectively which is approximately zero (0). Note that the error bars for Set Nos. 2 and 3 intersect the Control error bars. Also note that the standard deviation for Set No. 2 is quite large indicating that the expansion in the five prisms varied greatly. The Rates of Expansion are summarized in Table 6.2.

The regression analysis reveals a linear correlation between expansion and time with regression coefficients (R^2) generally greater than 0.90. The linear regression analysis reveals that initially expansion is slow. Then the lines increase with varying slopes for up to 160 days and eventually plateau though not totally horizontally. Note that treatment was applied at approximately 45 days. The slope of the middle best-fit-line seems to correlate to the severity of the concrete expansion. For example, the maximum expansion from highest to lowest is Set Nos. 3, 1, and 2 with expansion of 2.27%, 2.18%, and 1.68% respectively. The slope of the middle best-fit-line correlates to the Set Nos. 3, 1, and 2 with 0.0136, 0.0107, and 0.0091 respectively. The Linear Regression Analysis is summarized in Table 6.1.

The regression analysis reveals that there is a linear correlation between standard deviation and expansion measurements for a limited period of time. The slope of the best-fit-line is known as the coefficient of variation (COV). The COV of

the Control prisms (Set No. 1) is 0.2148 in^{-1} with a regression coefficient of 0.9965. The linear relationship terminates on day 115 with an expansion value of 0.7222%. The coefficient of variance, termination days and expansion value are similar. The COV of the Radcon Formula #7 (Set No. 3) is 0.2076 in^{-1} with a regression coefficient of 0.9869. The linear relationship terminates on day 119 with an expansion value of 0.7702%. In contrast, the COV for ChimneySaver (Set No. 2) prisms is twice as high as the Control at 0.4089 in^{-1}. Unlike Set Nos. 1 and 2 the linear relationship lasts up to Day 264 and an expansion value of 1.6476%. The Coefficients of Variance are summarized in Table 6.3.

6.1.2 Dequest 2060S (Set Nos. 4 – 6)

Expansion graphs for Set Nos. 4, 5, and 6 are shown in Figures 6.13 to 6.24. Out of these three sets the prisms treated with Dequest 2060S (Set No. 4) was the only set to exhibit a smaller expansion than the Control (Set No. 1). Dequest 2060S (Set No. 4) experienced a maximum expansion of 1.82% with a maximum expansion rate of 0.0160 %/day on Day 160. Prisms treated with Dequest 2060S and ChimneySaver (Set No. 5) experienced the worst expansion of 2.36% and the maximum expansion rate of 0.0214 %/day on Day 160. Prisms treated with Dequest 2060S and Radcon Formula #7 (Set No. 6) reached a maximum expansion of 2.24% and experienced the highest rate of expansion of 0.0225 %/day on Day 160. The rate of expansion on Day 300 for Set Nos. 4, 5, and 6 were 0.0013 %/day, 0.0012 %/day and 0.0019 %/day respectively. The rate of expansion for Set Nos. 4, 5, and 6 never reached a true asymptote and it seems that the expansion continues indefinitely. Note that the error bars for Set Nos. 4, 5, and 6 intersect the Control (Set No. 1) error bars

indicating no distinguishable difference in the expansion between the treated prisms and the untreated prisms. The Rates of Expansion are summarized in Table 6.2.

The regression analysis reveals a linear correlation between expansion and time with regression coefficients (R^2) generally greater than 0.98 for the middle best-fit-line. The steeper the slope of the middle best-fit-line indicates the greater propensity for expansion. The maximum expansion from highest to lowest are Set Nos. 5, 6, and 4 with expansions of 2.36%, 2.24% and 1.82% respectively. The slope of the middle best-fit-line correlates to 0.0140 %/day, 0.0141 %/day and 0.0108 %/day. Note the significant difference in expansion as well as slopes of the middle best-fit-line between Set Nos. 4 and 5 and the control Set No. 1. The Linear Regression Analysis is summarized in Table 6.1.

The regression analysis reveals that there is a linear correlation between standard deviation and expansion measurements of Set Nos. 4, 5, and 6 for a limited period of time. Although the range of the linear relationship is between Days 18 and 144 and the expansion values are generally around 0.66% for all three sets the COVs vary significantly. The COV for Set Nos. 4, 5, and 6 are 0.5545 in^{-1}, 0.2655 in^{-1}, and 0.4092 in^{-1}. The range and expansion values are higher than the Control (Set No. 1) values. The COV for Set No. 5 is very close to the Control (Set No.1-0.2148 in^{-1}) however the COVs of Set Nos. 4 and 6 are twice as high. Coefficients of Variation (COV) are summarized in Table 6.3.

6.1.3 Good-Rite K-752 (Set Nos. 7 – 9)

Expansion graphs for Set Nos. 7, 8, and 9 are shown in Figures 6.25 to 6.36. The expansions of all three Good-Rite K752 sets were lower than the Control (Set

No. 1). However, the rates of expansion in the three sets were still higher than the Control. The error bars on these three sets do not intersect as much as the five other treated sets indicating that Good-Rite K752 was somewhat successful at reducing expansion in the prisms. The combination of Good-Rite K752 with ChimneySaver (Set No. 8) yielded the lowest expansion at 1.68% and had a maximum expansion rate of 0.0198 %/day on Day 130. The next highest was the combination of Good-Rite K752 with Radcon Formula #7 (Set No. 9) which yielded an expansion of 1.81% with a maximum expansion rate of 0.0180 %/day on Day 150. The Good-Rite K752 (Set No. 7) reached a maximum average expansion of 1.86% with an expansion rate of 0.0180 %/day. The rates of expansion on Day 300 for Set Nos. 7, 8, and 9 were 0.0022 %/day, 0.0022 %/day and 0.0020 %/day respectively. The rates of expansion never reached true asymptotes and it seems that the expansion continues indefinitely. The Rates of Expansion are summarized in Table 6.2.

The regression analysis reveals a linear correlation between expansion and time with regression coefficients (R^2) exceeding 0.99 for the middle best-fit-line. Trends in the previous six sets indicate that the steeper the slope of the middle best-fit-line the greater propensity for expansion. This trend is only true for Set Nos. 8 & 9. The maximum expansion from highest to lowest is Set Nos. 7, 9, and 8 with expansions of 1.86%, 1.81% and 1.68% respectively. However, the slope of the middle best-fit-line from highest to lowest is Set Nos. 9, 7, and 8 with 0.0116 %/day, 0.0107 %/day, and 0.0102 %/day. Set No. 7 has the highest expansion but only the second highest slope. The slopes are approximately close to the Control (Set No. 1 – 0.0107) and the difference between the highest and lowest slopes is only 0.0014

in/day. The differences are not negligible however a broad correlation between the maximum expansion and slope of the regression can still be made. The Linear Regression Analysis is summarized in Table 6.1.

The regression analysis reveals that there exists a linear correlation between standard deviation and expansion measurements of Set Nos. 7, 8, and 9. The COV for Set Nos. 7, 8, and 9 do not vary as much as the other treated sets. The range of the linear relationship is between 14 and 158 days and the expansion values are approximately 0.85%. The COV for Set Nos. 7, 8, and 9 are 0.2373 in^{-1}, 0.2148 in^{-1} and 0.1873 in^{-1} which are approximate to the Control VOC of 0.2148. The Coefficients of Variance are summarized in Table 6.3.

6.1.4 Summary of Expansion Results

Table 6.1 summarizes the linear regression analyses performed on the expansion measurements with respect to time. Table 6.2 summarizes the maximum expansion rate and the final expansion rate at Day 300. Table 6.3 summarizes the linear regression analysis of the expansion versus standard deviation graphs. The Coefficient of Variation value is equal to the slope of the best-fit-line. Table 6.4 summarizes the maximum expansion, rate of expansion, slope of best-fit-line, and COV values with corresponding rankings (from highest to lowest). Note that the ChimneySaver (Set No. 2) had the lowest maximum expansion, maximum rate of expansion, and slope of the best-fit-line. Figure 6.37 summarizes the expansion versus time curves for all nine sets.

6.2 Weight Change Results

Five 3" x 3" x 11.25" concrete prisms per set were used for weight change and expansion measurements. Each point on the graphs represents the average of the five weight change measurements. The standard deviation of the five measurements was calculated for each data point and plotted as the vertical error bars. Measurements were recorded twice at 3 to 5-day intervals for the first 180 days then once a week thereafter for a total of 300 days. Linear regression analysis was performed on the measurements and plotted on a graph. The rate of weight change (first derivative) was calculated and curves were developed. The maximum rate of weight change was achieved on the second set (Day 4) of measurements. This was due to the fact that prisms were initially dry when placed in the storage solution. A linear relationship was developed between weight change and expansion. A total of three graphs were developed for each set and are described as follows:

- Graph 1 – Linear Regression Analysis Graph with Error Bars (Best Fit Lines)
- Graph 2 – Rate of Change versus Time (First Derivative)
- Graph 3 – Weight Change versus Expansion

Weight change results are described per groups of three sets in Sections 6.2.1 to 6.2.3. Results of all nine sets are summarized in Tables 6.5 to 6.8, in Section 6.2.4. Concrete prisms were fully submerged in water to accelerate the growth of ettringite which consequently also caused permanent weight gain. Overall, two sets experienced weight changes above 7% and two sets below 6%. The remaining five sets experienced weight changes between 6% and 7%. All eight of the treated sets experienced a weight change smaller than the Control (Set 1) which experienced a maximum 7.70% weight gain. Similar to the expansion measurement data a general

relationship can be established between maximum weight change and slope of the weight change versus time graphs. Also, much like the expansion measurements, this trend is not true for all sets. The trend is observed in Table 6.8 by comparing the rankings of the maximum weight change (%) and the slope of weight change versus time best-fit-lines. The maximum weight gain was reached in the final days or the plateau.

Shimada (2005) hypothesized that the weight gain was a result of the volume increase caused by the concrete expansion. Ettringite growth induces stresses in the cement paste and aggregate matrix causing defects such as cracks. Since the prisms are fully submerged in solution the defects should be completely filled with the solution. Furthermore, Shimada (2005) assumes that solution absorbed by the concrete prism is the sole cause of the weight gain. Based on this hypothesis a linear relationship could be established between weight gain and expansion of concrete prisms.

6.2.1 Control & Water Repellents (Set Nos. 1 – 3)

Weight change graphs for Set Nos. 1, 2, and 3 are shown in Figures 6.38 to 6.46. The Control prisms (Set 1) experienced a maximum average weight gain of 7.70% with a trendline slope of 0.1033 %/day. The ChimneySaver (Set No. 2) exhibited a maximum weight gain of 6.15% with a trendline slope of 0.00192 %/day. The Radcon Formula #7 had a similar curve to the Control and the only set with a slope greater than Control. Radcon Formula #7 (Set No. 3) exhibited a maximum weight gain of 7.55% with trendline slope of 0.00192 %/day. The rate of weight gain on the final day of measurement (Day 300) for Set Nos. 1, 2, and 3 were 0.0047

%/day, 0.0020 %/day, and 0.0006 %/day respectively. The rates seem to indicate that Set Nos. 1 & 2 were still absorbing water due to continuing formation of cracks while Set No. 3 was close to reaching an asymptote.

A linear regression analysis between the expansion and weight change data revealed that the slopes of the Set Nos. 1, 2, and 3 exhibited linear relationships with a 0.99 regression coefficients (R^2). The respective slopes of Set Nos. 1, 2, and 3 are 0.7851 % per %, 0.8154 % per %, and 0.7975 % per %. The slopes indicate that expansion is occurring slower than the weight gain. Take for instance the Control (Set No. 1) which is expanding at 0.7851% for every 1.0% in weight gain.

6.2.2 Dequest 2060S (Set Nos. 4 – 6)

Weight change graphs for Set Nos. 4, 5, and 6 are shown in Figures 6.47 to 6.55. The prisms treated with Dequest 2060S (Set No. 4) experienced a maximum average weight gain of 5.33% with a maximum trendline slope of 0.0071 %/day. Both values were the lowest out of the nine sets. The prisms treated with Dequest and ChimneySaver (Set No. 5) exhibited a maximum weight gain of 6.20% with a trendline slope of 0.0095 %/day. The prisms treated with Dequest and Radcon Formula #7 (Set No. 6) exhibited a maximum weight gain of 6.33% with a trendline slope of 0.0089 %/day. The rates of weight gain on the final day of measurement (Day 300) for Set Nos. 4, 5, and 6 were 0.0036 %/day, -0.0004 %/day, and 0.0009 %/day. The rates seem to indicate that Set No. 4 was still absorbing water due to continuing formation of cracks while Set Nos. 5 & 6 were close to reaching an asymptote.

Linear regression analysis between the expansion and weight change data revealed that the slopes of Set Nos. 4, 5, and 6 exhibited linear relationships with a 0.99 regression coefficients (R^2). The respective slopes of Set Nos. 4, 5, and 6 are 1.1052 % per %, 1.0352 % per %, and 1.0896 % per %. Slopes indicate that expansion and weight gain are occurring at a slightly equal to or greater than one to one. Take for instance Set No. 5 which is expanding at 1.0352% for every 1.0% in weight gain. Set Nos. 4, 5, and 6 were the only sets to exhibit an approximate one to one expansion to weight gain ratio. The remaining six sets had ratios less than one.

6.2.3 Good-Rite K-752 (Set Nos. 7 – 9)

Weight change graphs for Set Nos. 7, 8, and 9 are shown in Figures 6.56 to 6.64. The prisms treated with Good-Rite K752 (Set No. 7) experienced a maximum average weight gain of 6.13% with a trendline slope of 0.0098 %/day. The prisms treated with K752 and ChimneySaver (Set No. 8) exhibited a maximum weight gain of 5.93% with a trendline slope of 0.0091 %/day. The prisms treated with K752 and Radcon Formula #7 (Set No. 8) exhibited a maximum weight gain of 6.63% with a trendline slope of 0.0098 %/day. The rates of weight gain on the final day of measurement (Day 300) for Set Nos. 7, 8, and 9 were 0.0052 %/day, 0.0025 %/day, and 0.0067 %/day respectively. The rates seem to indicate that all three sets were still absorbing water due to continuing formation of cracks.

Linear regression analysis between the expansion and weight change data revealed the slopes of the Set Nos. 4, 5, and 6 exhibited linear relationships with a 0.99 regression coefficient (R^2). The respective slopes of Set Nos. 4, 5, and 6 are

0.8455 % per %, 0.8032 % per %, and 0.8172 % per %. Slopes indicate that expansion was occurring at a slower pace than the weight gain.

6.2.4 Summary of Weight Change Results

Table 6.5 summarizes the linear regression analysis performed on the weight change measurements with respect to time. Table 6.6 summarizes the maximum rate of weight change and the final expansion rate at Day 300. Table 6.7 summarizes the linear regression analysis of the expansion versus weight change. Table 6.8 summarizes the maximum weight change, rate of weight change, slope of best-fit-line, and expansion to weight change regression values with corresponding rankings (from highest to lowest). Figures 6.65 and 6.66 summarize weight change versus time and expansion versus weight change for all nine sets.

6.3 Compression Test Results

Compression tests were performed at 30 days, 90 days and 240 days after the completion of the UMD/FHWA Modified Duggan Cycle. The compressive strength test results reported in Table 6.9 and Figure 6.67 are averages for three 4" diameter x 8" high cylinders. The standard deviation of the three measurements is plotted as the error bars. All nine sets of cylinders were stored in lime water for the duration of the project, the same as the prisms. Initial compressive strength at thirty days varied between 3100 psi to 3800 psi. Overall, all nine sets of cylinders were reduced in strength at 90 days and 240 days after the completion of the Duggan Cycle.

Only two sets outperformed the Control set at 90 days and no sets at 240 days. The strength reduction varied from 5% to 33% at 90 days. The smallest reduction at

90 days was by Set No. 6 at 5% and the largest by Set No. 2 at 33%. However, at 240 days six of the nine sets were reduced in strength by approximately 85% and the remaining three sets (Set Nos. 1, 6, & 9) reduced in strength by approximately 65%. Compression test results per groups of three sets are described in Sections 6.3.1 to 6.3.3.

6.3.1 Control & Water Repellents (Set Nos. 1 – 3)

The Control (Set No. 1) exhibited a 14% loss of strength at 90 days and 62% loss at 240 days. The Control set was one of the better performers in the compression tests at both 90 and 240 days. Only two sets (Set Nos. 6 & 9) outperformed the Control set at 90 days and no sets at 240 days. Set No. 2 (ChimneySaver) exhibited a 33% loss at 90 days and a 86% loss at 240 days. Set No. 3 (Radcon Formula #7) experienced similar results to Set No. 2 with 25% loss at 90 days and 85% loss at 240 days. Set Nos. 2 and 3 performed the poorest when compared to the other nine sets of concrete cylinders.

6.3.2 Dequest2060S (Set Nos. 4 – 6)

Set Nos. 4, 5, and 6 were treated with Dequest 2060S and a combination of water repellent. Compared to all nine sets, Set No. 6 (Dequest & Radcon) exhibited the least amount of strength loss at 90 days with 5% and the second smallest reduction at 240 days with 65%. In contrast, Set No. 4 (Dequest) and Set No. 5 (Dequest & ChimneySaver) were poor performers with an average reduction of 27% at 90 days and 88% at 240 days. Both Set Nos. 4 and 5 exhibited significant more strength reduction than the Control specimens.

6.3.3 Good-Rite K-752 (Set Nos. 7 – 9)

Set Nos. 7, 8, and 9 were treated with Good-Rite K752 and a combination of water repellent. Set No. 9 (K752 & Radcon) exhibited the least amount of strength loss at 90 days and 240 days with 11% and 68% respectively. At 90 days Set Nos. 7, 8, and 9 only differed in strength loss by 5%. However at 240 days the difference was 20% between Set No. 9 and Set Nos. 7 and 8. At 90 days Set No. 7 (K752) and Set No. 8 (K752 & ChimneySaver) exhibited reductions of 16% and 21% respectively. At 240 days Set Nos. 7 and 8 exhibited reductions of 87% and 85% respectively. Both Set Nos. 7 and 8 exhibited significantly more reduction than the Control specimens.

6.4 SEM and EDAX Analysis Results

SEM analysis with EDAX was performed on all nine sets at 30, 90, and 240 days after the completion of the Duggan Cycle. One prism per set was fractured and two samples were prepared. One sample was prepared from the exterior portion of the prism and the second one from an interior portion. Eighteen (18) samples were prepared at each interval for a total of fifty-four (54). Each sample was analyzed to determine if ettringite was present. If ettringite was found the morphology, location, the amount of ettringite was noted. It is impossible to quantify ettringite because of the scaling factor and depth uncertainties of the electron microscope. However, it is significant to note that very small samples (~5mm diameter) yielded large quantities of ettringite. Ettringite was identified visually and from the EDAX analysis. EDAX consistently gave "good" results meaning Ca-S-Al ratios around 6-3-2. Recall that

the chemical composition of ettringite is $3CaO{\cdot}Al_2O{\cdot}3CaSO_4{\cdot}32H_2O$ or, in chemists notation, $C_6A\hat{S}_3H_{32}$.

Ettringite morphologies are summarized in Tables 6.10 to 6.13. Typical morphologies in the fifty-four samples are shown in Figures 6.68 to 6.73. Most samples had an abundant amount of ettringite in a variety of forms. A few of the samples exhibited no ettringite which was most likely due to poor samples. Samples typically produced ettringite with similar morphologies including spheres, laths, and needles. Spheres were the most common at 30 days. Lamellar, spheres, and needles were more common at 90 days and 240 days. Ettringite was found in cavities, on the surface and in the cement matrix. Ettringite in the cement matrix supports the Uniform Paste Theory of Expansion. Scrivener and Taylor (1993) and Johanson et al. (1993) proposed the Uniform Paste Expansion Theory, which suggests that the concrete expands and then the ettringite forms in the newly created gaps.

6.5 Discussion of Results

The analysis of the expansion data, particularly Figure 6.37, reveals that three out of the four mitigation products outperformed the control. The water repellent, ChimneySaver, and both crystal inhibitors, Dequest 2060S and Good-Rite K752, when applied as a single treatment, reduced expansion when compared to the control set. At 300 days, ChimneySaver was the best performer experiencing a 30% reduction in expansion. The cross combination sets of water repellent and crystal inhibitor proved to be insignificant. The expansion of Dequest 2060S cross combination sets (Set Nos. 5 & 6) appeared to be performing well until Day 150 when expansion rose sharply and eventually overtook the control set. The Good-Rite

K752 cross combination sets (Set Nos. 8 & 9) tended to remain in line with the single treatment set (Set No. 7) implying that the inhibitor was most responsible for the reduction in expansion. The fourth product, water repellent Radcon Formula #7 (Set No. 2), appears to have the opposite effect from its intended purpose. A chemical reaction between the product and the concrete actually accelerated the expansion to the point of severely exceeding the control.

Similar correlations can be derived from the weight change data, however the separation between the sets is less pronounced (see Figure 6.65). Three of the four products, ChimneySaver, Dequest 2060S and Good-Rite K752, exhibited noticeably smaller weight changes than the control set. The fourth product, Radcon Formula #7, experienced the most weight change of the products and the graph is nearly parallel to the control. Much like the expansion results the cross combination treatment (Set Nos. 5, 6, 8 and 9) proved to be inconsequential.

It is difficult to correlate compression test results and SEM analysis with expansion and weight change results. The compression tests revealed varying degrees of concrete deterioration in all nine sets making comparisons of the product's effectiveness impracticable. For example, at 240 days, the ChimneySaver set had 1.65% expansion and 86% loss of strength. Simultaneously the control experienced a larger expansion of 2.08% and lower strength loss of 62%. The task of quantifying and characterizing ettringite through SEM in a small sample taken from a 3" x 3" x 11.25" prism is challenging and for the most part subjective. In this study, common ettringite morphologies included spheres, laths, and needles.

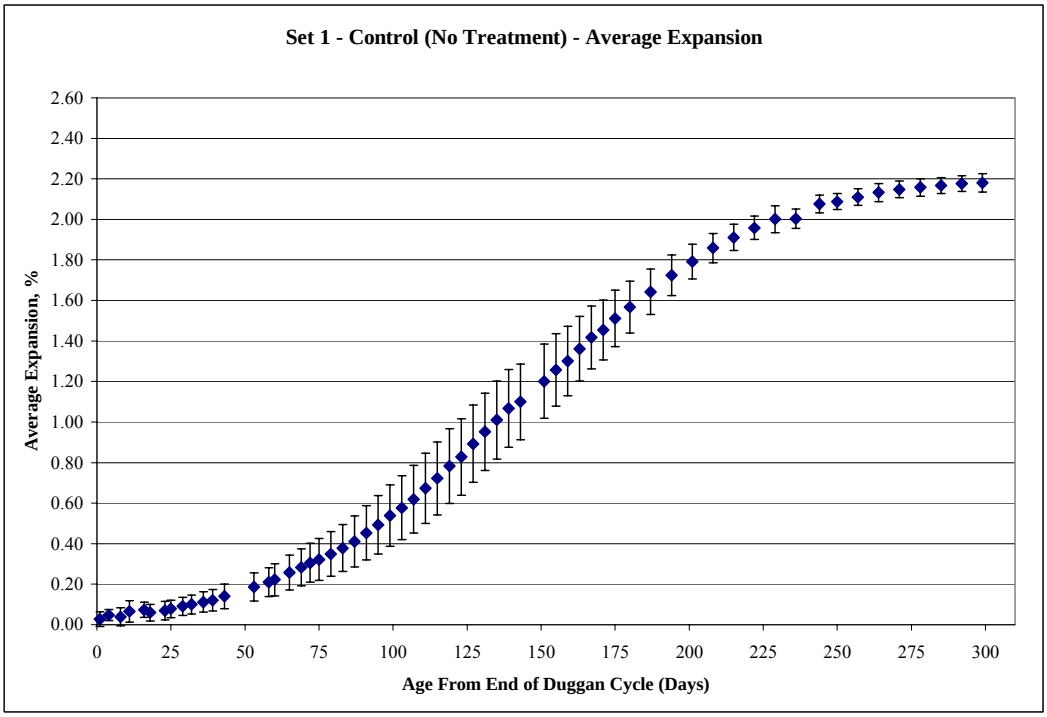

Figure 6.1 - SET 1 Expansion versus Time with Error Bars

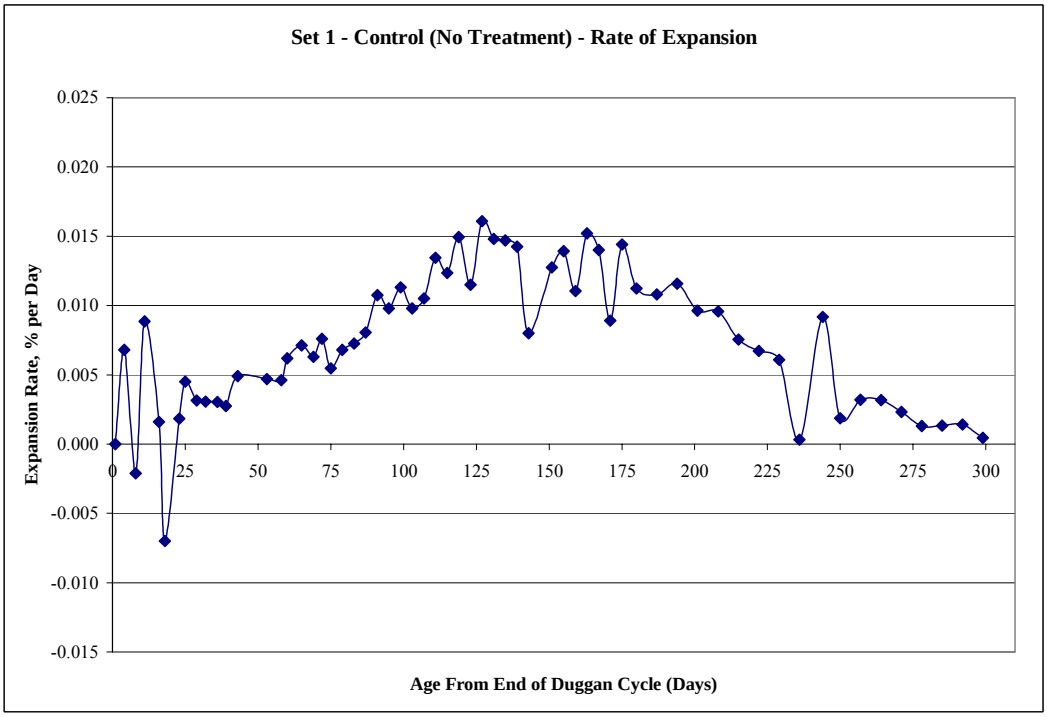

Figure 6.2 - SET 1 Rate of Expansion versus Time (First Derivative)

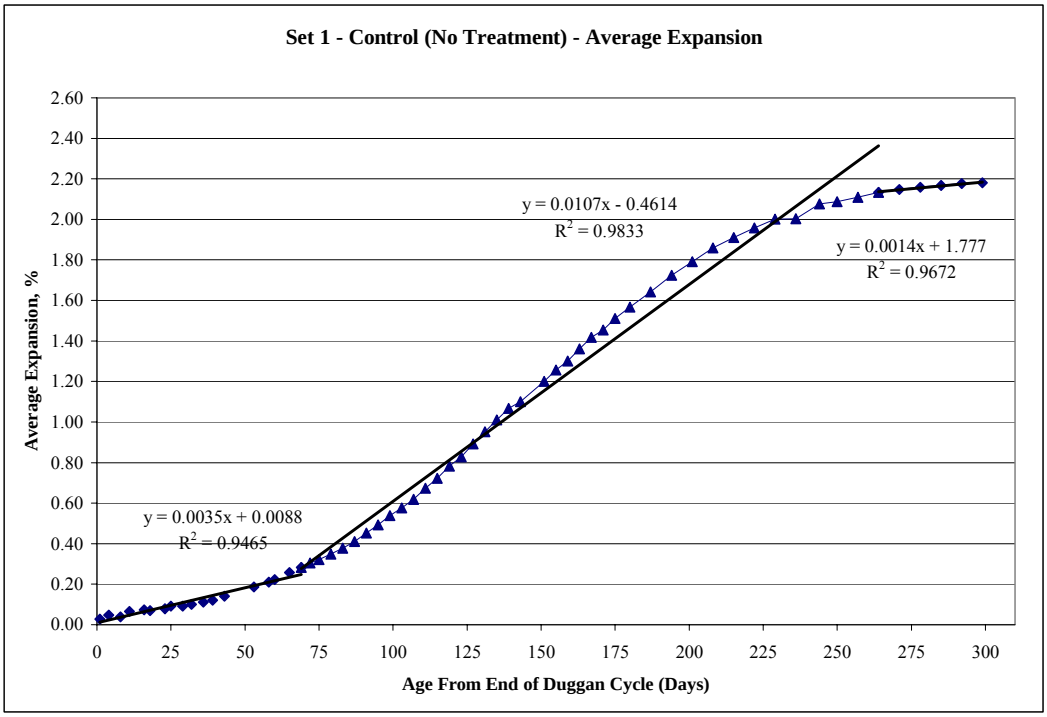

Figure 6.3 - SET 1 Linear Regression Analysis Graph (Best Fit Lines)

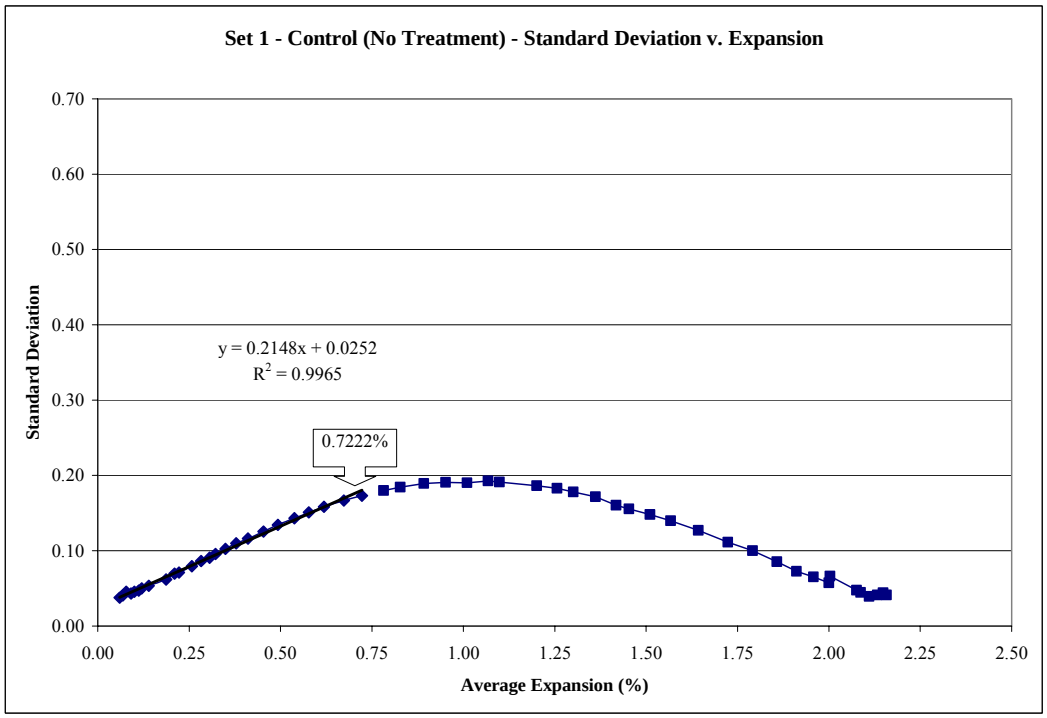

Figure 6.4 - SET 1 Standard Deviation versus Expansion

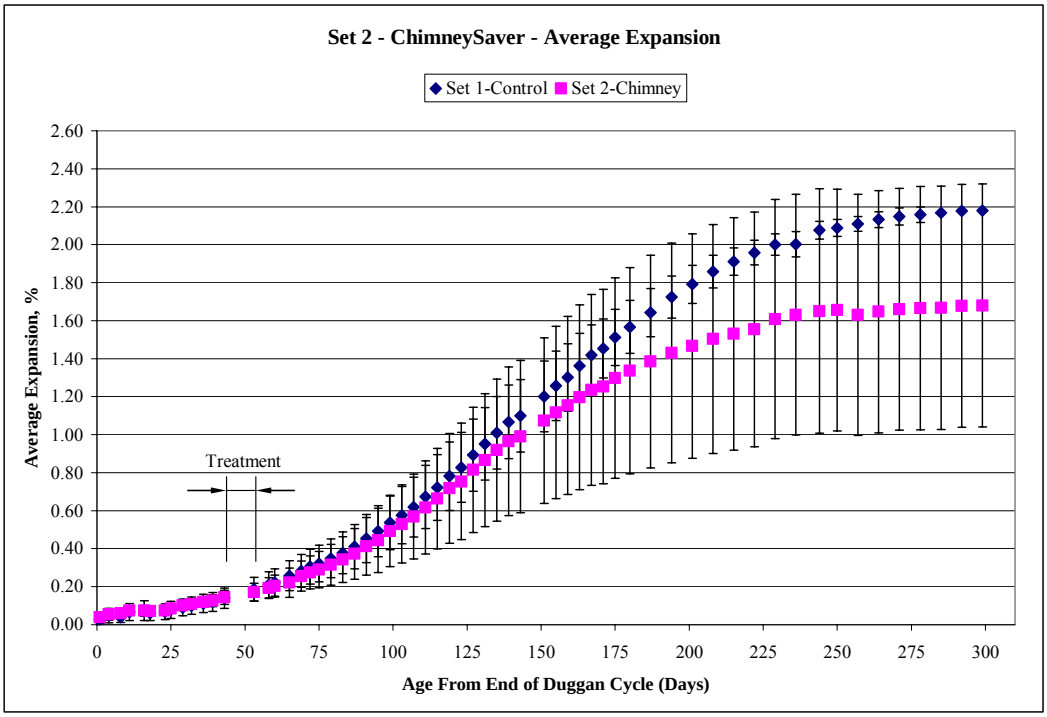

Figure 6.5 - SET 2 Expansion versus Time with Error Bars

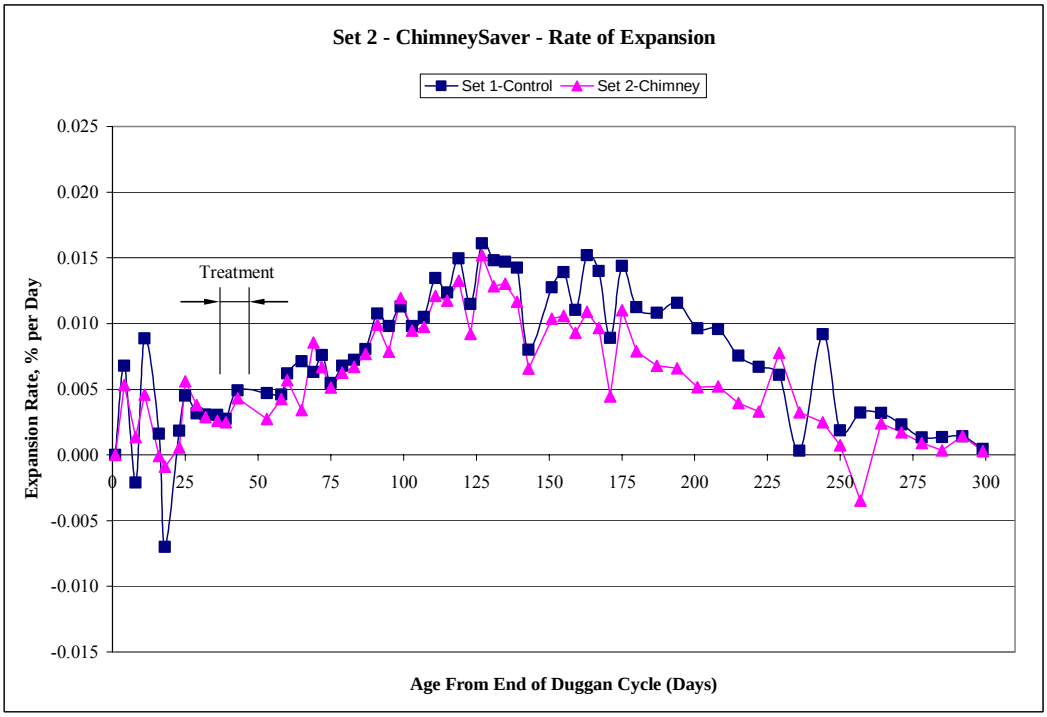

Figure 6.6 - SET 2 Rate of Expansion versus Time (First Derivative)

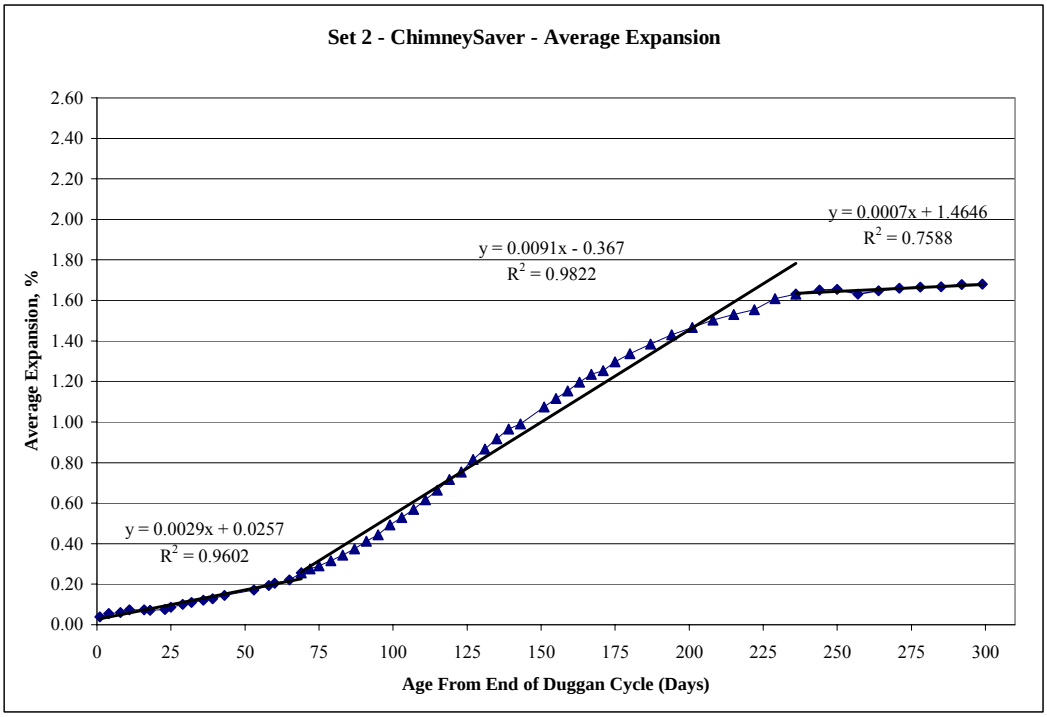

Figure 6.7 - SET 2 Linear Regression Analysis Graph (Best Fit Lines)

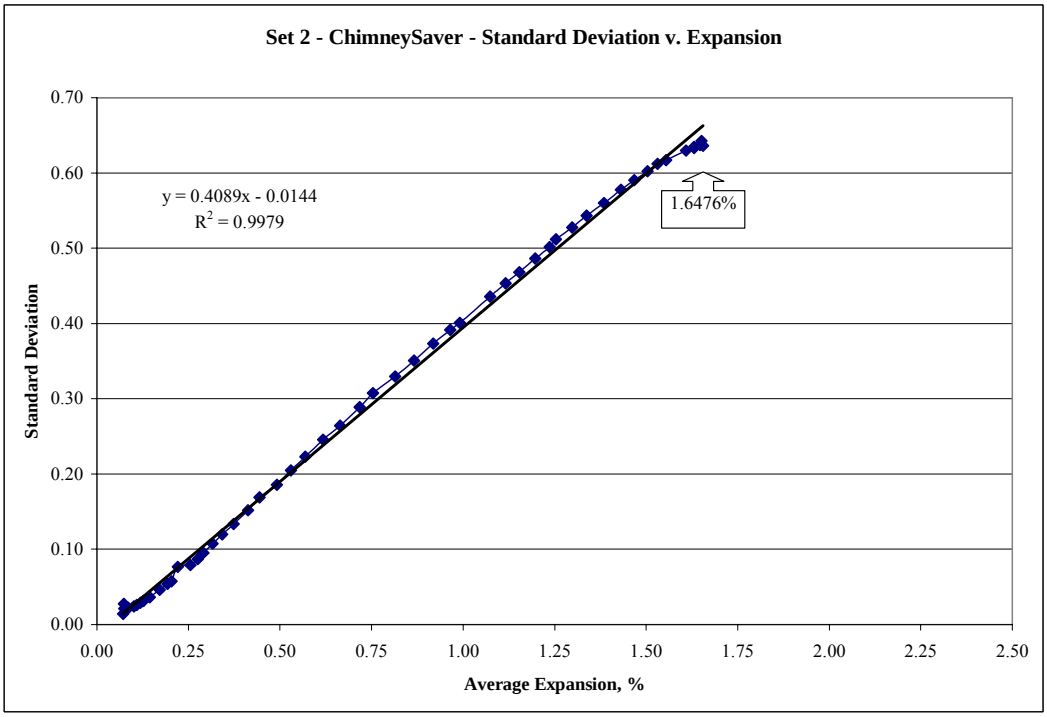

Figure 6.8 - SET 2 Standard Deviation versus Expansion

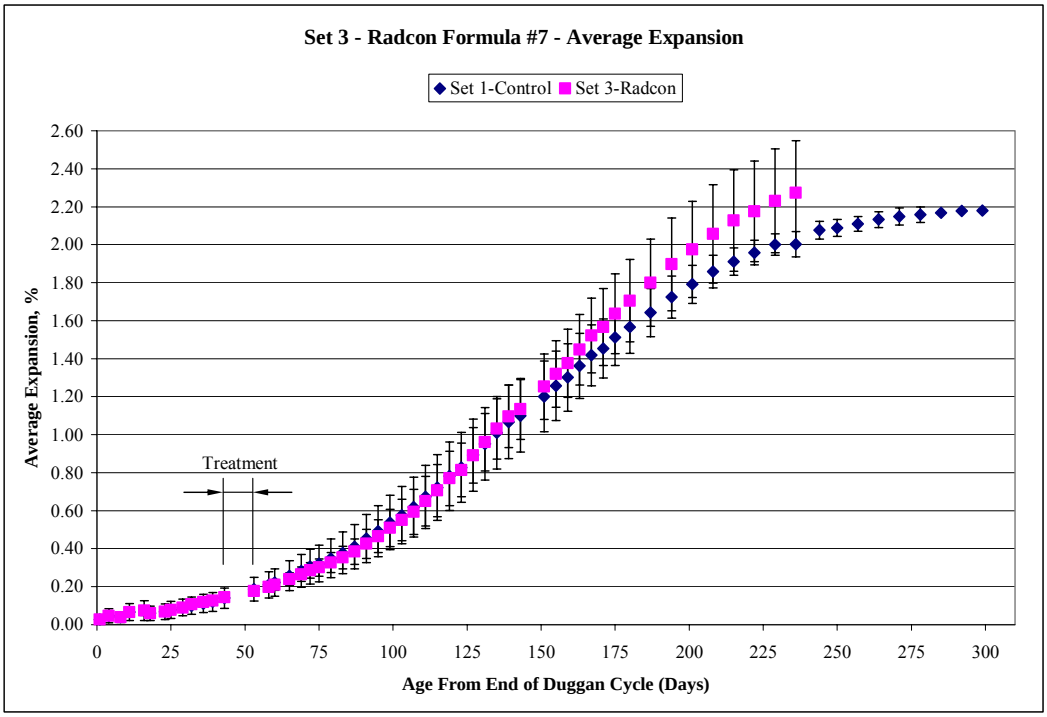

Figure 6.9 - SET 3 Expansion versus Time with Error Bars

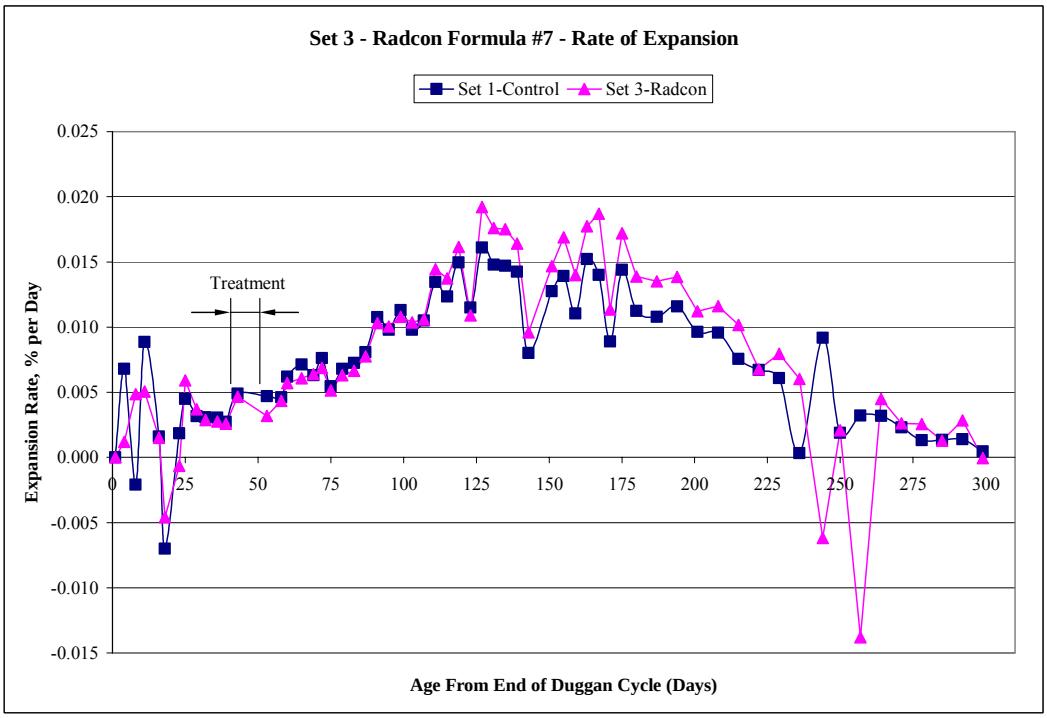

Figure 6.10 - SET 3 Rate of Expansion versus Time (First Derivative)

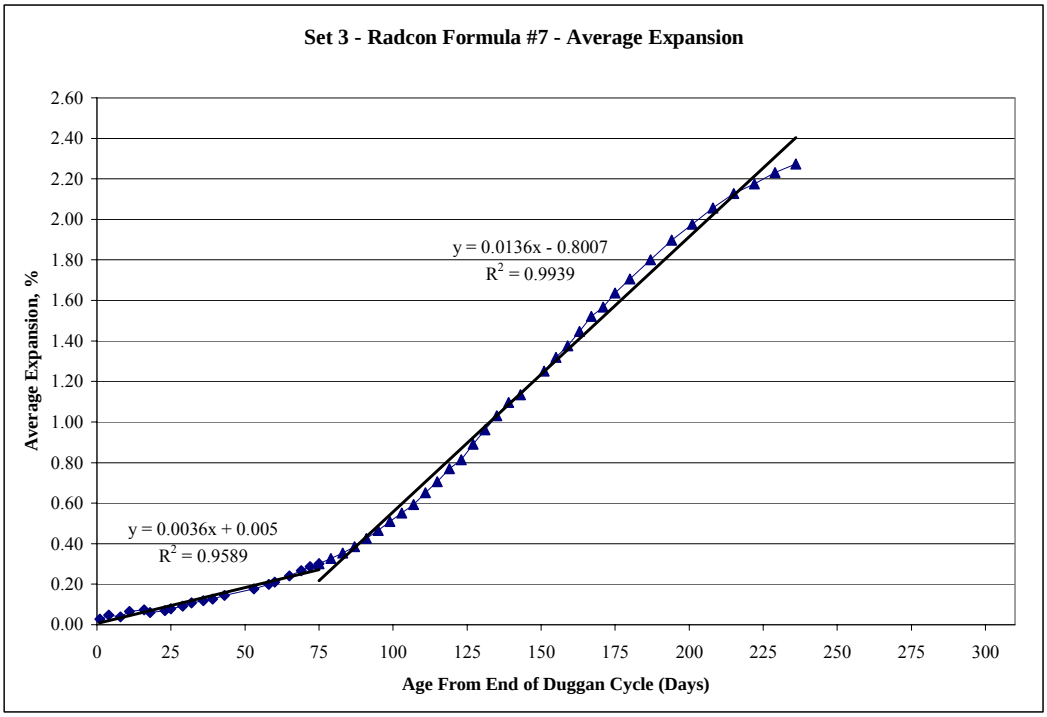

Figure 6.11 - SET 3 Linear Regression Analysis Graph (Best Fit Lines)

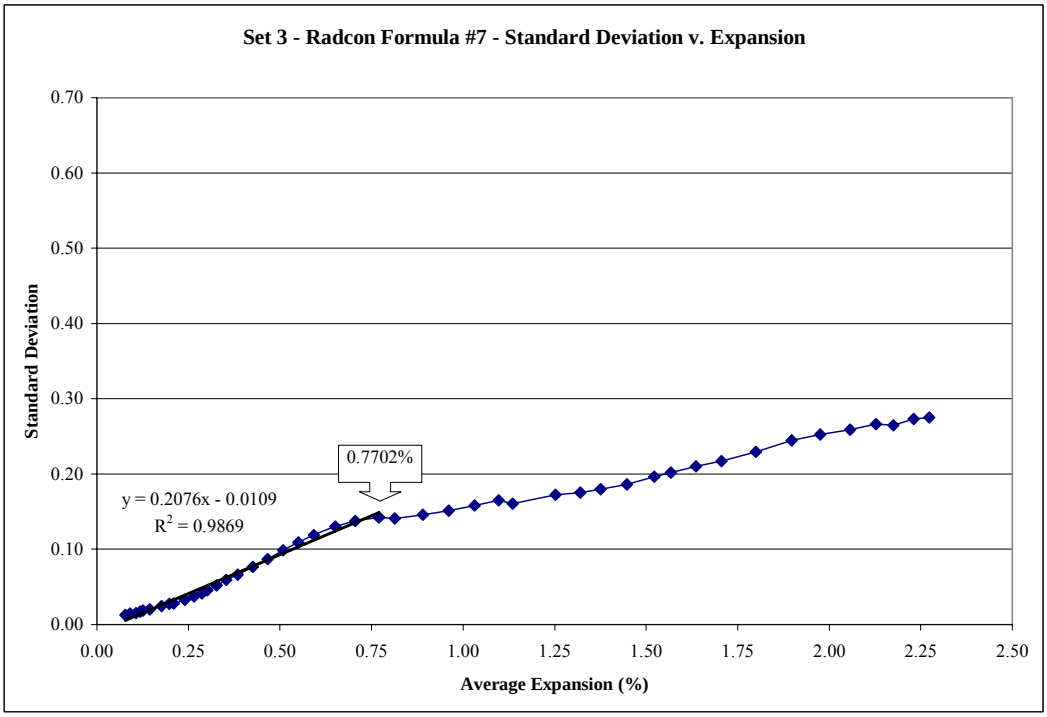

Figure 6.12 - SET 3 Standard Deviation versus Expansion

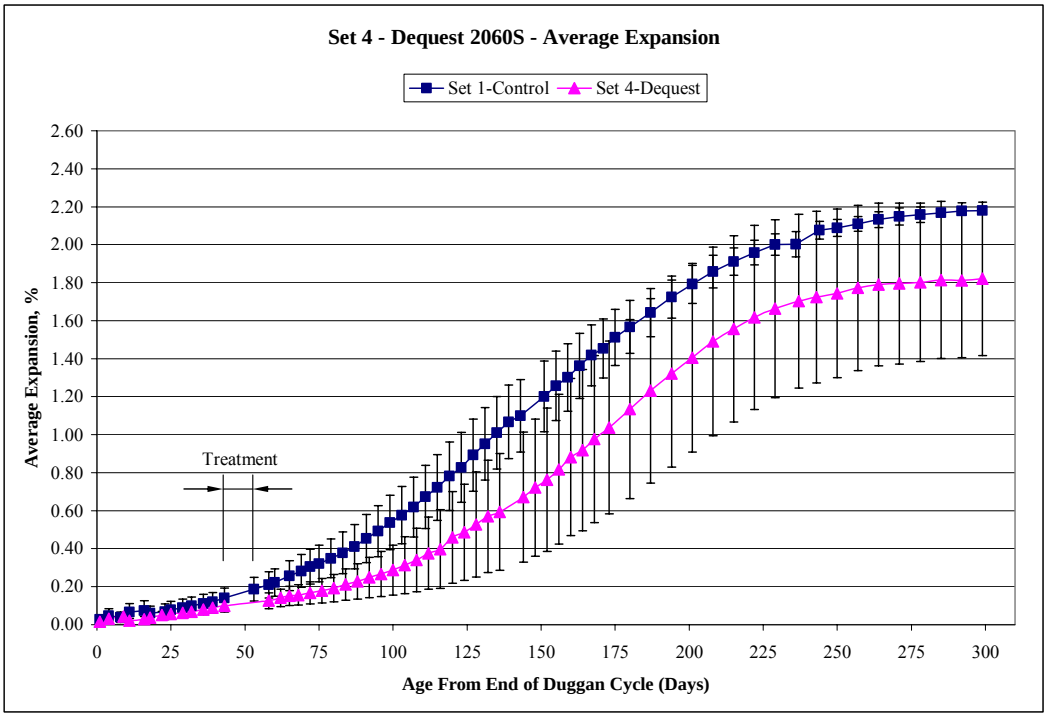

Figure 6.13 - SET 4 Expansion versus Time with Error Bars

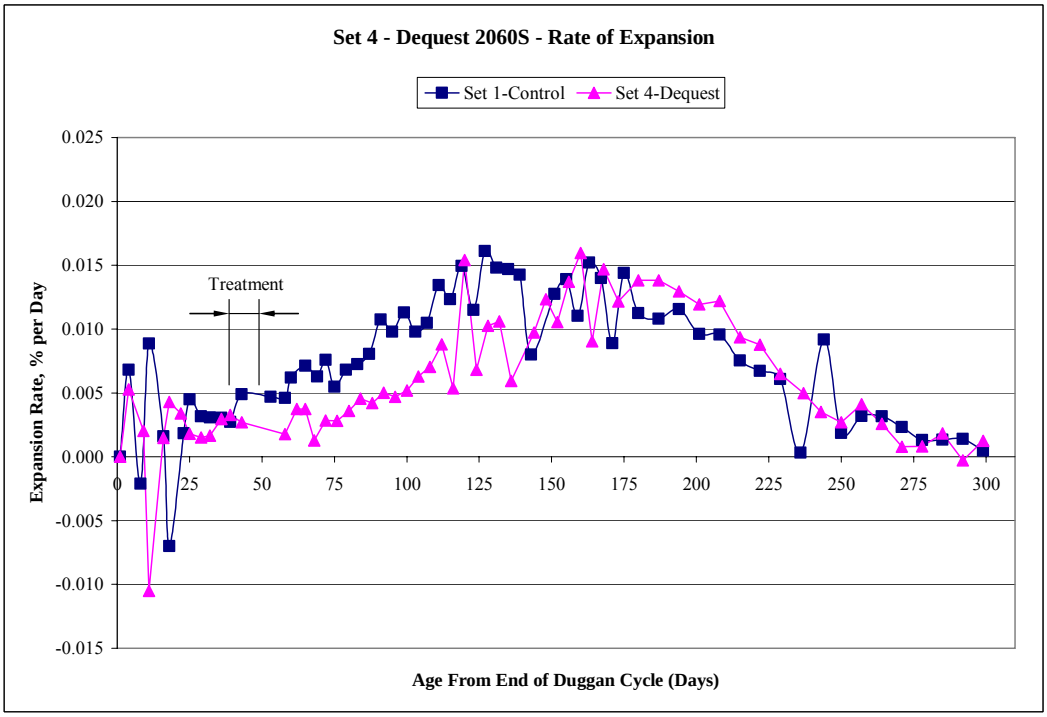

Figure 6.14 - SET 4 Rate of Expansion versus Time (First Derivative)

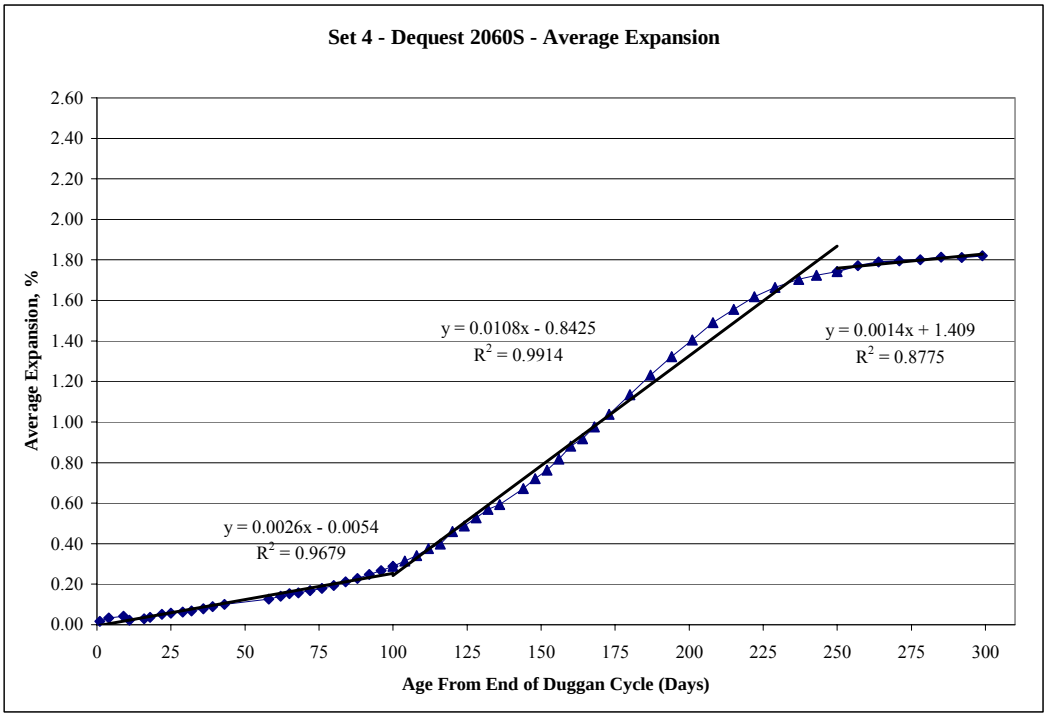

Figure 6.15 - SET 4 Linear Regression Analysis Graph (Best Fit Lines)

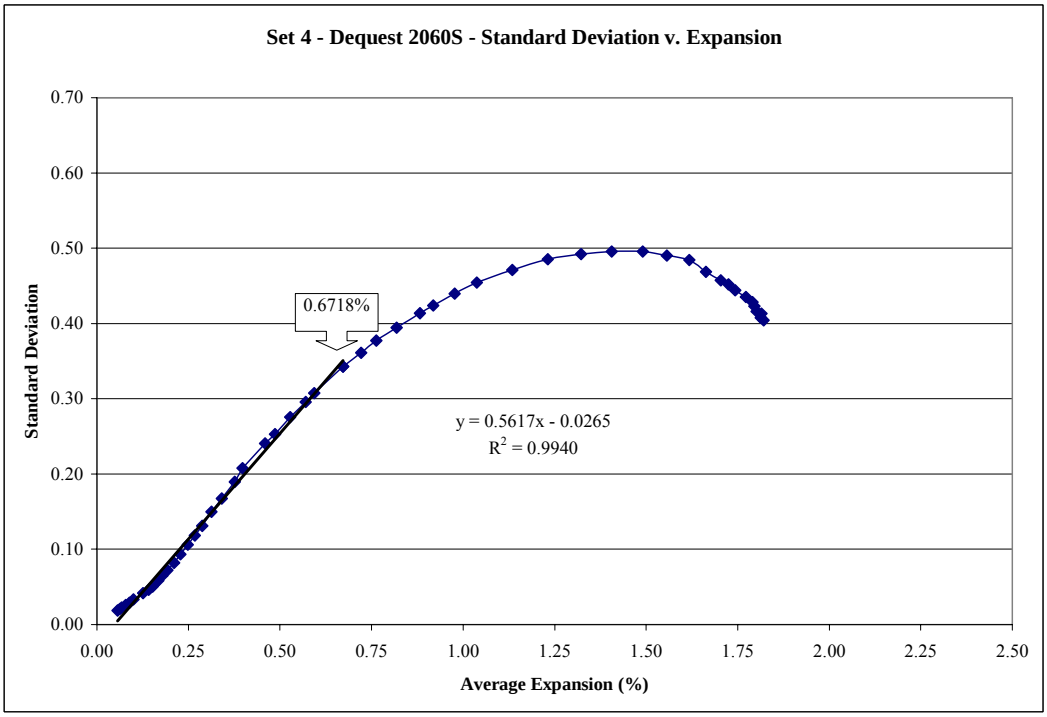

Figure 6.16 - SET 4 Standard Deviation versus Expansion

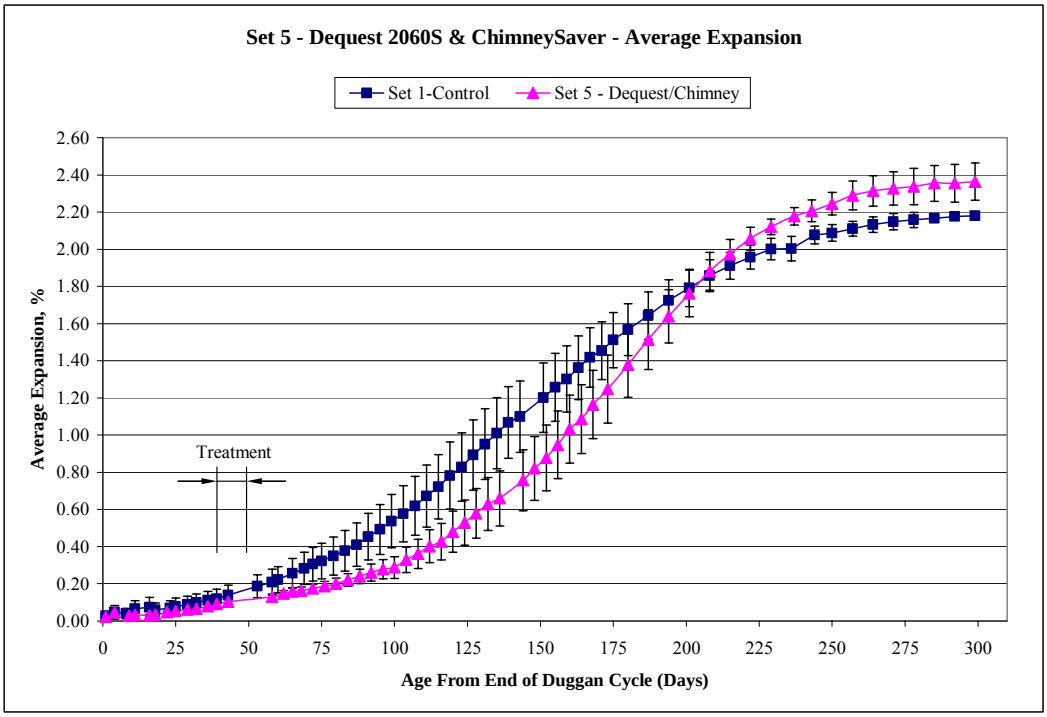

Figure 6.17 - SET 5 Expansion versus Time with Error Bars

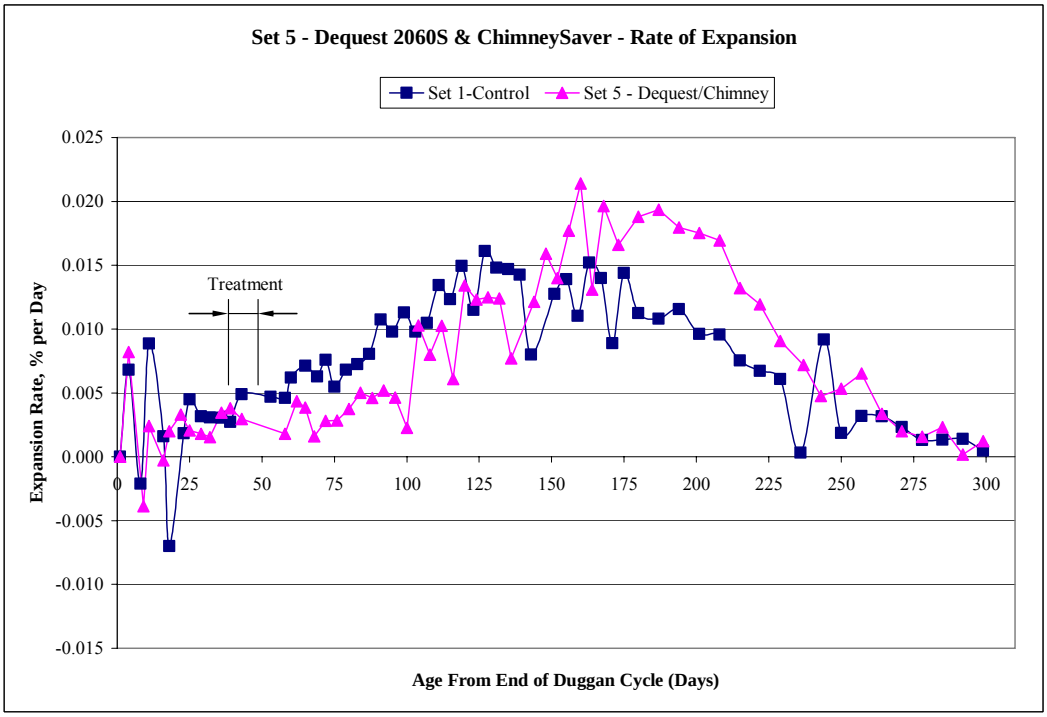

Figure 6.18 - SET 5 Rate of Expansion versus Time (First Derivative)

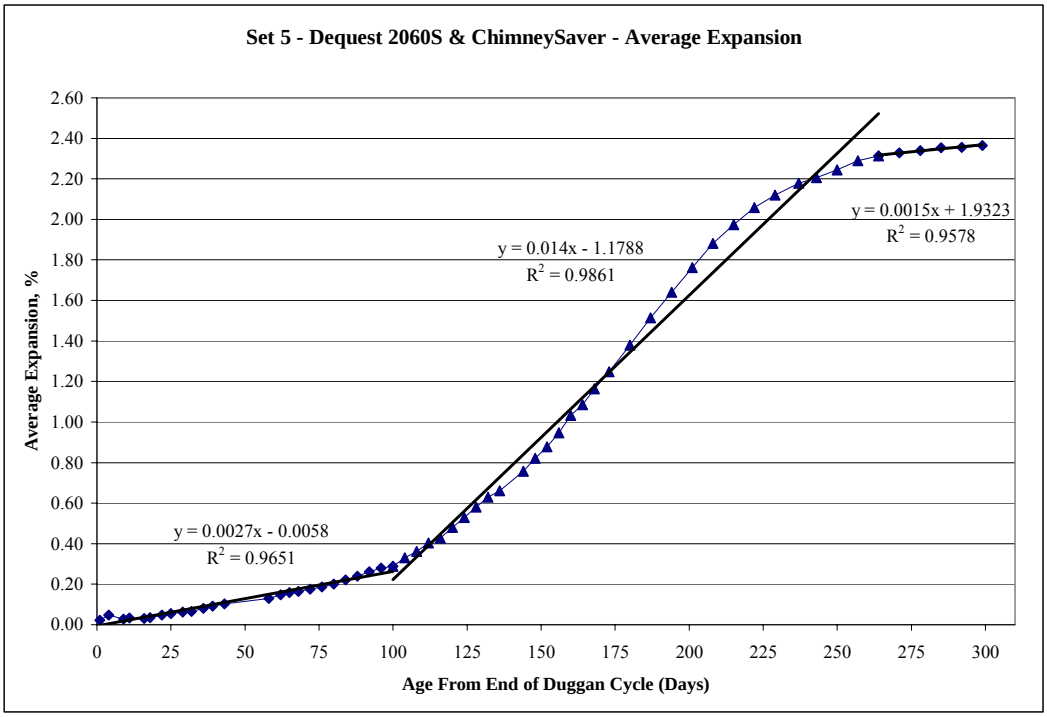

Figure 6.19 - SET 5 Linear Regression Analysis Graph (Best Fit Lines)

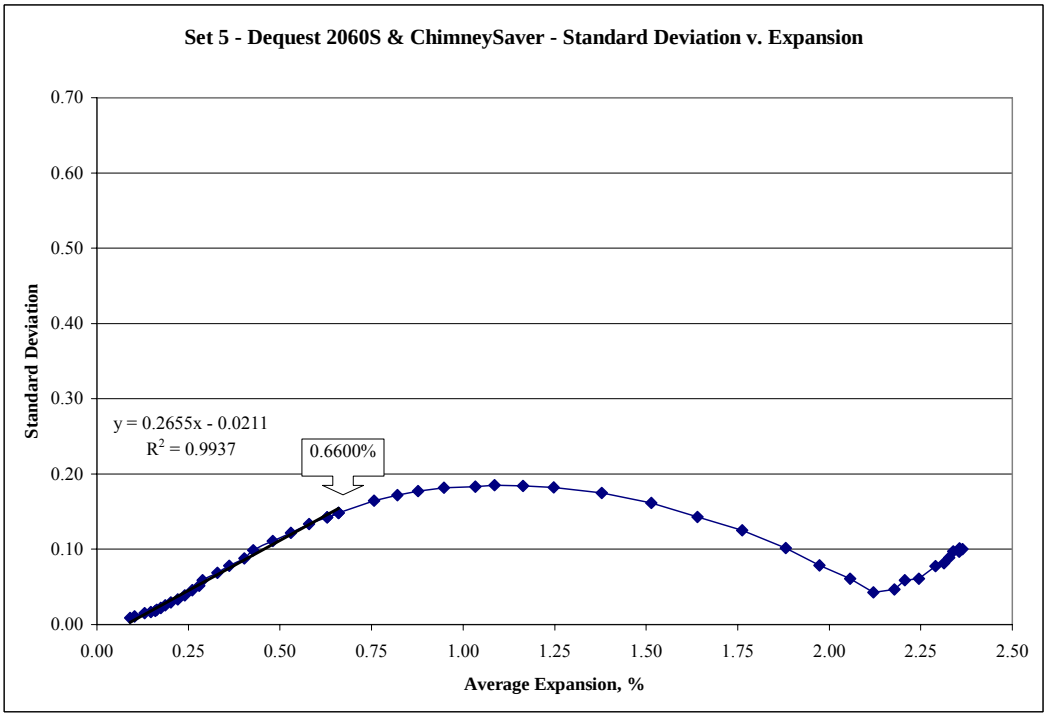

Figure 6.20 - SET 5 Standard Deviation versus Expansion

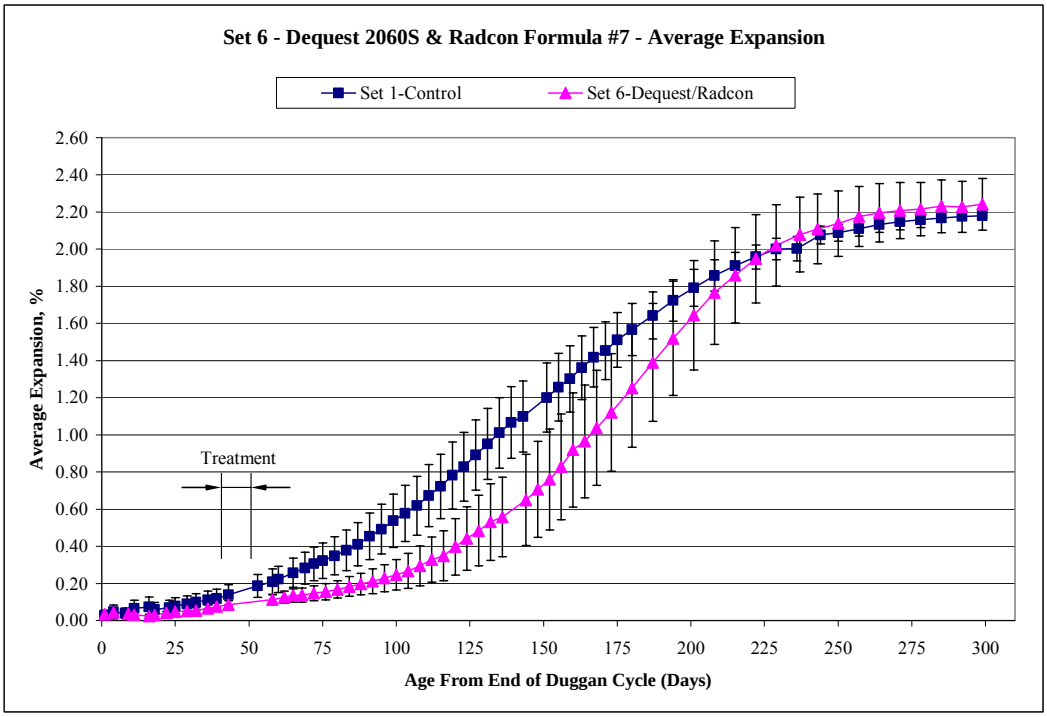

Figure 6.21 - SET 6 Expansion versus Time with Error Bars

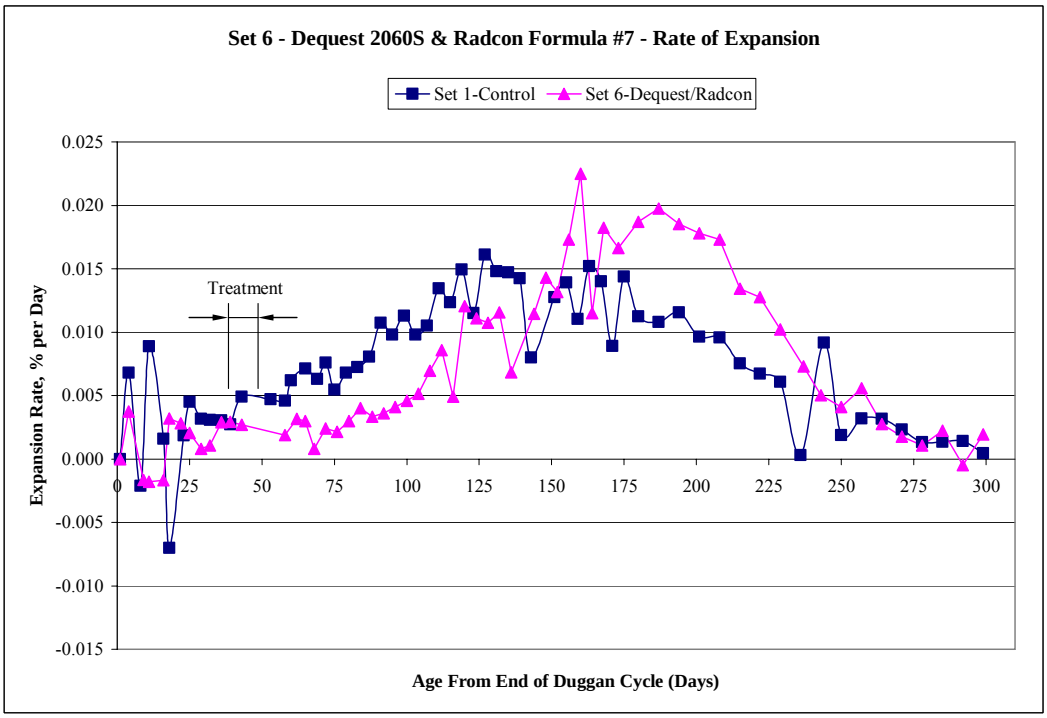

Figure 6.22 - SET 6 Rate of Expansion versus Time (First Derivative)

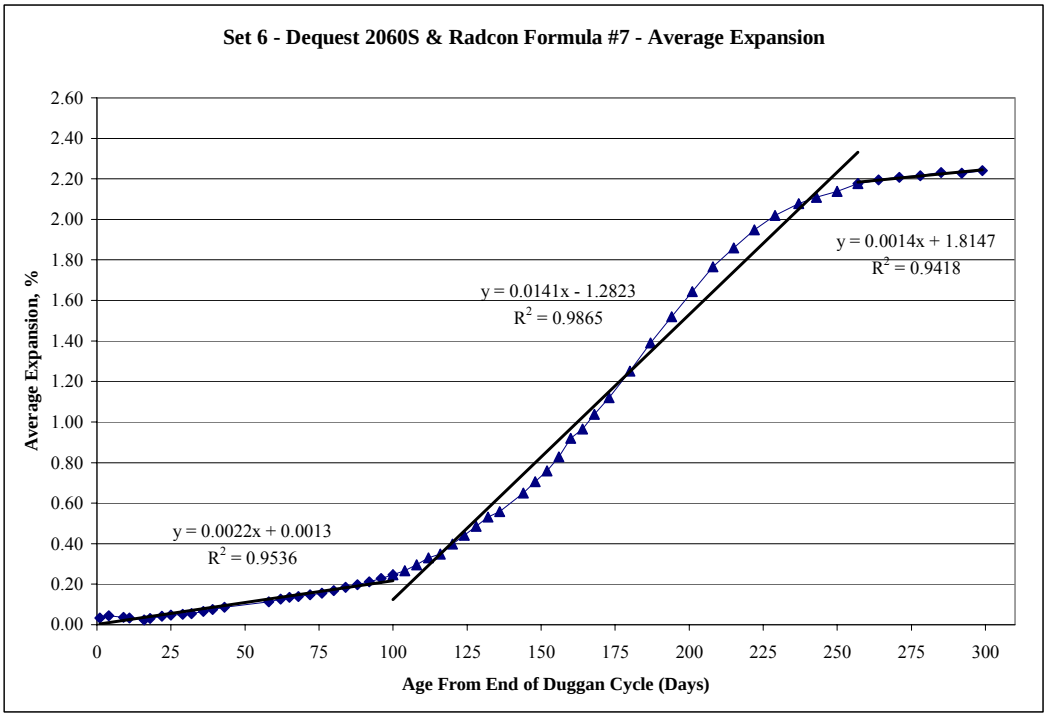

Figure 6.23 - SET 6 Linear Regression Analysis Graph (Best Fit Lines)

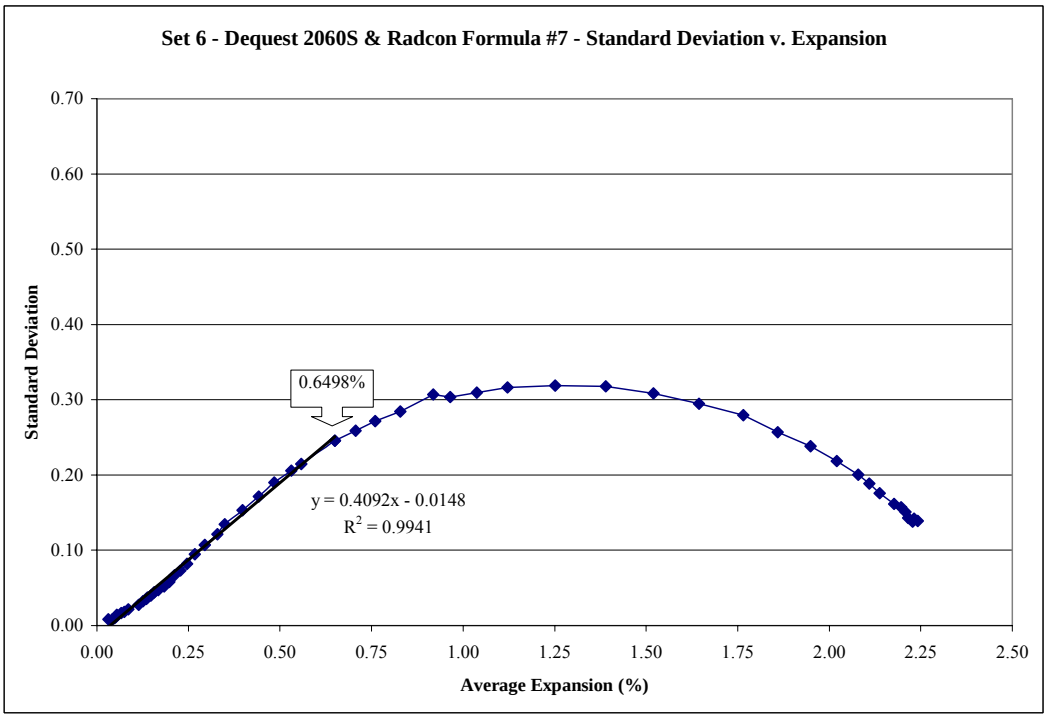

Figure 6.24 - SET 6 Standard Deviation versus Expansion

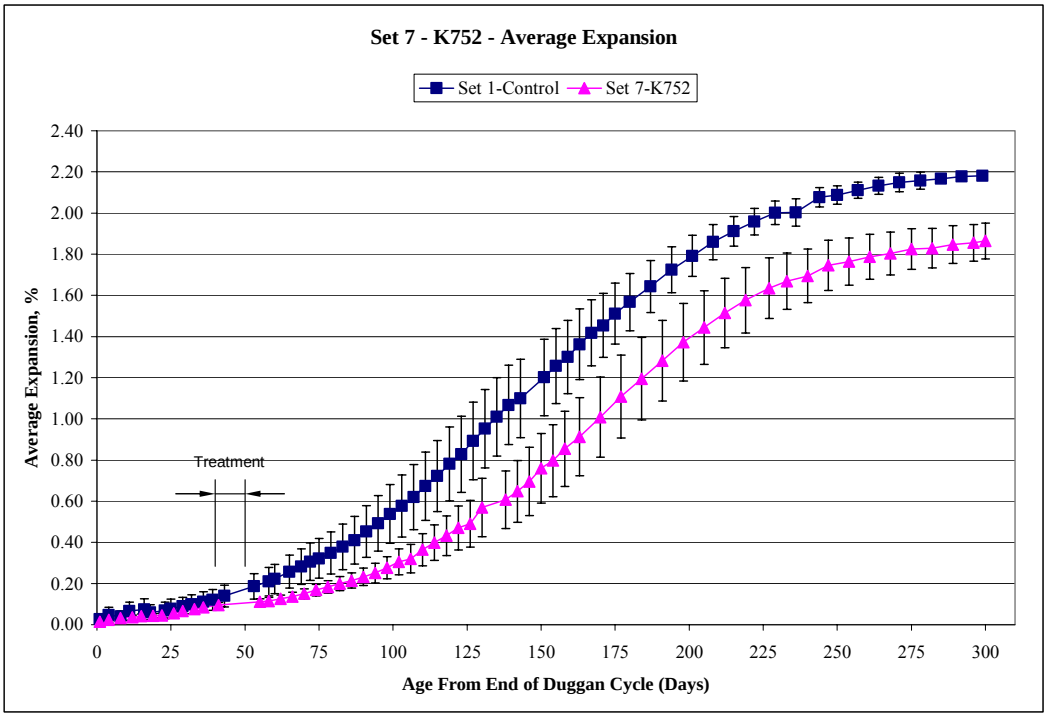

Figure 6.25 - SET 7 Expansion versus Time with Error Bars

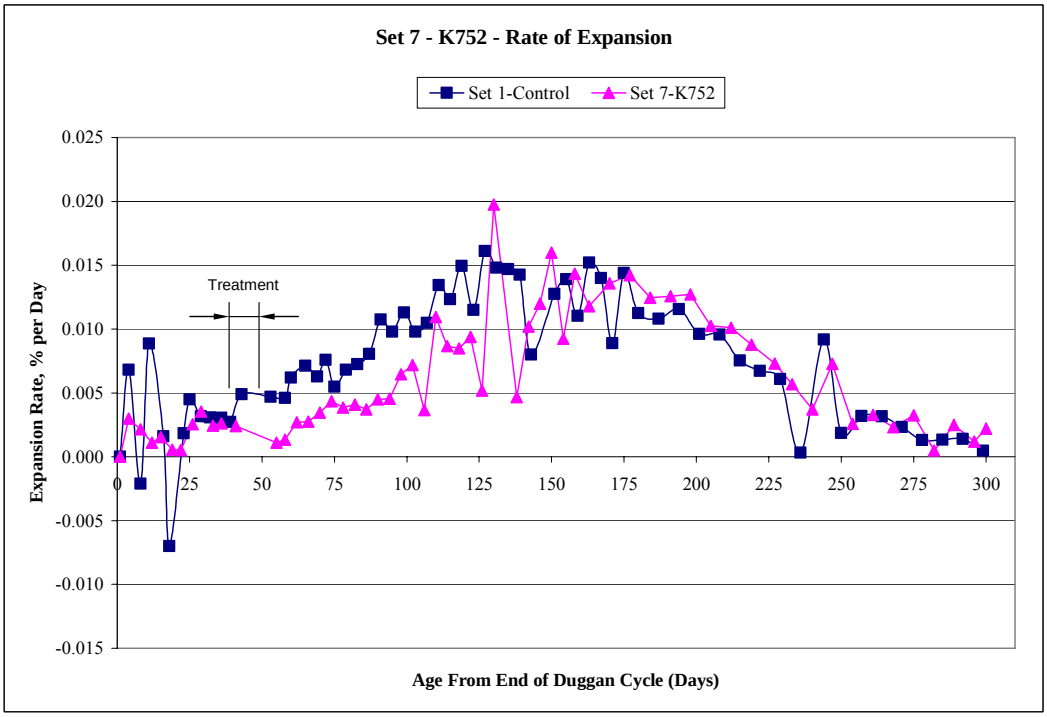

Figure 6.26 - SET 7 Rate of Expansion versus Time (First Derivative)

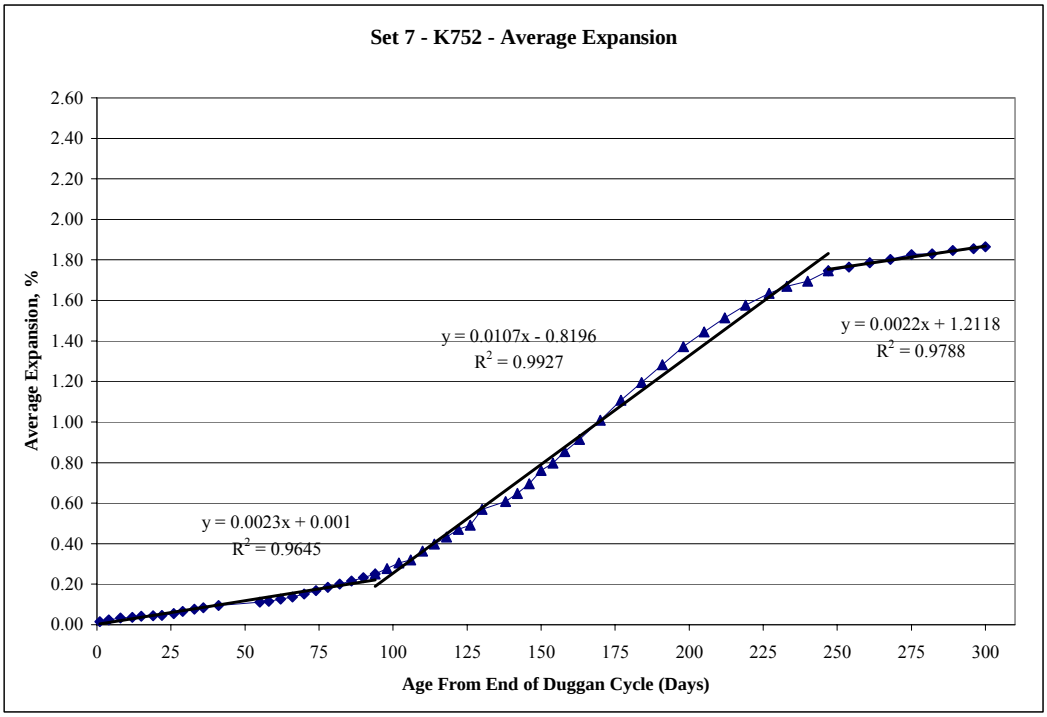

Figure 6.27 - SET 7 Linear Regression Analysis Graph (Best Fit Lines)

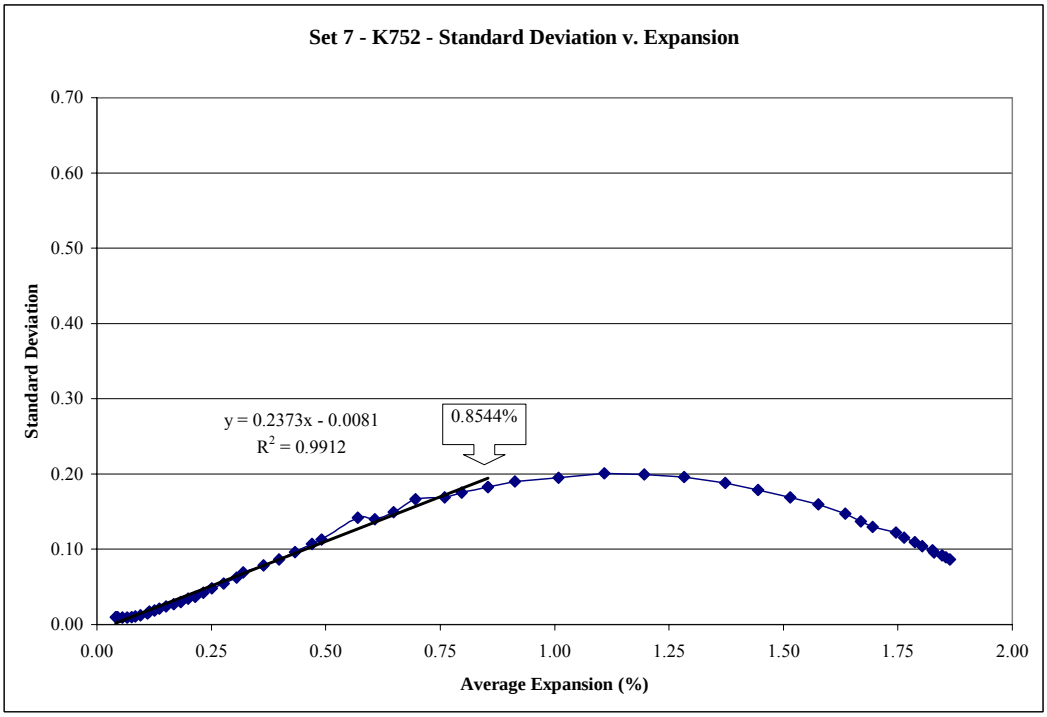

Figure 6.28 - SET 7 Standard Deviation versus Expansion

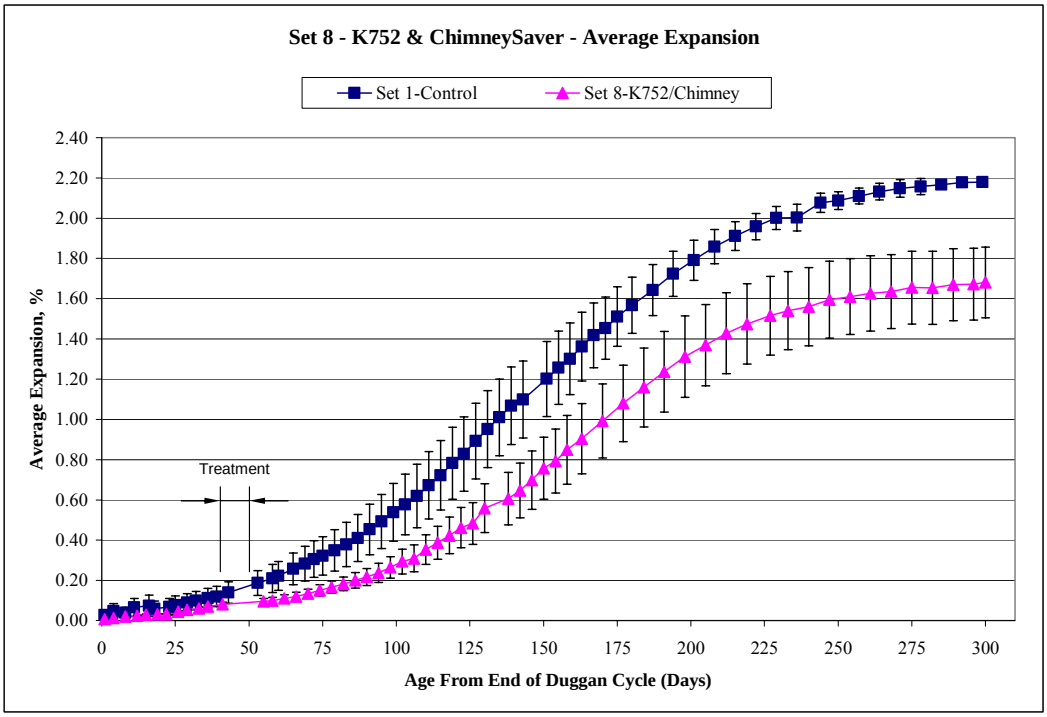

Figure 6.29 - SET 8 Expansion versus Time with Error Bars

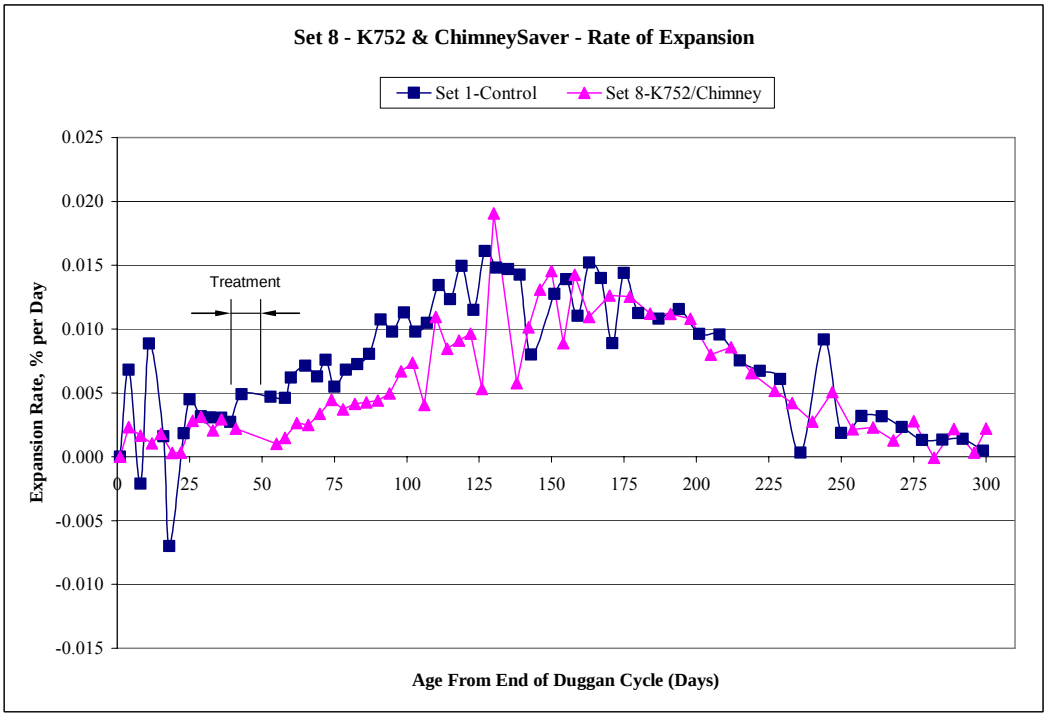

Figure 6.30 - SET 8 Rate of Expansion versus Time (First Derivative)

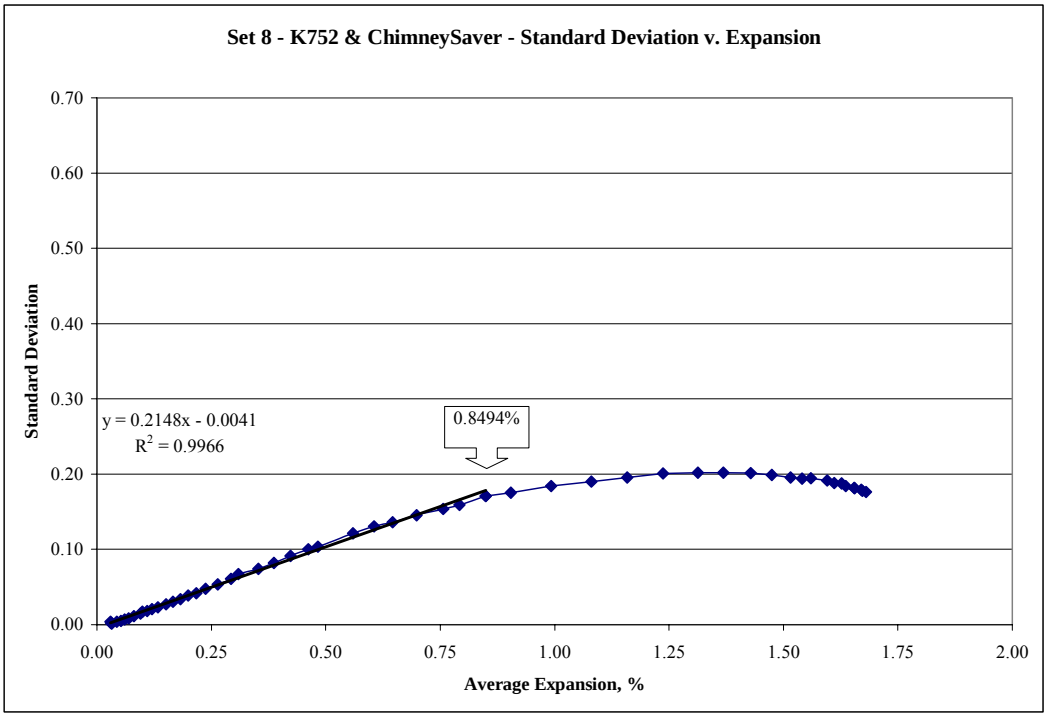

Figure 6.31 - SET 8 Linear Regression Analysis Graph (Best Fit Lines)

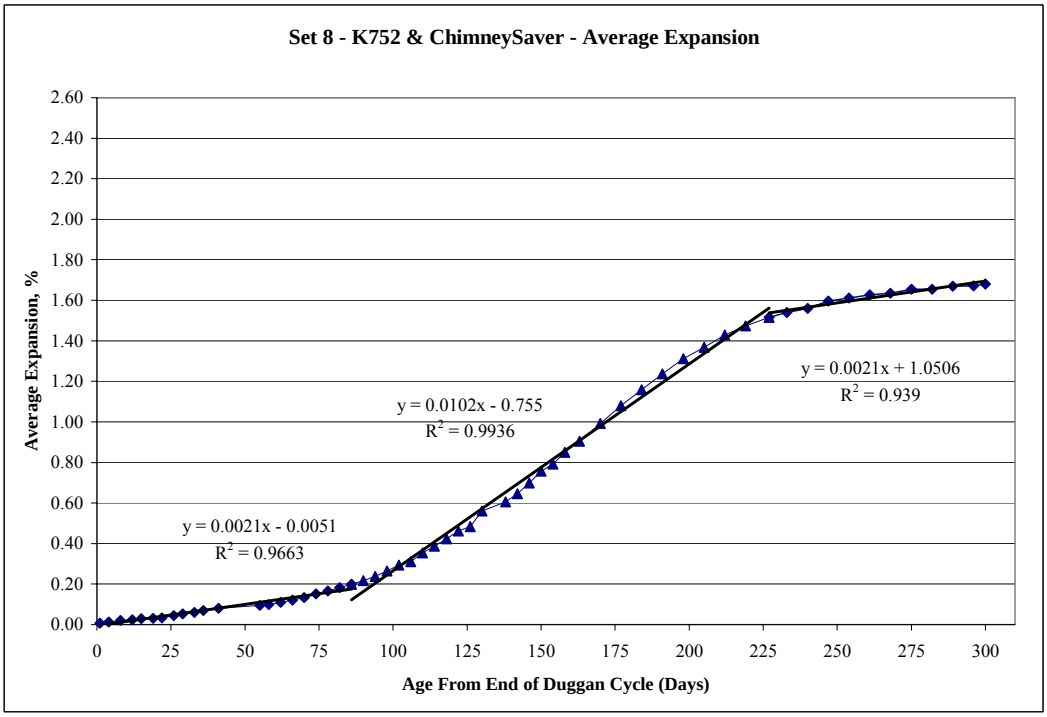

Figure 6.32 - SET 8 Standard Deviation versus Expansion

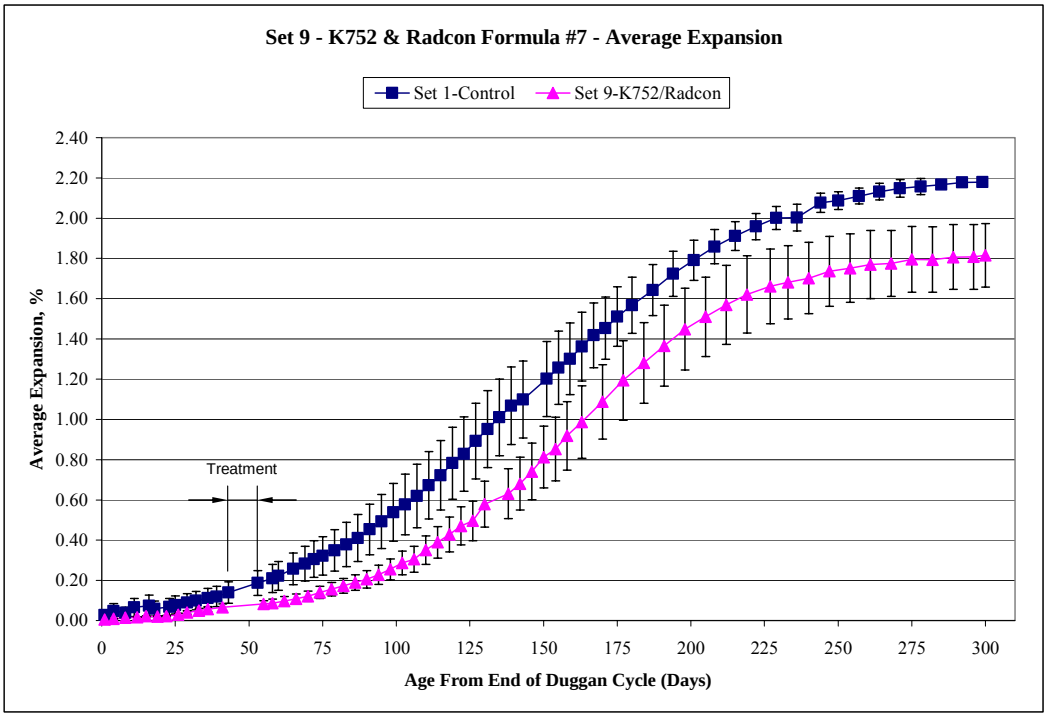

Figure 6.33 - SET 9 Expansion versus Time with Error Bars

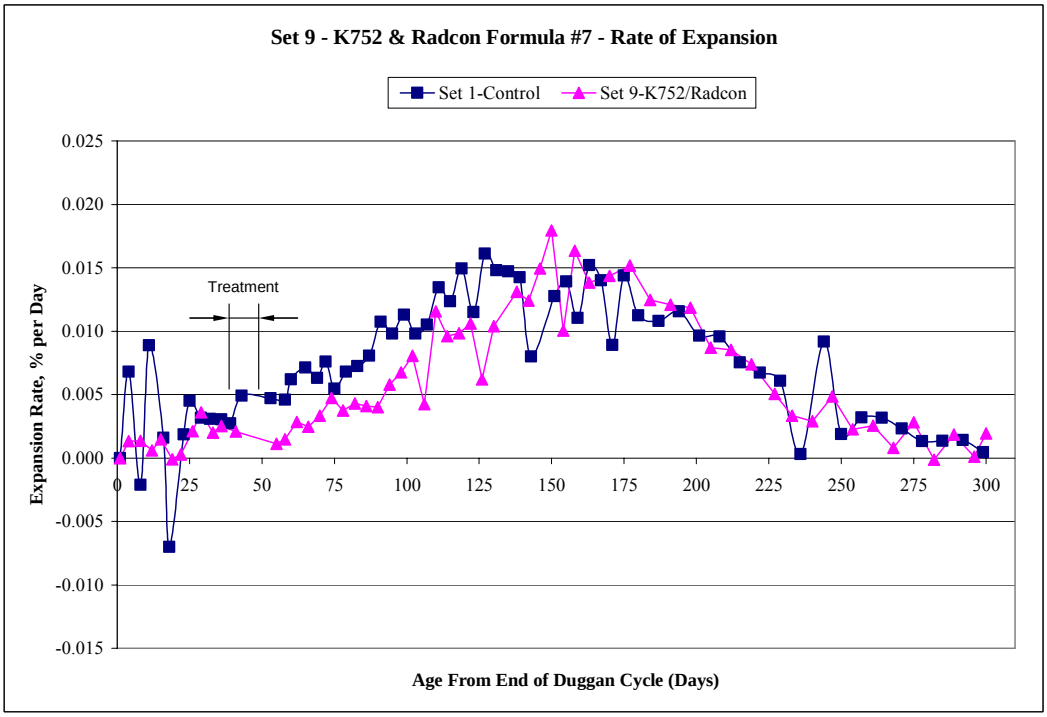

Figure 6.34 - SET 9 Rate of Expansion versus Time (First Derivative)

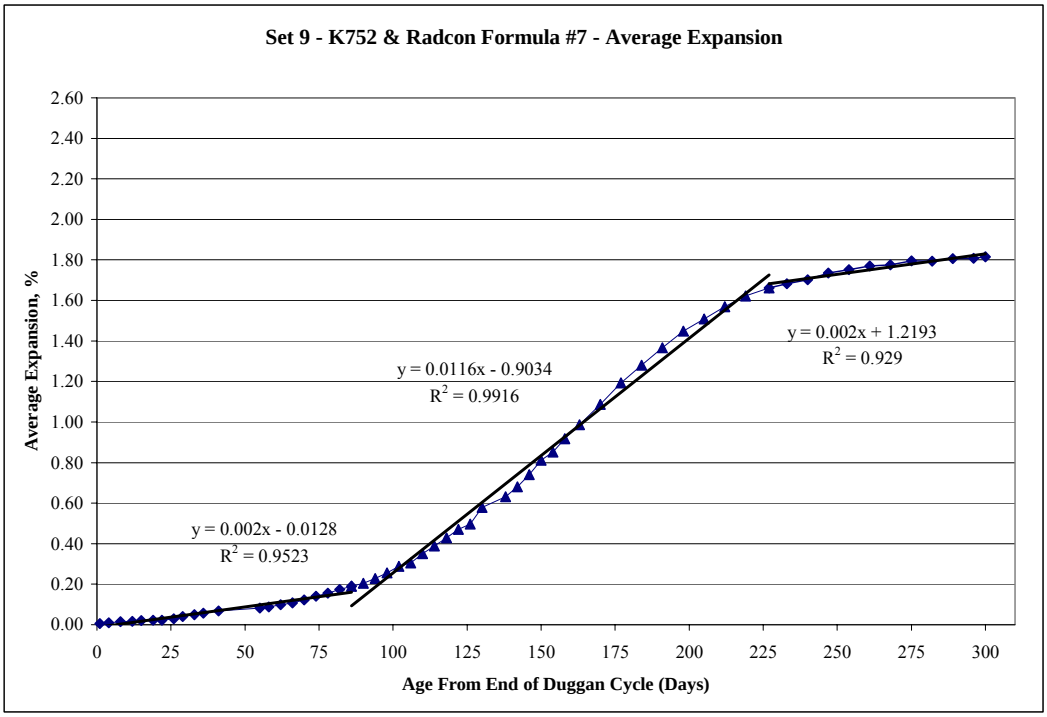

Figure 6.35 - SET 9 Linear Regression Analysis Graph (Best Fit Lines)

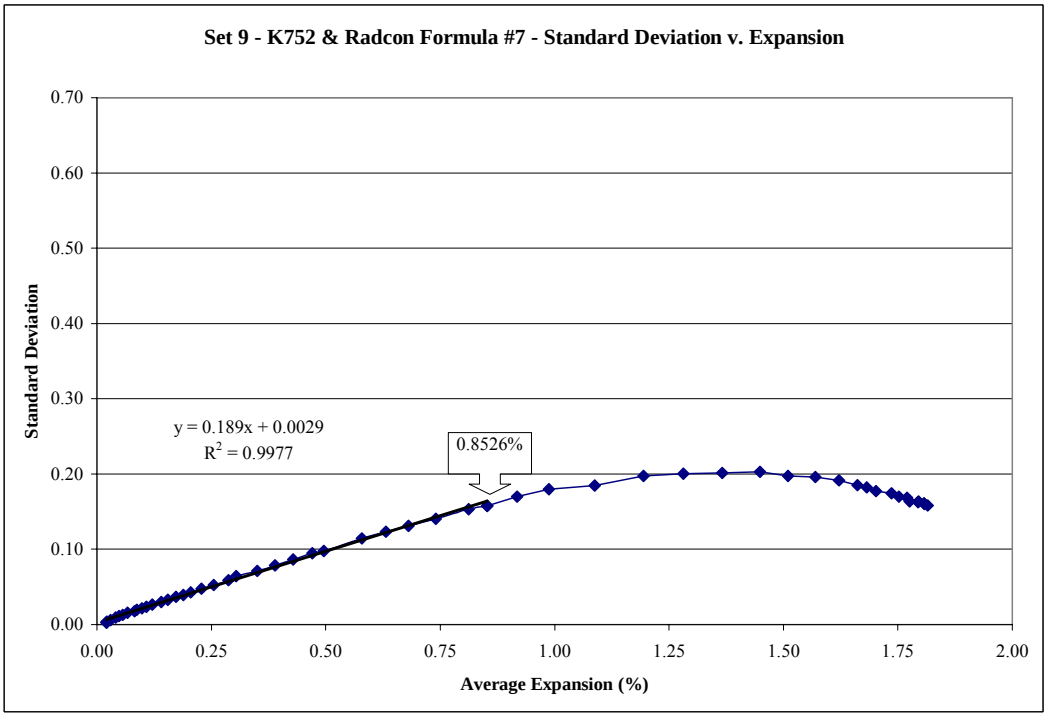

Figure 6.36 - SET 9 Standard Deviation versus Expansion

Table 6.1 - Summary of Linear Regression Analysis

EXPANSION MEASUREMENTS - LINEAR REGRESSION SUMMARY

Set 1	Maximum	Day 1 - 69	y = 0.0035x + 0.0088	R^2 = 0.9465
Control	Expansion	Day 69 - 264	y = 0.0107x - 0.4614	R^2 = 0.9833
	2.18%	Day 264 - 300	y = 0.0014x + 1.7770	R^2 = 0.9672
Set 2	Maximum	Day 1 - 69	y = 0.0029x + 0.0257	R^2 = 0.9602
ChimneySaver	Expansion	Day 69 - 236	y = 0.0091x - 0.3670	R^2 = 0.9822
	1.68%	Day 236 - 300	y = 0.0007x + 1.4646	R^2 = 0.7588
Set 3	Maximum	Day 1 - 75	y = 0.0036x + 0.005	R^2 = 0.9589
Radcon #7	Expansion	Day 75 - 236	y = 0.0136x - 0.8007	R^2 = 0.9939
	2.27%			
Set 4	Maximum	Day 1 - 100	y = 0.0026x - 0.0054	R^2 = 0.9679
Dequest 2060S	Expansion	Day 100 - 250	y = 0.0108x - 0.8425	R^2 = 0.9914
	1.82%	Day 250 - 300	y = 0.0014x + 1.4090	R^2 = 0.8775
Set 5	Maximum	Day 1 - 100	y = 0.0027x - 0.0058	R^2 = 0.9651
Dequest 2060S	Expansion	Day 100 - 264	y = 0.0140x - 1.1788	R^2 = 0.9861
ChimneySaver	2.36%	Day 264 - 300	y = 0.0015x + 1.9323	R^2 = 0.9578
Set 6	Maximum	Day 1 - 100	y = 0.0022x -0.0013	R^2 = 0.9536
Dequest 2060S	Expansion	Day 100 - 257	y = 0.0141x - 1.2823	R^2 = 0.9865
Radcon #7	2.24%	Day 257 - 300	y = 0.0014x + 1.8147	R^2 = 0.9418
Set 7	Maximum	Day 1 - 82	y = 0.0023x + 0.0010	R^2 = 0.9645
Noveon K752	Expansion	Day 82 - 261	y = 0.0107x - 0.8196	R^2 = 0.9927
	1.86%	Day 261 - 300	y = 0.0022x + 1.2118	R^2 = 0.9788
Set 8	Maximum	Day 1 - 86	y = 0.0021x - 0.0051	R^2 = 0.9663
Noveon K752	Expansion	Day 86 - 227	y = 0.0102x - 0.7550	R^2 = 0.9936
ChimneySaver	1.68%	Day 227 - 300	y = 0.0021x + 1.0506	R^2 = 0.9390
Set 9	Maximum	Day 1 - 86	y = 0.0020x - 0.0128	R^2 = 0.9523
Noveon K752	Expansion	Day 86 - 227	y = 0.0116x - 0.9034	R^2 = 0.9916
Radcon #7	1.81%	Day 227 - 300	y = 0.0020x + 1.2193	R^2 = 0.9290

Table 6.2 - Summary of Expansion Rate

Rate of Expansion Summary

Set No. - Treatment	Day	Max. Rate of Exp. (%/day)	Day 300 - Rate of Expan. (%/day)
Set 1 - Control	127	0.0161	0.0005
Set 2 - ChimneySaver	127	0.0152	0.0003
Set 3 - Radcon Formula #7 *	127	0.0192	0.0060
Set 4 - Dequest 2060S	160	0.0160	0.0013
Set 5 - Dequest / Chimney	160	0.0214	0.0012
Set 6 - Dequest / Radcon	160	0.0225	0.0019
Set 7 - Noveon K752	130	0.0198	0.0022
Set 8 - K752 / Chimney	130	0.0191	0.0022
Set 9 - K752 / Radcon	150	0.0180	0.0020

* - Expansion Measurements Discontinued at Day 236

Table 6.3 - Summary of Standard Deviation versus Expansion COV

EXPANSION MEASUREMENTS V. STANDARD DEVIATION SUMMARY

Set #	Interval	Expansion Value	Trendline	R Squared
Set 1	Day 18 - 115	0.7222%	y = 0.2148x + 0.0252	$R^2 = 0.9965$
Set 2	Day 16 - 264	1.6476%	y = 0.4089x - 0.0144	$R^2 = 0.9979$
Set 3	Day 25 - 119	0.7702%	y = 0.2076x - 0.0109	$R^2 = 0.9869$
Set 4	Day 25 - 144	0.6718%	y = 0.5545x - 0.0250	$R^2 = 0.9940$
Set 5	Day 39 - 136	0.6600%	y = 0.2655x - 0.0211	$R^2 = 0.9937$
Set 6	Day 18 - 144	0.6498%	y = 0.4092x - 0.0148	$R^2 = 0.9941$
Set 7	Day 15 - 158	0.8544%	y = 0.2373x - 0.0081	$R^2 = 0.9912$
Set 8	Day 15 - 158	0.8494%	y = 0.2148x - 0.0041	$R^2 = 0.9966$
Set 9	Day 15 - 154	0.8526%	y = 0.1873x + 0.0032	$R^2 = 0.9977$

Table 6.4 - Summary of Expansion Values and Rankings

Summary of Expansion Values

Set	Exp. (%)	Slope (%/day)	Max. Rate (d% / d day)	COV
1	2.18	0.0107	0.0161	0.2148
2	1.68	0.0091	0.0152	0.4089
3	2.27	0.0136	0.0192	0.2076
4	1.82	0.0108	0.01595	0.5545
5	2.36	0.0140	0.0214	0.2655
6	2.24	0.0141	0.0225	0.4092
7	1.86	0.0107	0.0198	0.2373
8	1.68	0.0102	0.0191	0.2148
9	1.81	0.0116	0.0180	0.1873

Set Ranking - Highest to Lowest Values

Exp. (Set No.)	Slope (Set No.)	Max. Rate (Set No.)	COV (Set No.)
5	6	6	4
3	5	5	6
6	3	7	2
1	9	3	5
7	4	8	7
4	7	9	8
9	1	1	1
8	8	4	3
2	2	2	9

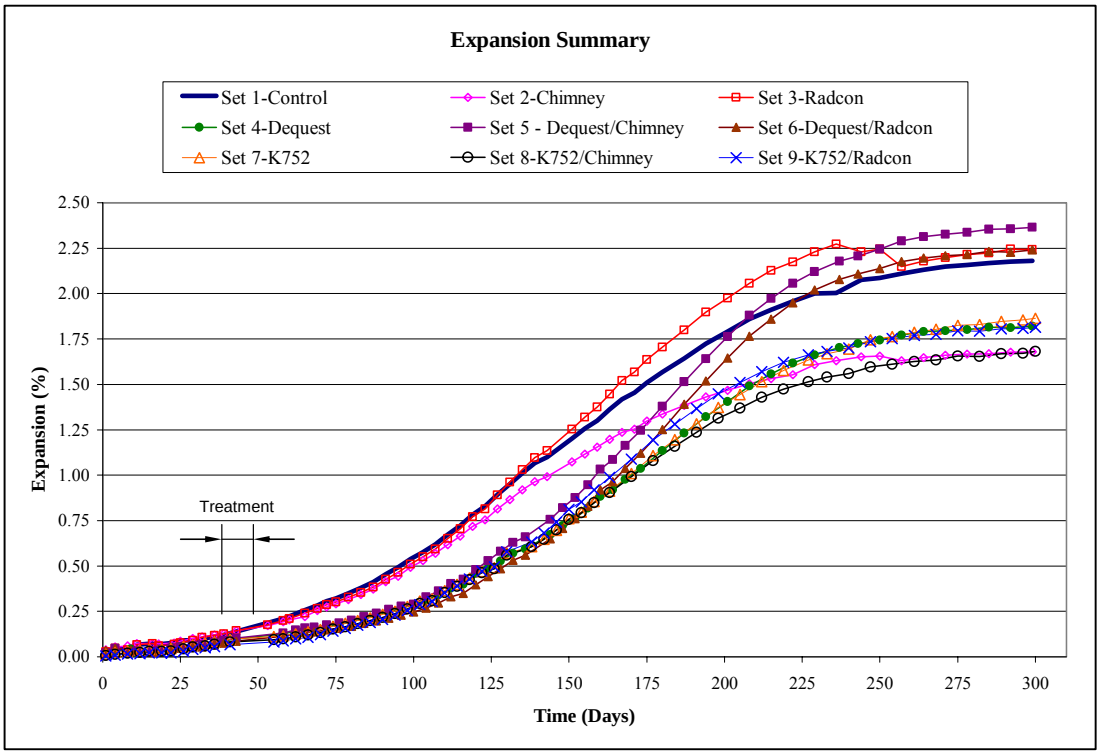

Figure 6.37 - Summary of Expansion versus Time (Nine Sets)

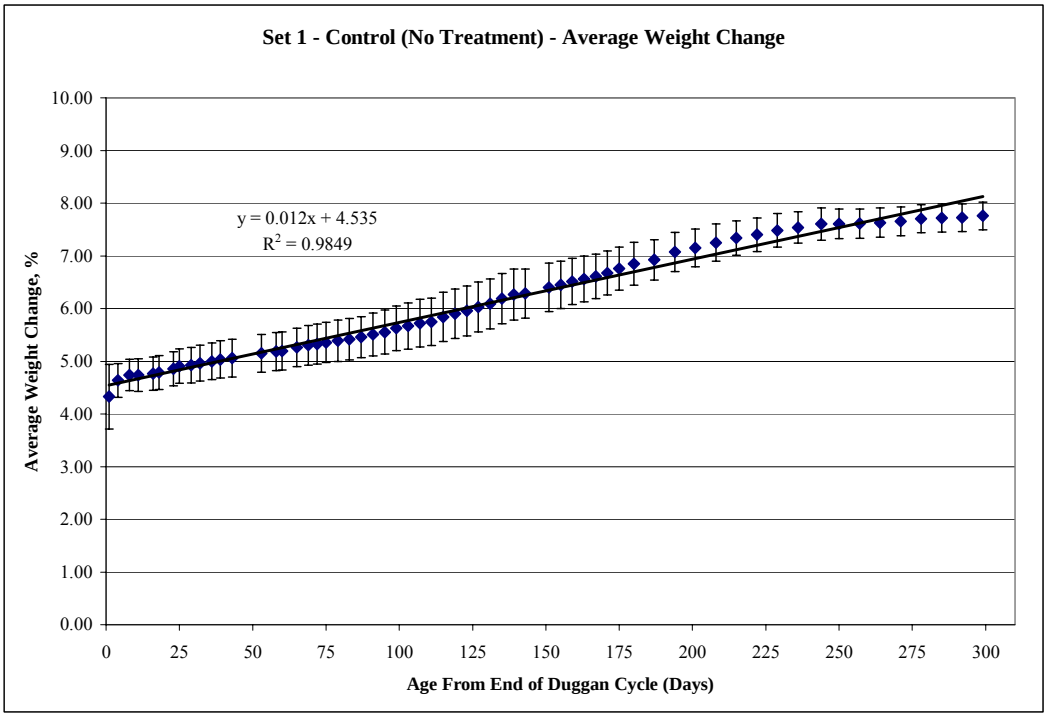

Figure 6.38 - SET 1 Weight Change versus Time with Error Bars

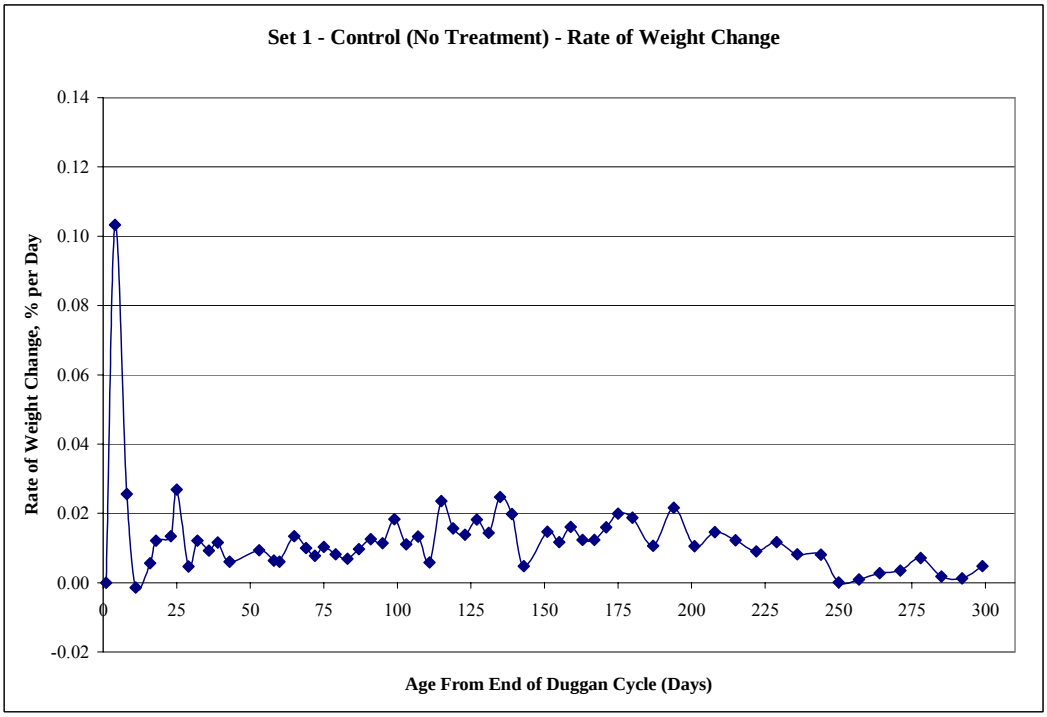

Figure 6.39 - SET 1 Rate of Weight Change versus Time (First Derivative)

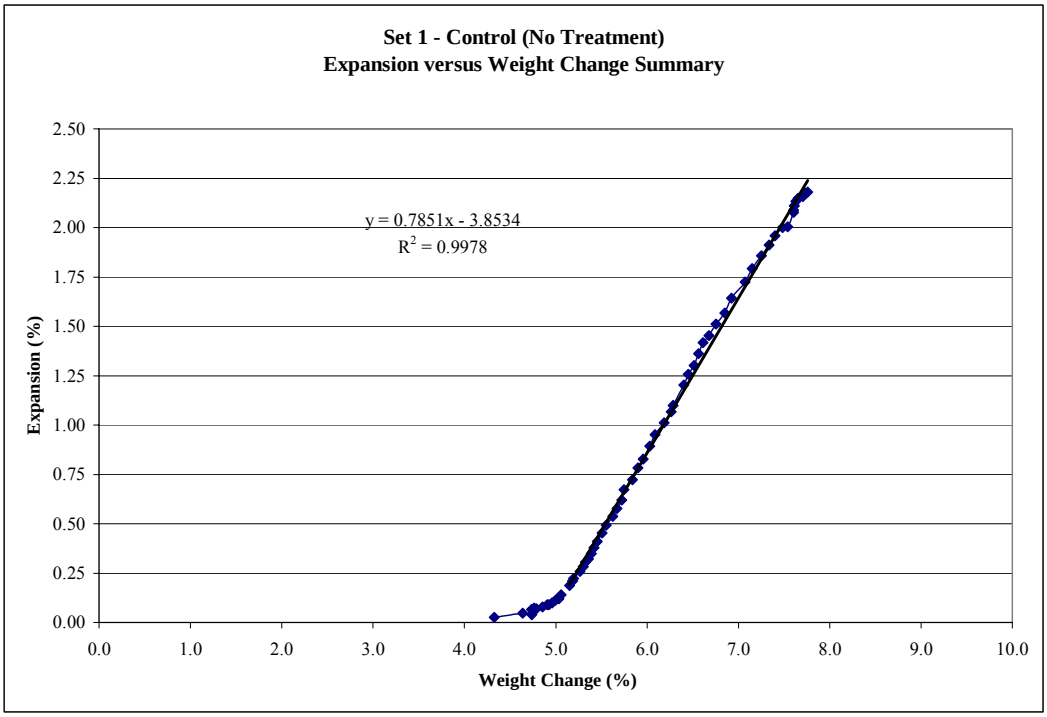

Figure 6.40 - SET 1 Expansion versus Weight Change

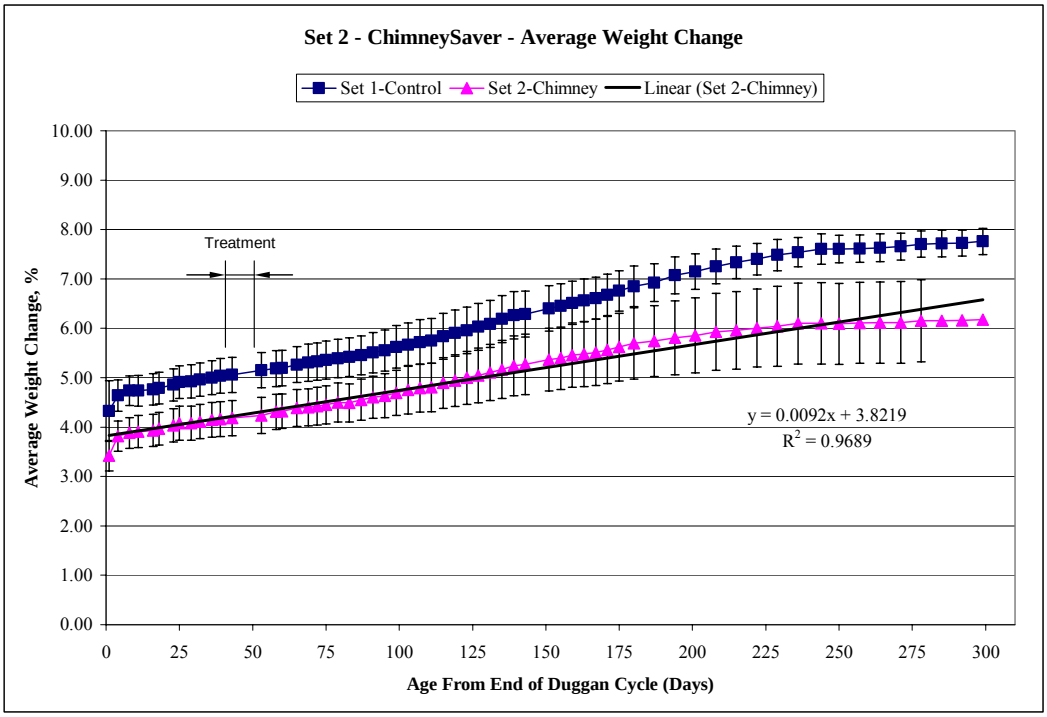

Figure 6.41 - SET 2 Weight Change versus Time with Error Bars

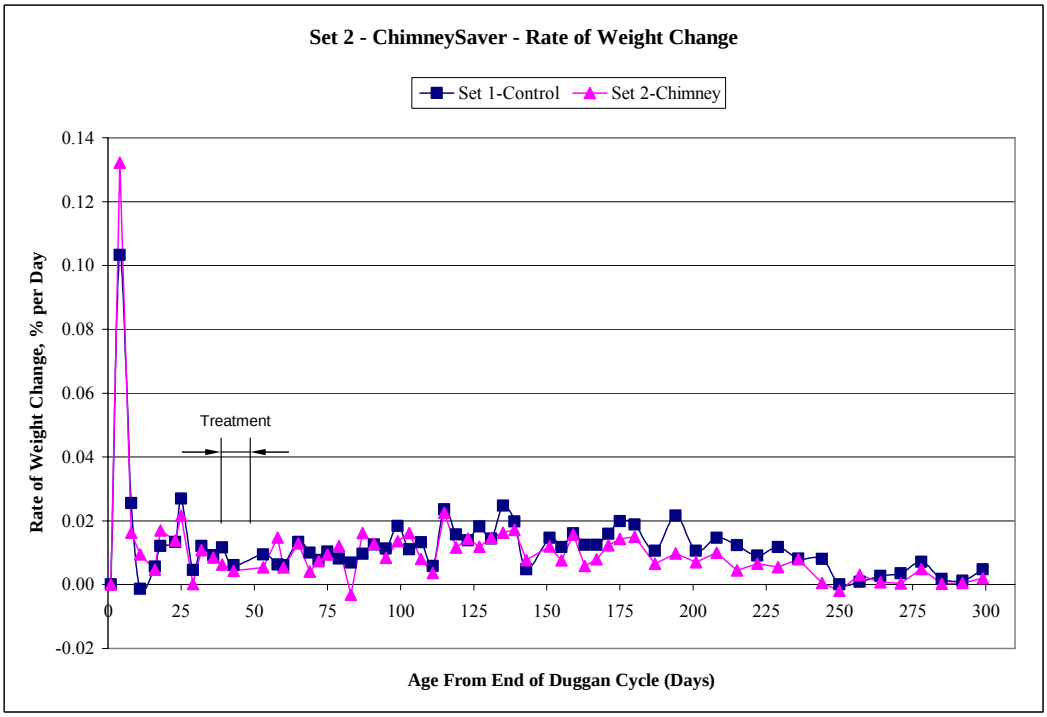

Figure 6.42 - SET 2 Rate of Weight Change versus Time (First Derivative)

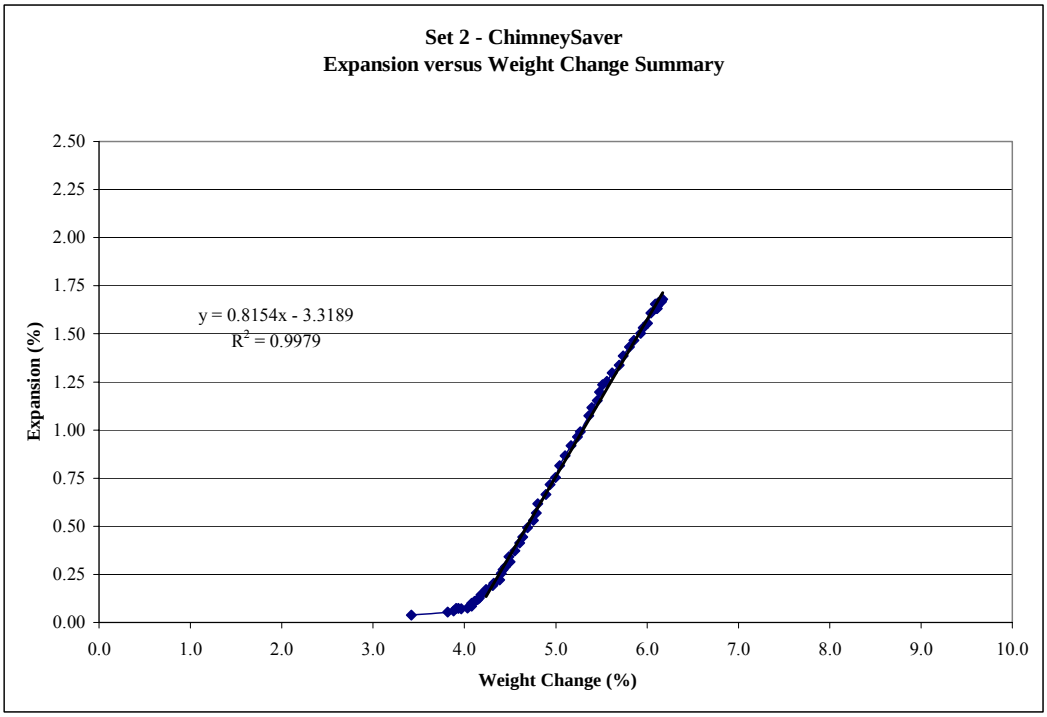

Figure 6.43 - SET 2 Expansion versus Weight Change

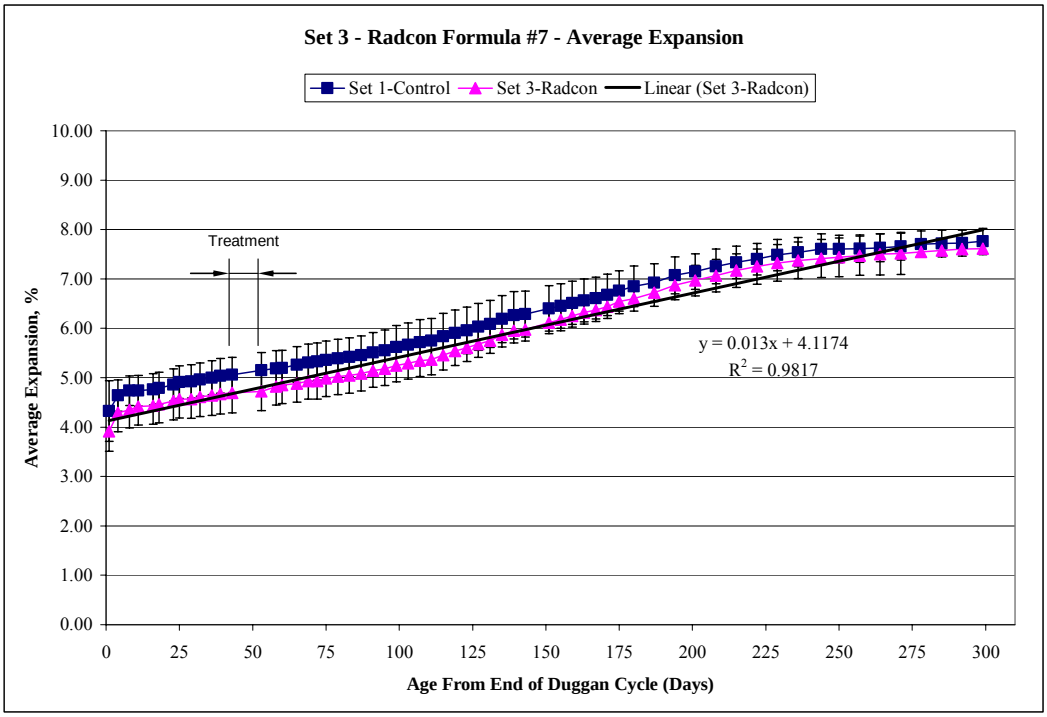

Figure 6.44 - SET 3 Weight Change versus Time with Error Bars

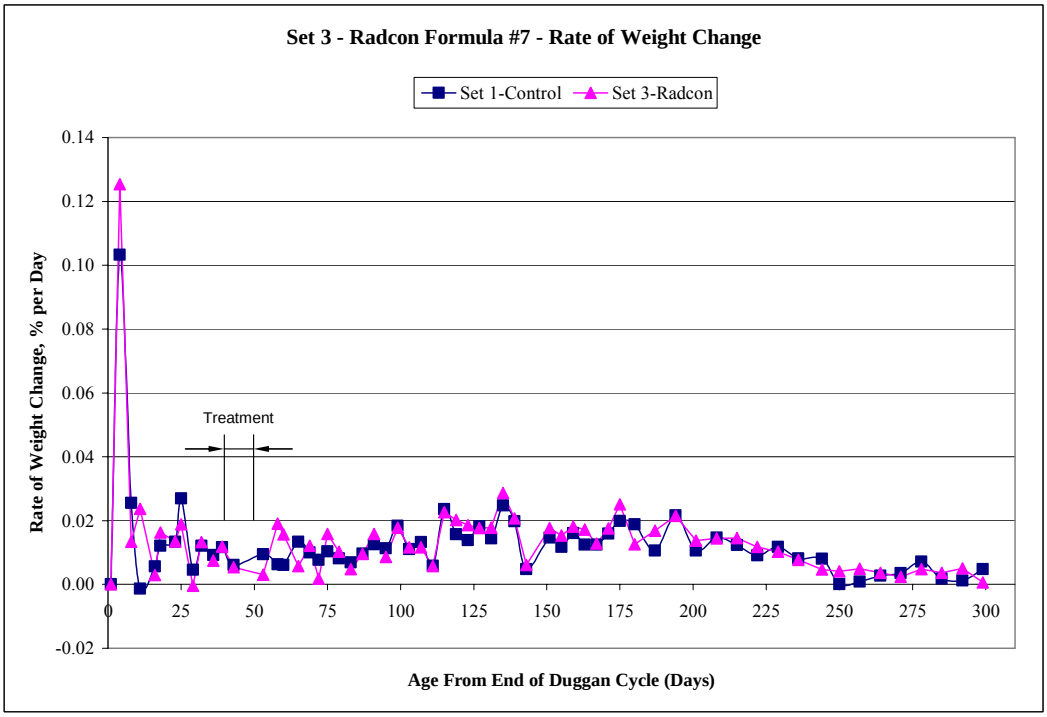

Figure 6.45 - SET 3 Rate of Weight Change versus Time (First Derivative)

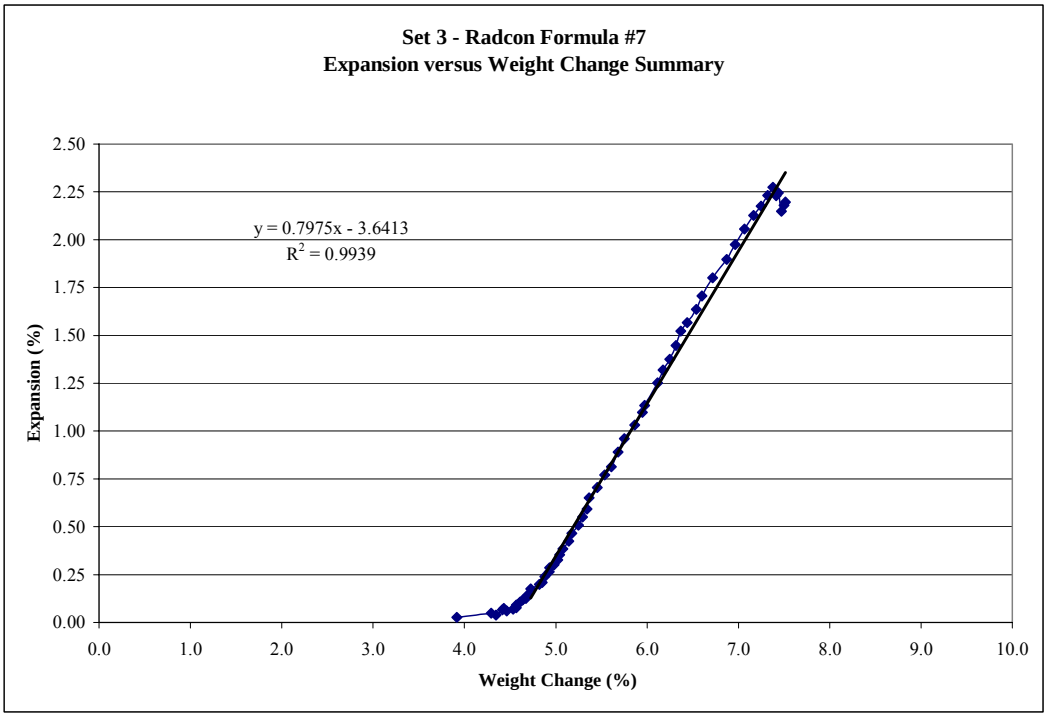

Figure 6.46 - SET 3 Expansion versus Weight Change

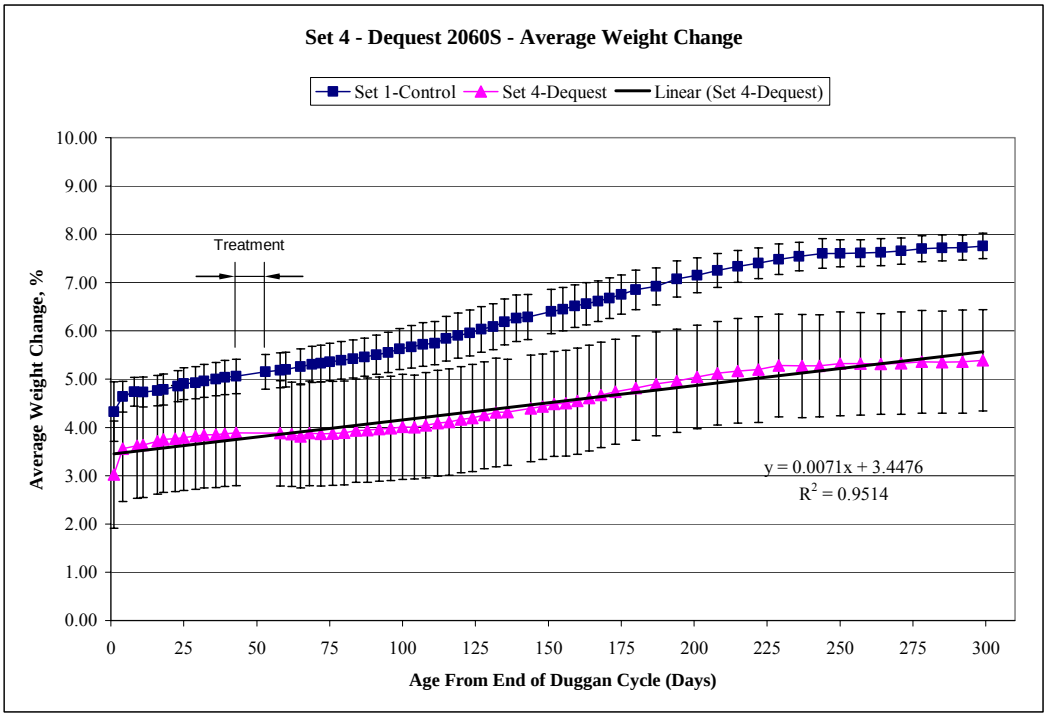

Figure 6.47 - SET 4 Weight Change versus Time with Error Bars

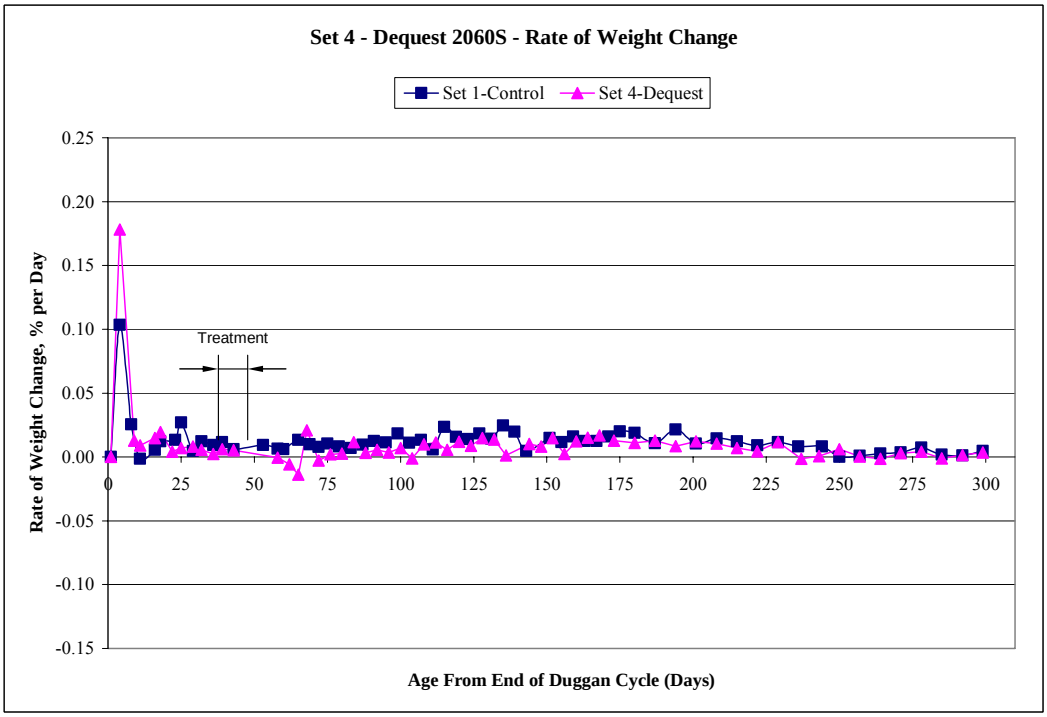

Figure 6.48 - SET 4 Rate of Weight Change versus Time (First Derivative)

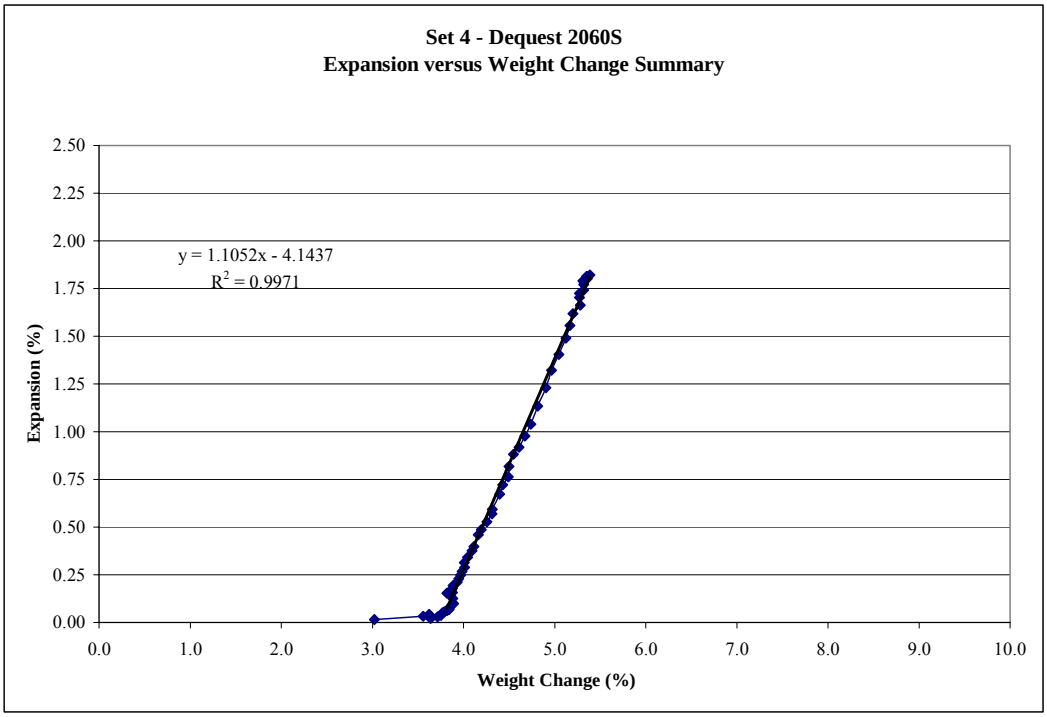

Figure 6.49 - SET 4 Expansion versus Weight Change

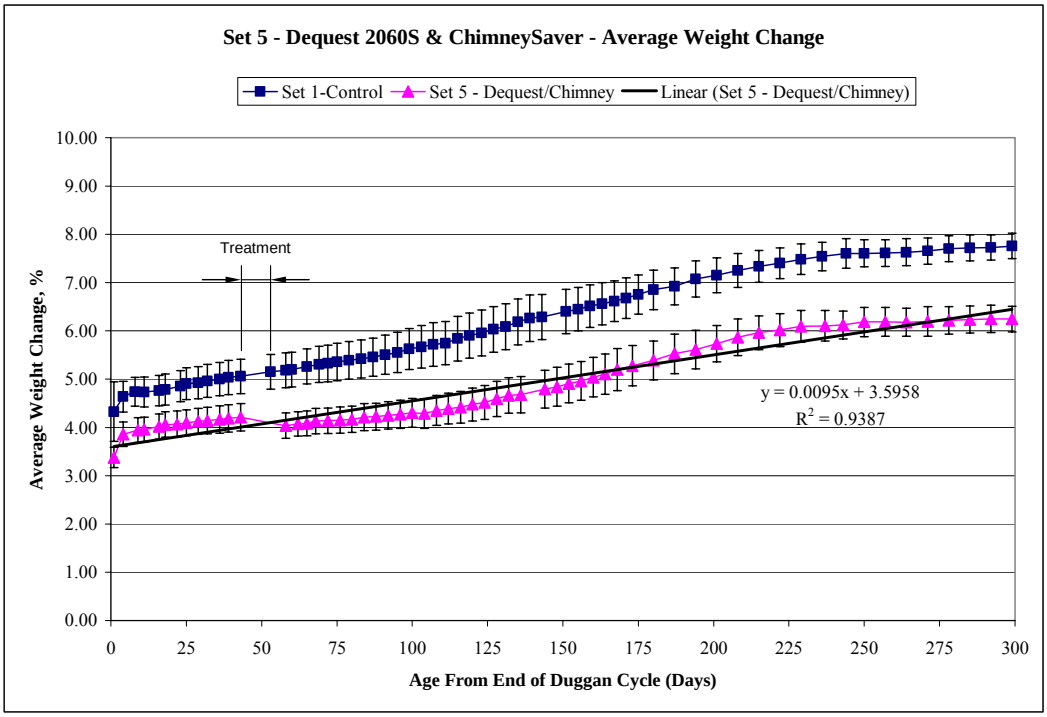

Figure 6.50 - SET 5 Weight Change versus Time with Error Bars

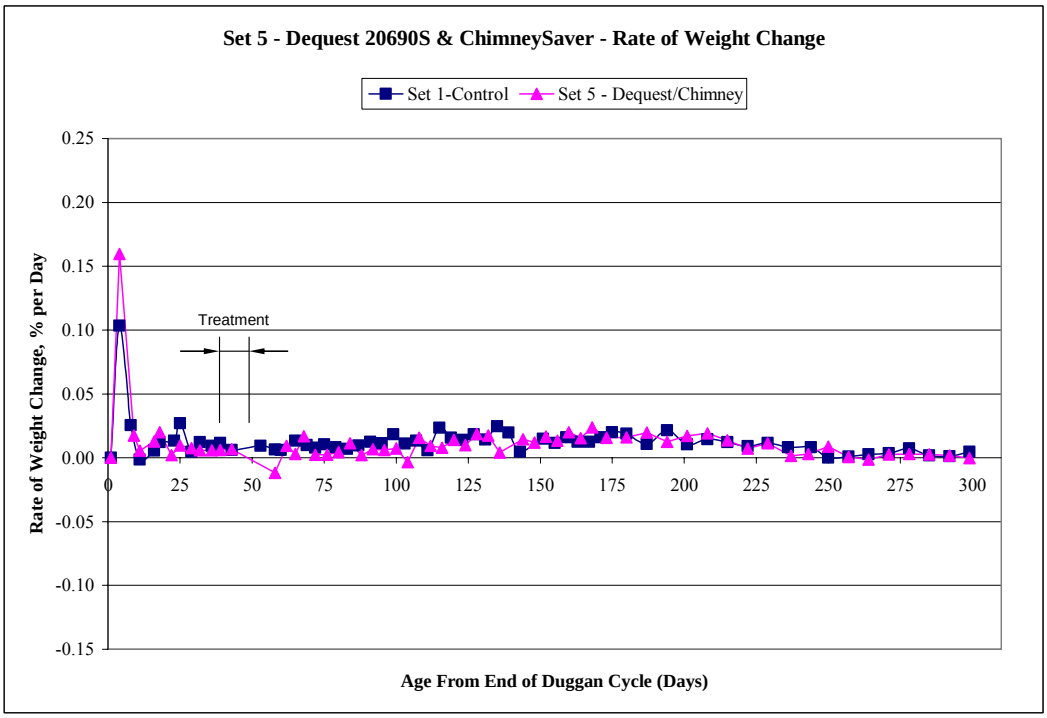

Figure 6.51 - SET 5 Rate of Weight Change versus Time (First Derivative)

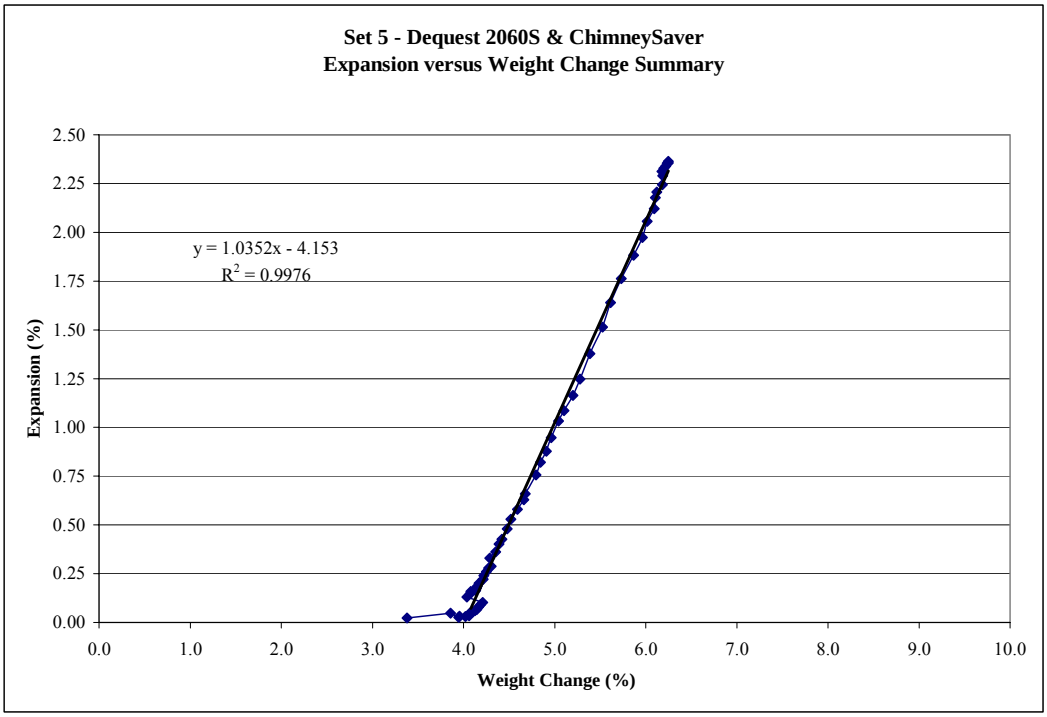

Figure 6.52 - SET 5 Expansion versus Weight Change

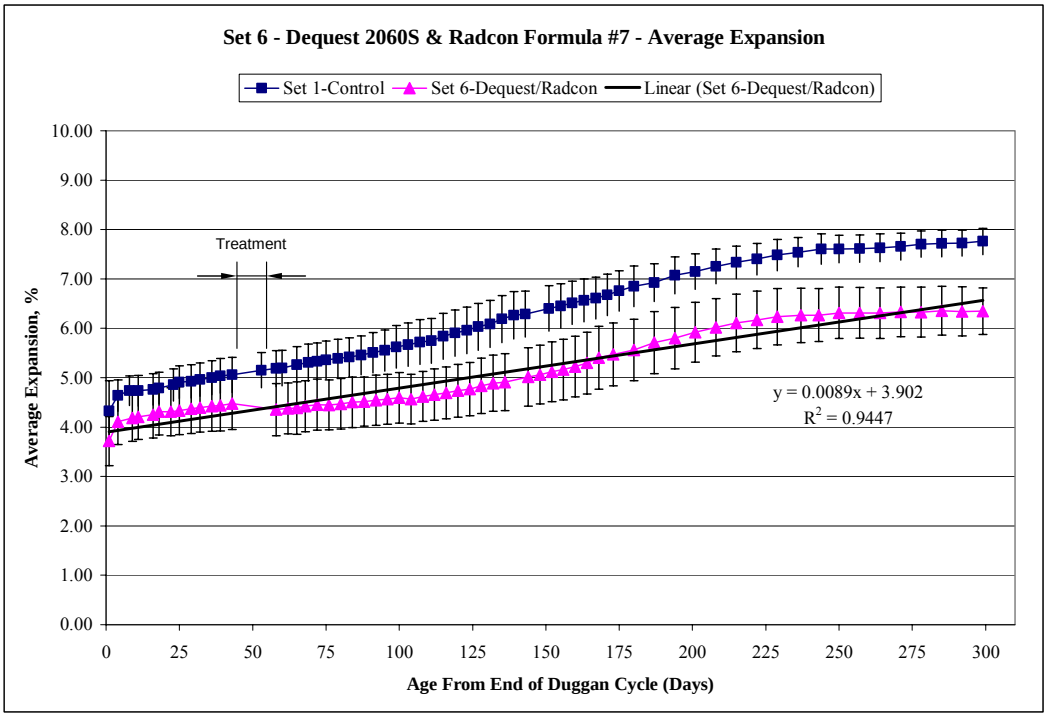

Figure 6.53 - SET 6 Weight Change versus Time with Error Bars

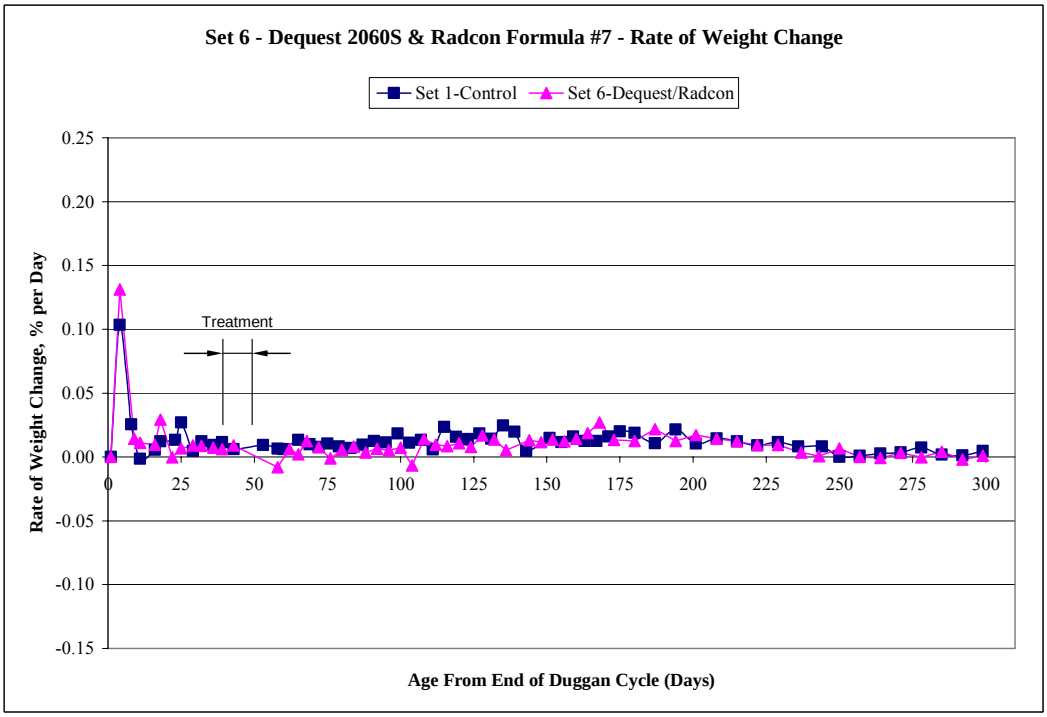

Figure 6.54 - SET 6 Rate of Weight Change versus Time (First Derivative)

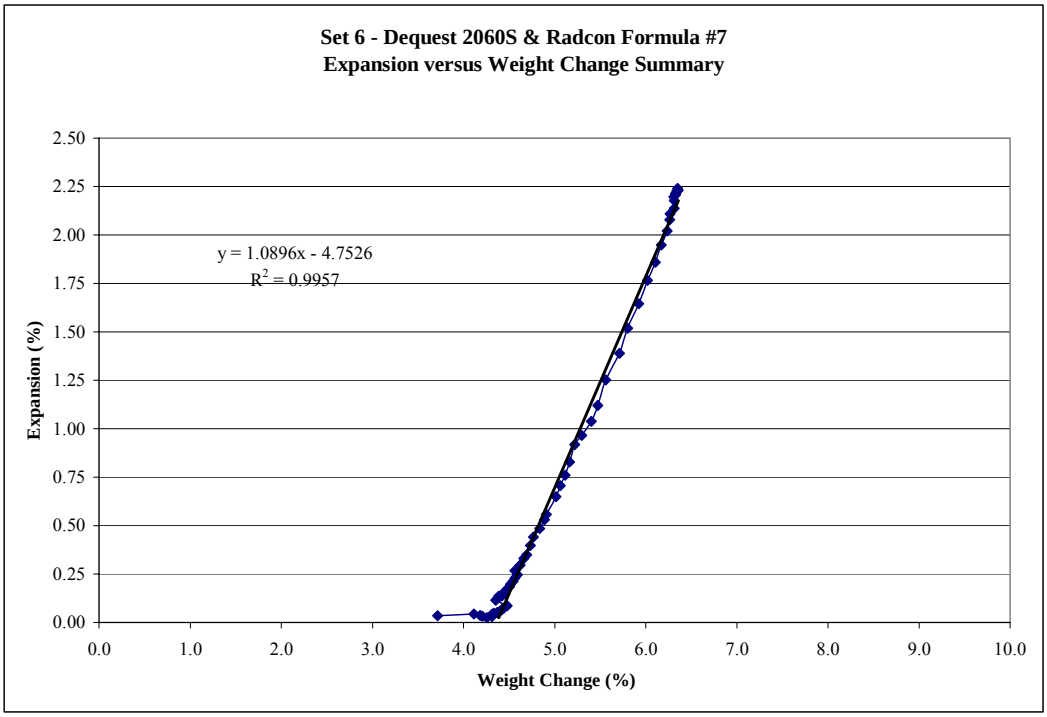

Figure 6.55 - SET 6 Expansion versus Weight Change

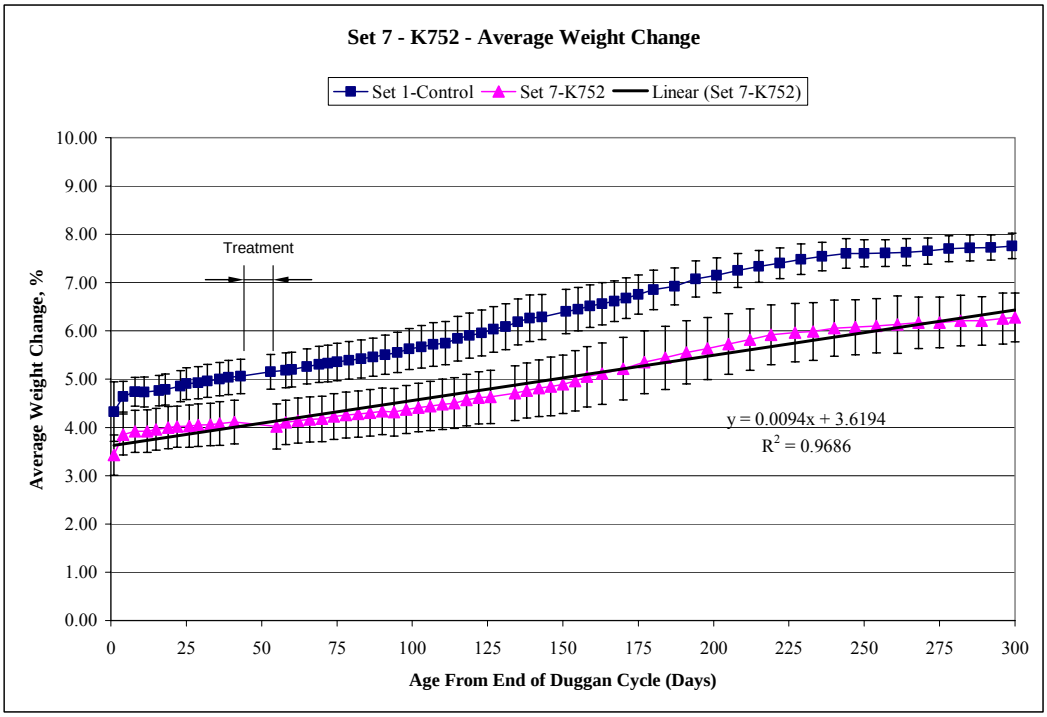

Figure 6.56 - SET 7 Weight Change versus Time with Error Bars

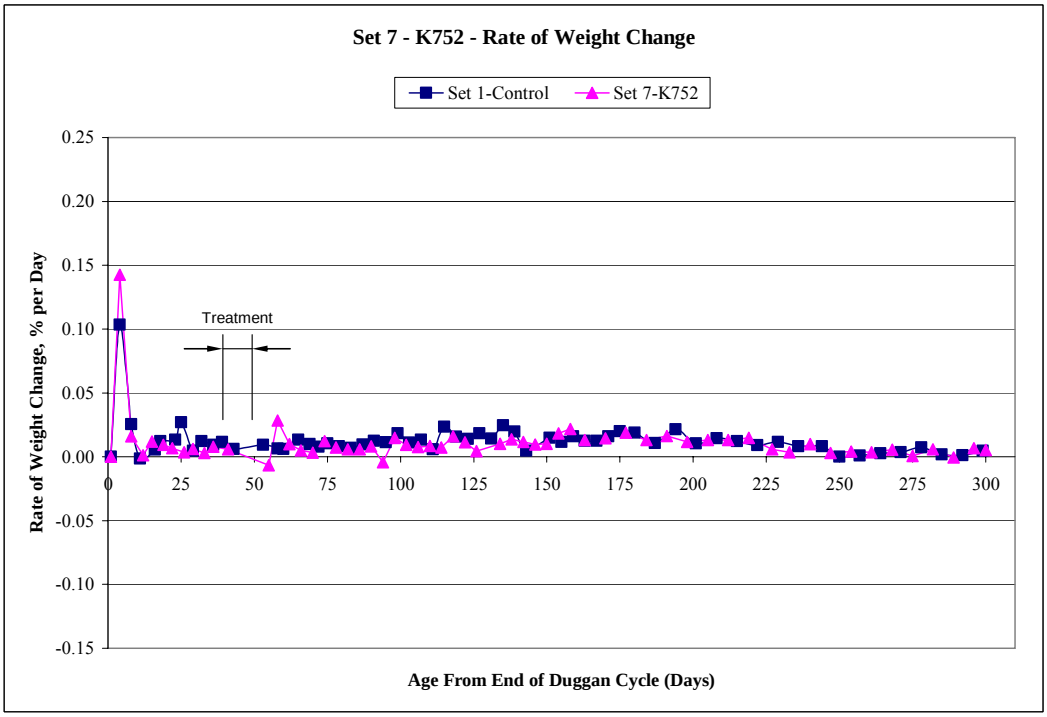

Figure 6.57 - SET 7 Rate of Weight Change versus Time (First Derivative)

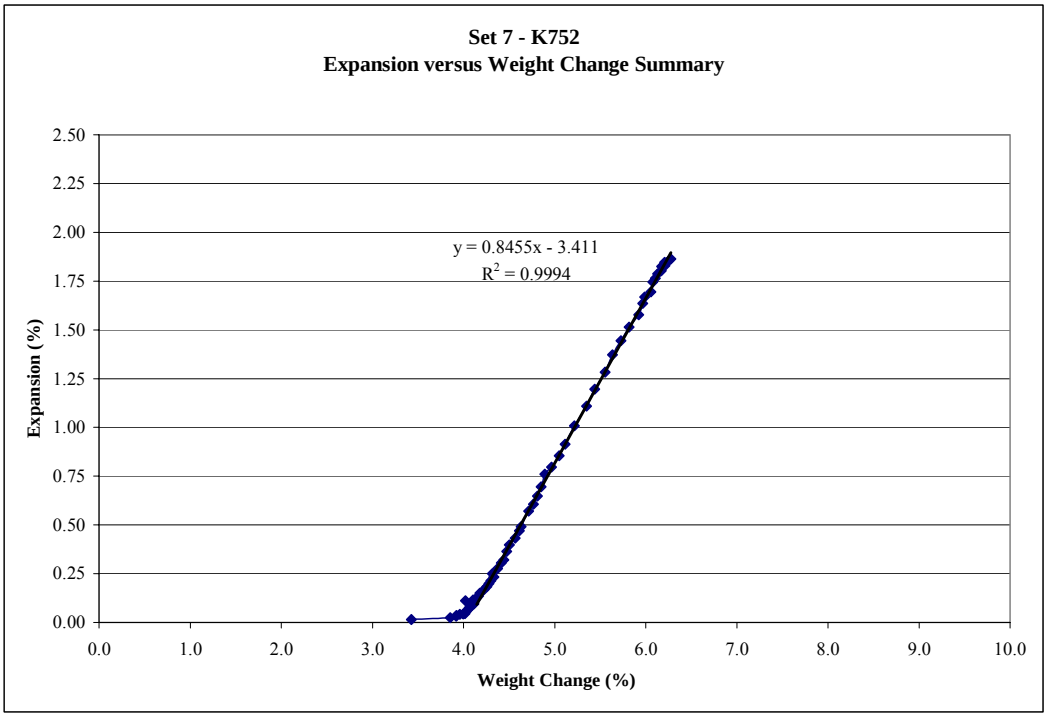

Figure 6.58 - SET 7 Expansion versus Weight Change

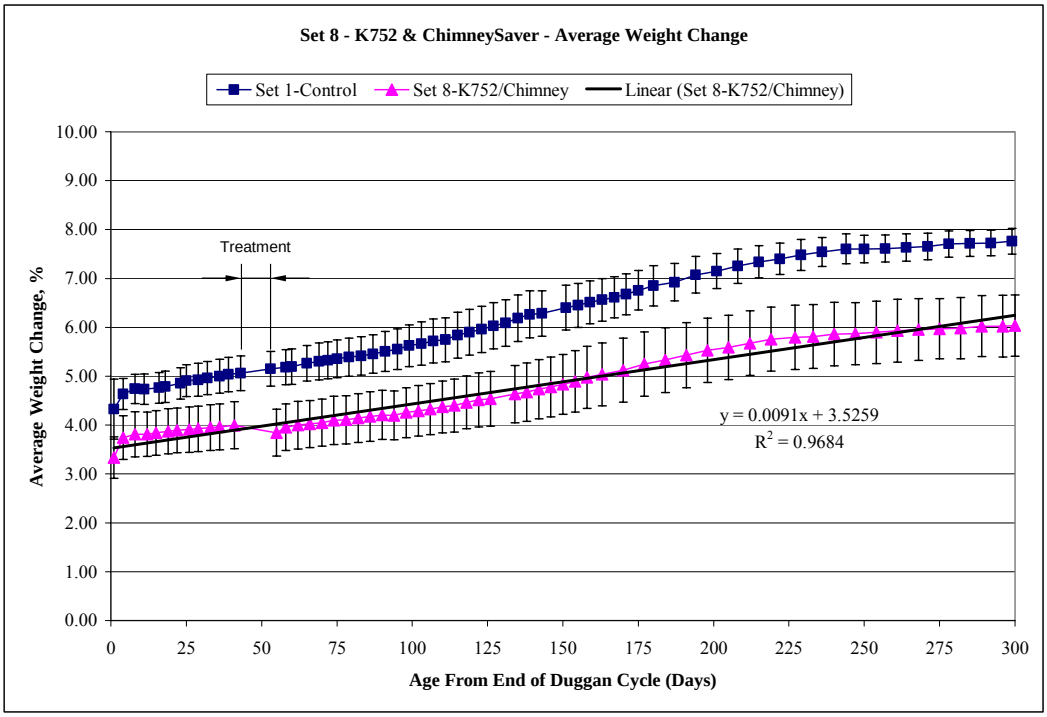

Figure 6.59 - SET 8 Weight Change versus Time with Error Bars

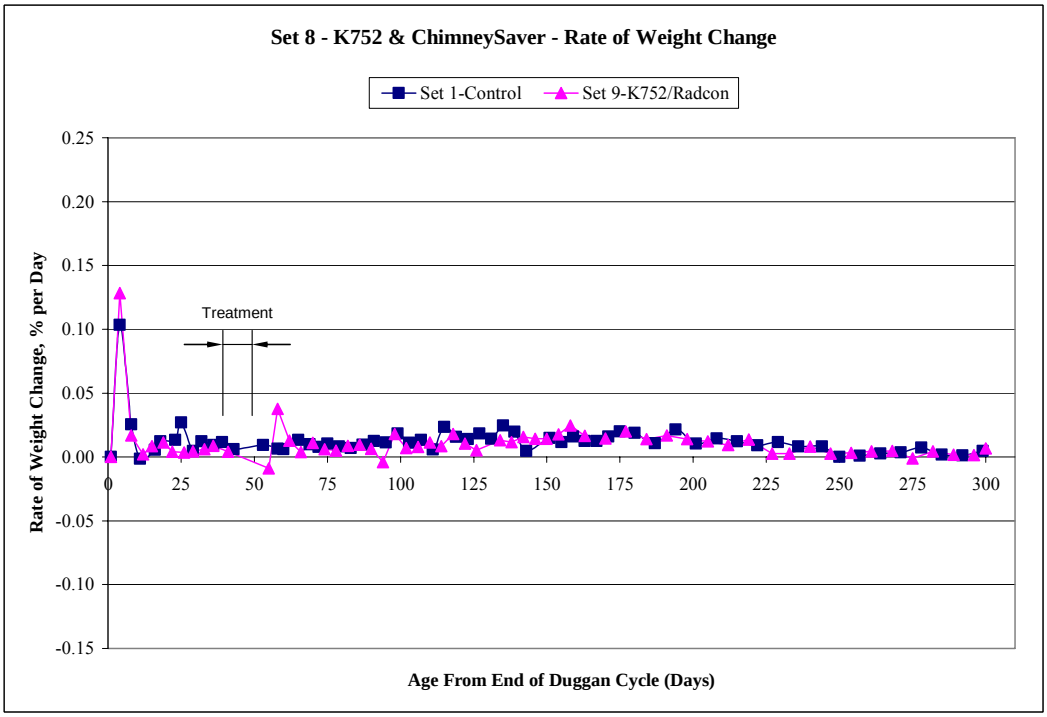

Figure 6.60 - SET 8 Rate of Weight Change versus Time (First Derivative)

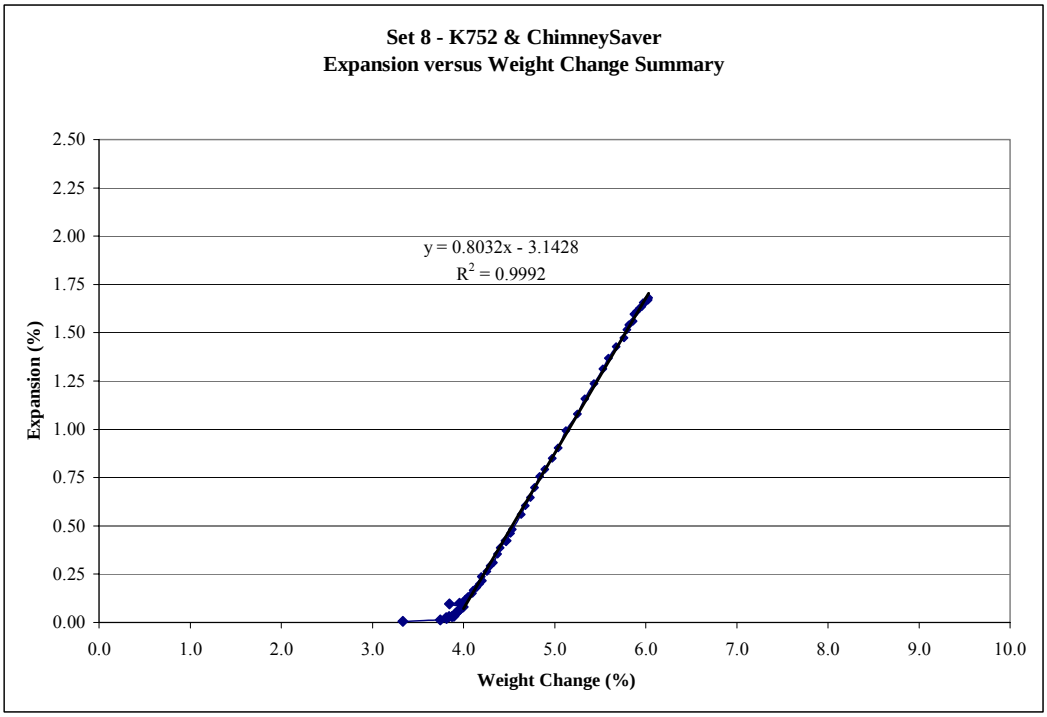

Figure 6.61 - SET 8 Expansion versus Weight Change

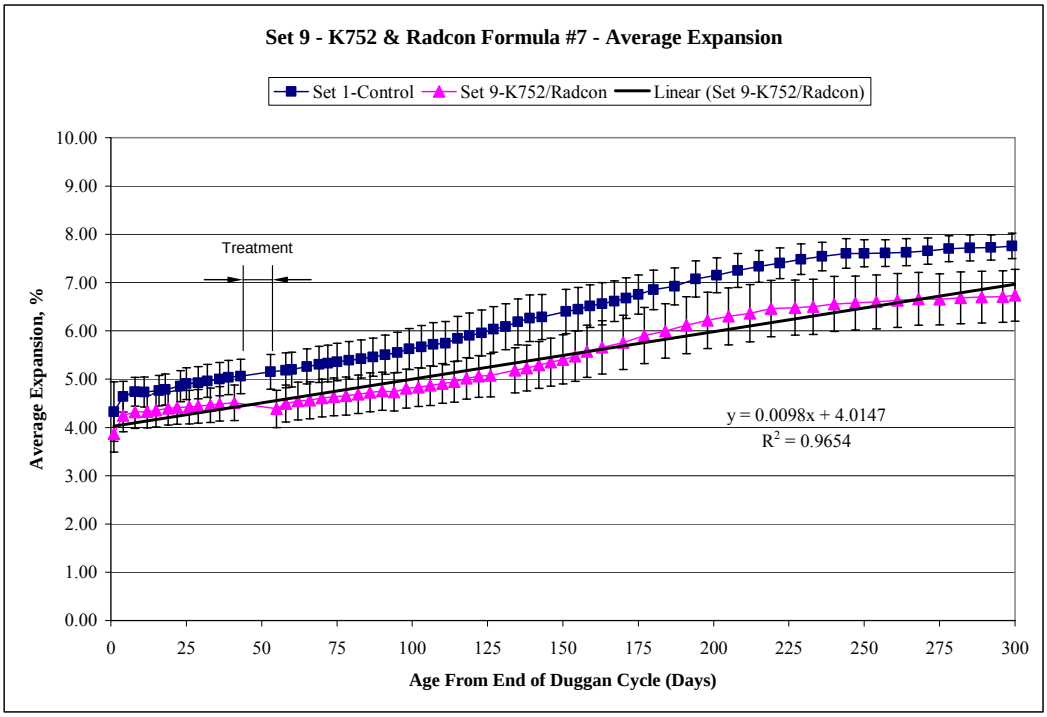

Figure 6.62 - SET 9 Weight Change versus Time with Error Bars

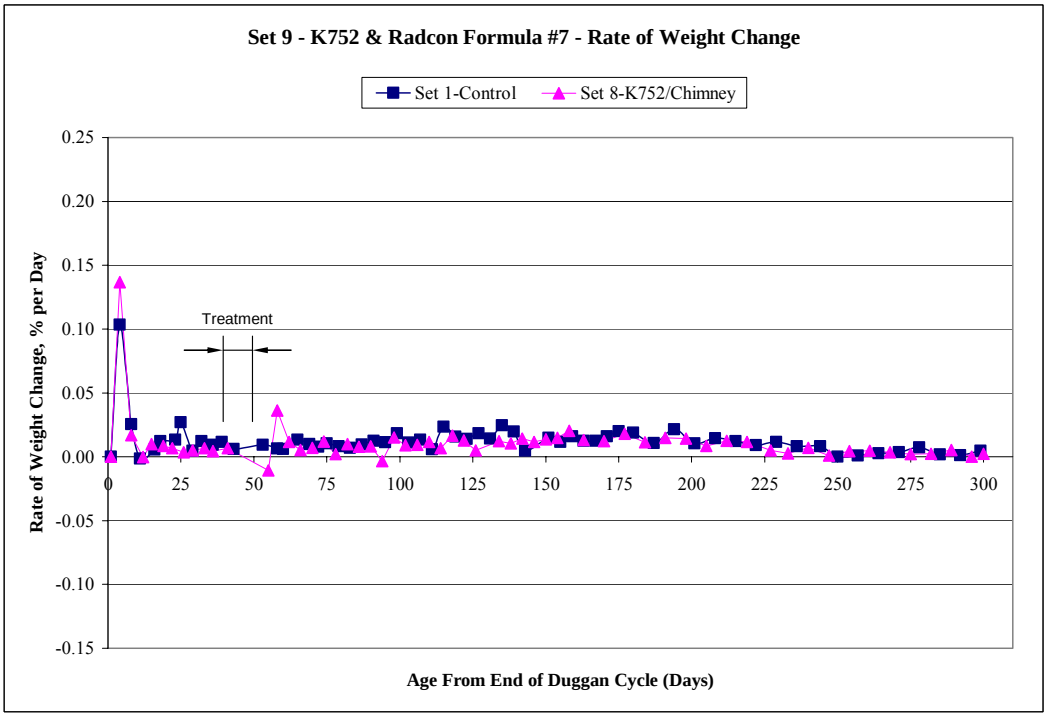

Figure 6.63 - SET 9 Rate of Weight Change versus Time (First Derivative)

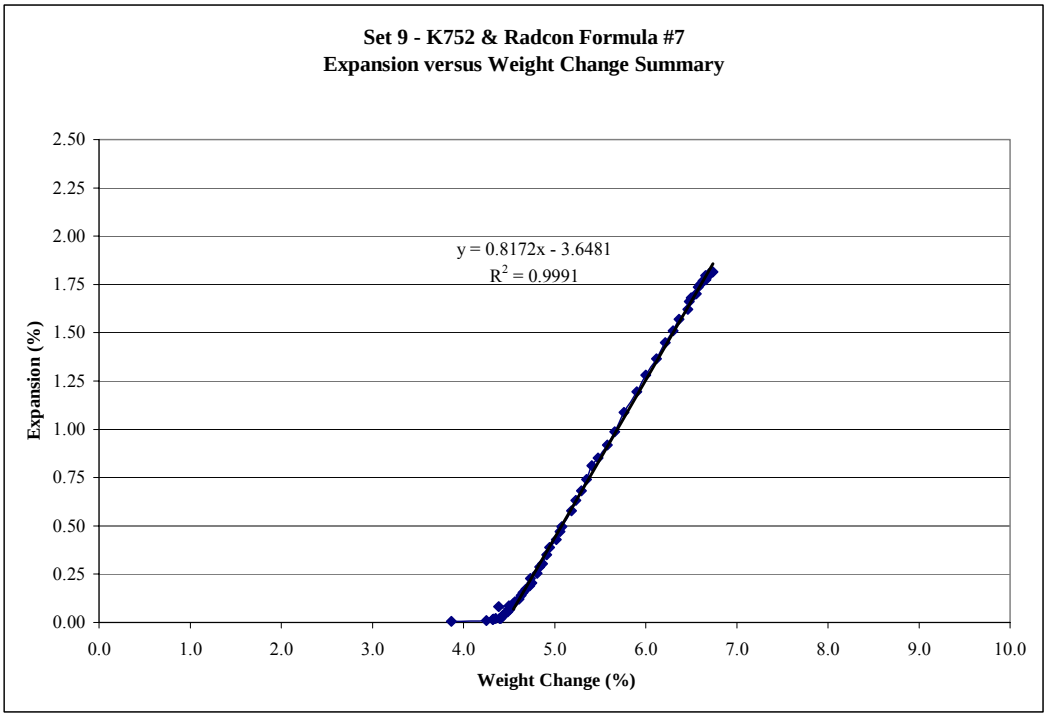

Figure 6.64 - SET 9 Expansion versus Weight Change

Table 6.5 - Summary of Linear Regression Analysis

WEIGHT SUMMARY

	Max. Change	Interval	Trendline	R Squared
Set 1	7.70%	Day 1 - 300	y = 0.0120x + 4.5350	R^2 = 0.9849
Set 2	6.15%	Day 1 - 300	y = 0.0092x + 3.8219	R^2 = 0.9689
Set 3	7.55%	Day 1 - 300	y = 0.0130x + 4.1174	R^2 = 0.9817
Set 4	5.33%	Day 1 - 300	y = 0.0071x + 3.4476	R^2 = 0.9514
Set 5	6.20%	Day 1 - 300	y = 0.0095x + 3.5958	R^2 = 0.9515
Set 6	6.33%	Day 1 - 300	y = 0.0089x + 3.9020	R^2 = 0.9447
Set 7	6.13%	Day 1 - 300	y = 0.0094x + 3.6194	R^2 = 0.9686
Set 8	5.93%	Day 1 - 300	y = 0.0091x + 3.5259	R^2 = 0.9684
Set 9	6.63%	Day 1 - 300	y = 0.0098x + 4.0147	R^2 = 0.9654

Table 6.6 - Summary of Rate of Weight Change

Rate of Weight Change Summary

Set No. - Treatment	Day	Max. Rate (%/day)	Day 300 (%/day)
Set 1 - Control	4	0.1033	0.0047
Set 2 - ChimneySaver	4	0.1322	0.0020
Set 3 - Radcon Formula #7	4	0.1254	0.0006
Set 4 - Dequest 2060S	4	0.1780	0.0036
Set 5 - Dequest / Chimney	4	0.1597	-0.0004
Set 6 - Dequest / Radcon	4	0.1314	0.0009
Set 7 - Noveon K752	4	0.1425	0.0052
Set 8 - K752 / Chimney	4	0.1367	0.0025
Set 9 - K752 / Radcon	4	0.1285	0.0067

Table 6.7 - Summary of Expansion versus Weight Change

WEIGHT CHANGE V. EXPANSION SUMMARY

Set #	Interval	Trendline	R Squared
Set 1	Day 58 - 300	y = 0.7851x - 3.8534	R^2 = 0.9978
Set 2	Day 58 - 300	y = 0.8154x - 3.3189	R^2 = 0.9979
Set 3	Day 58 - 271	y = 0.7975x - 3.6413	R^2 = 0.9939
Set 4	Day 65 - 300	y = 1.1052x - 4.1437	R^2 = 0.9971
Set 5	Day 65 - 300	y = 1.0352x - 4.1530	R^2 = 0.9976
Set 6	Day 65 - 300	y = 1.0896x -4.7526	R^2 = 0.9957
Set 7	Day 62 - 300	y = 0.8455x - 3.4110	R^2 = 0.9994
Set 8	Day 62 - 300	y = 0.8032x - 3.1428	R^2 = 0.9992
Set 9	Day 62 - 300	y = 0.8172x - 3.6481	R^2 = 0.9991

Table 6.8 - Summary of Weight Change Value and Rankings

Summary of Weight Change Values

Set	Weight Gain (%)	Slope (%/day)	Max. Rate (d % / d day)	Exp./Wt. Slope (% / %)
1	7.70	0.0120	0.1033	0.7851
2	6.15	0.0092	0.1322	0.8154
3	7.55	0.0130	0.1254	0.7975
4	5.33	0.0071	0.1780	1.1052
5	6.20	0.0095	0.1597	1.0352
6	6.33	0.0089	0.1314	1.0896
7	6.13	0.0094	0.1425	0.8455
8	5.93	0.0091	0.1367	0.8032
9	6.63	0.0098	0.1285	0.8172

Set Ranking - Highest to Lowest Values

Weight Gain (Set No.)	Slope (Set No.)	Max. Rate (Set No.)	Exp./Wt. Slope (Set No.)
1	3	4	4
3	1	5	6
9	9	7	5
6	5	8	7
5	7	2	9
2	2	6	2
7	8	9	8
8	6	3	3
4	4	1	1

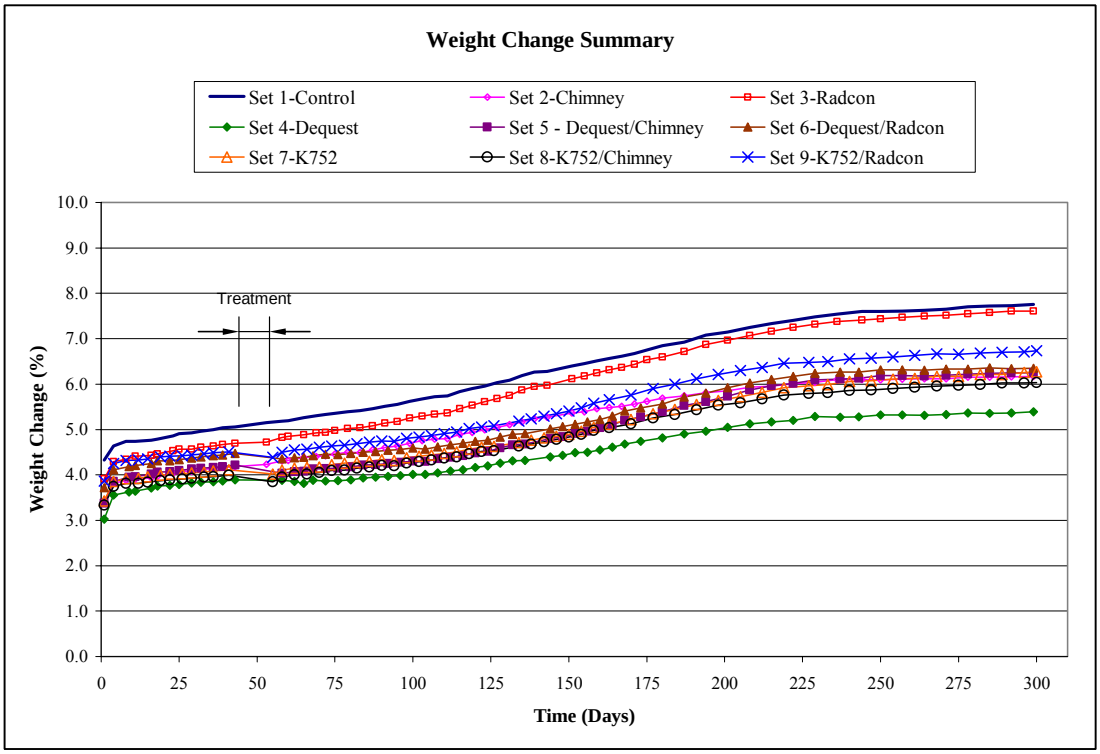

Figure 6.65 - Summary of Weight Change (Nine Sets)

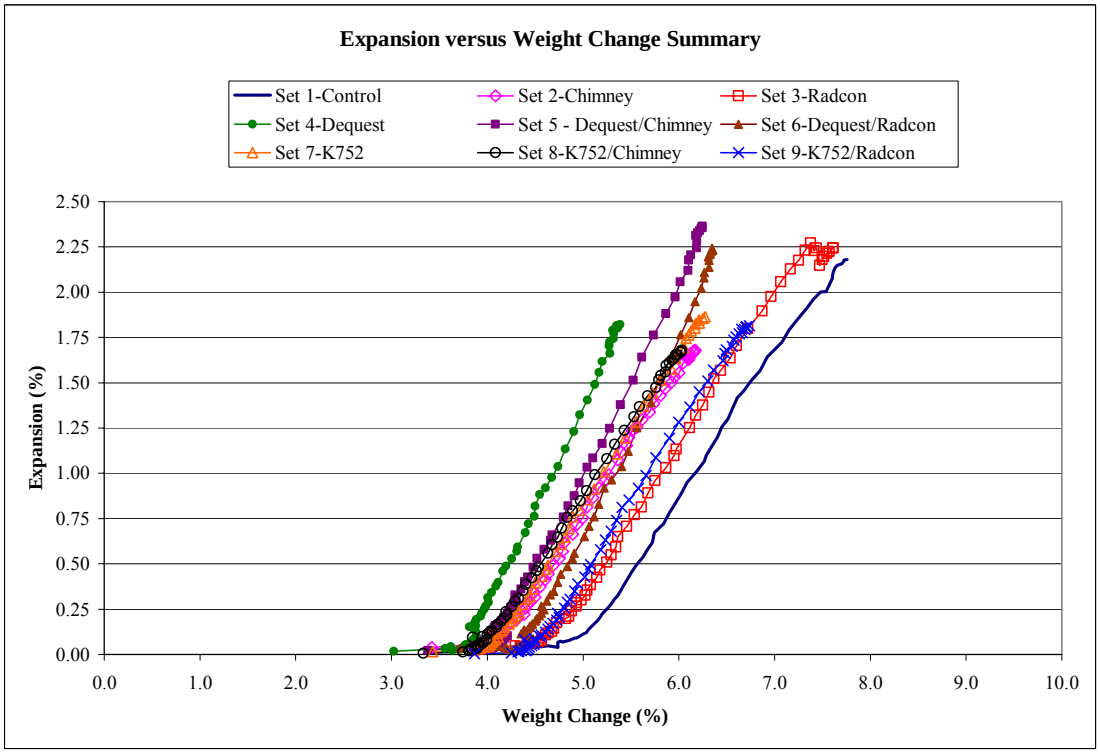

Figure 6.66 - Summary of Expansion versus Weight Change (Nine Sets)

Table 6.9 - Average Compressive Strength and Percent Reduction of 4" Diameter by 8" Tall Cylinders

	AVERAGE STRENGTH (PSI)			PERCENT REDUCTION	
	30 Days	90 Days	240 Days	90 Days	240 Days
	Stand. Dev.	Stand. Dev.	Stand. Dev.		
Set 1-Control	3146	2703	1206	-14%	-62%
	44	213	49		
Set 2-Chimney	3674	2479	501	-33%	-86%
	87	329	25		
Set 3-Radcon	3415	2554	511	-25%	-85%
	364	291	73		
Set 4-Dequest	3515	2547	473	-28%	-87%
	45	126	58		
Set 5-Dequest & Chimney	3613	2727	426	-25%	-88%
	211	221	32		
Set 6-Dequest & Radcon	3196	3036	1124	-5%	-65%
	61	101	76		
Set 7-K752	3739	3152	484	-16%	-87%
	26	145	26		
Set 8-K752 & Chimney	3686	2919	560	-21%	-85%
	143	34	88		
Set 9-K752 & Radcon	3792	3371	1222	-11%	-68%
	74	129	81		

* Stand. Dev. = Standard Deviation of Three Tested Cylinders

** Percent Reduction from 30 Day Compression Test

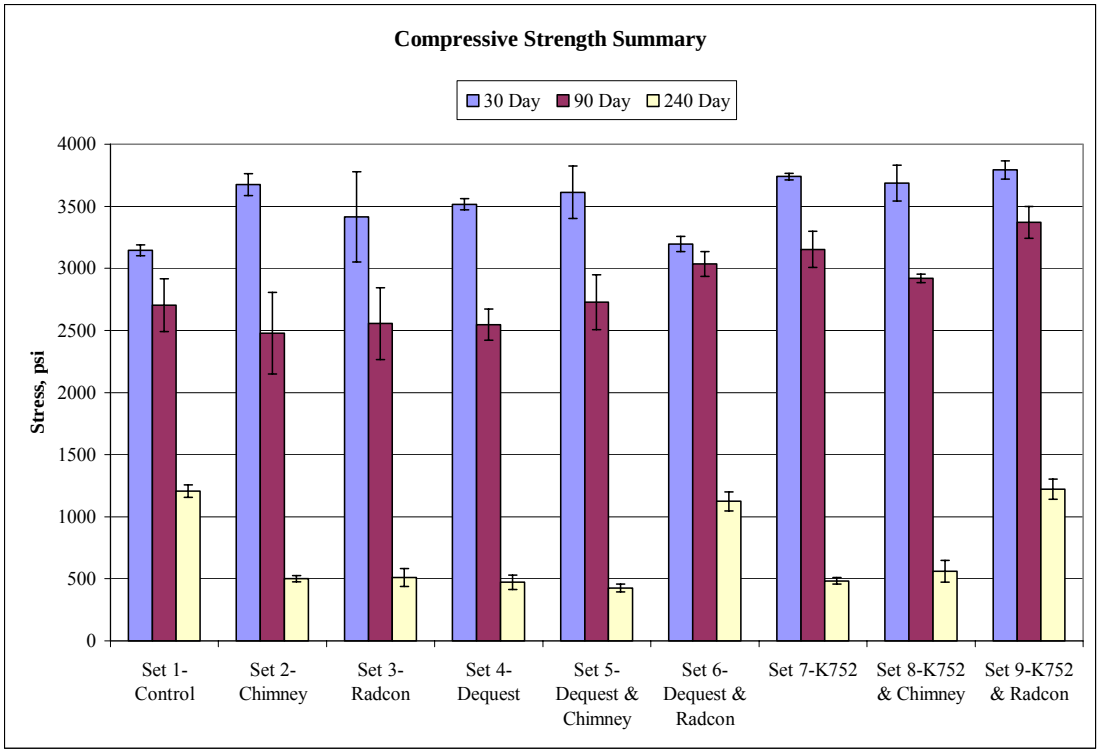

Figure 6.67 - Average Compressive Strength and Percent Reduction of 4" Diameter by 8" Tall Cylinders

Legend

Set 1 - Control
Set 2 - Chimney Saver
Set 3 - Radcon Formula #7
Set 4 - Dequest 2060S
Set 5 - Dequest 2060S & Chimney Saver
Set 6 - Dequest 2060S & Radcon Formula #7
Set 7 - Goodrite K752
Set 8 - Goodrite K752 & Chimney Saver
Set 9 - Goodrite K752 & Radcon Formula #7

Table 6.10 - 30 Day SEM Morphology Summary

30 DAY - SEM Morphology Summary

		UMD Sample ID	FHWA Sample ID	Ettringite Formation
SET 1	Exterior	S1-P6	1997	Clumps
	Interior	S1-P6	1998	No Ettringite Found
SET 2	Exterior	S2-P6	1999	Laminar with spheres and needles
	Interior	S2-P6	2000	Laminar
SET 3	Exterior	S3-P6	2001	Laminar
	Interior	S3-P6	2002	Laminar
SET 4	Exterior	S4-P6	2009	Spheres with needles in cavities
	Interior	S4-P6	2010	Spheres with needles in cavities
SET 5	Exterior	S5-P6	2011	Spheres with needles in cavities
	Interior	S5-P6	2012	Spheres with needles in cavities
SET 6	Exterior	S6-P6	2013	Spheres with needles in cavities
	Interior	S6-P6	2014	Spheres with needles in cavities
SET 7	Exterior	S7-P6	2027	Spheres in cavities
	Interior	S7-P6	2028	Spheres with needles in cavities
SET 8	Exterior	S8-P6	2029	Spheres with needles in cavities
	Interior	S8-P6	2030	Spheres with needles in cavities
SET 9	Exterior	S9-P6	2031	No Ettringite Found
	Interior	S9-P6	2032	Spheres in cavities

Table 6.11 - 90 Day SEM Morphology Summary

90 DAY - SEM Morphology Summary

		UMD Sample ID	FHWA Sample ID	Ettringite Formation
SET 1	Exterior	S1-P7	2080	Laminar
	Interior	S1-P7	2081	Laminar with spheres
SET 2	Exterior	S2-P7	2082	Packets of spheres
	Interior	S2-P7	2083	Spheres
SET 3	Exterior	S3-P7	2084	Laminar with needles and spheres
	Interior	S3-P7	2085	Laminar
SET 4	Exterior	S4-P7	2086	Laminar with spheres
	Interior	S4-P7	2087	Packets of needles
SET 5	Exterior	S5-P7	2088	Laminar with spheres and needles
	Interior	S5-P7	2089	Laminar with radiating needles
SET 6	Exterior	S6-P7	2090	Laminar with spheres and needles
	Interior	S6-P7	2091	Laminar with spheres and needles
SET 7	Exterior	S7-P7	2093	Laminar with spheres and needles
	Interior	S7-P7	2094	Laminar with spheres and needles
SET 8	Exterior	S8-P7	2095	Laminar with spheres and needles
	Interior	S8-P7	2096	Laminar with spheres and needles
SET 9	Exterior	S9-P7	2097	Clumps and spheres
	Interior	S9-P7	2098	Laminar with radiating needles

Table 6.12 - 240 Day SEM Morphology Summary

240 DAYS - SEM Morphology Summary

		UMD Sample ID	FHWA Sample ID	Ettringite Formation
SET 1	Exterior	S1-P8	2129	Spheres
	Interior	S1-P8	2130	Laminar with radiating needles
SET 2	Exterior	S2-P8	2131	Laminar; Clumps
	Interior	S2-P8	2132	Laminar with spheres and needles
SET 3	Exterior	S3-P8	2133	Spheres in cavities
	Interior	S3-P8	2134	Packets of poorly formed spheres
SET 4	Exterior	S4-P8	2136	Laminar with spheres and needles
	Interior	S4-P8	2137	Clumps
SET 5	Exterior	S5-P8	2138	Laminar with radiating needles
	Interior	S5-P8	2139	Laminar with radiating needles
SET 6	Exterior	S6-P8	2140	Laminar with radiating needles
	Interior	S6-P8	2141	Laminar with radiating needles
SET 7	Exterior	S7-P8	2142	Clumps
	Interior	S7-P8	2143	Laminar with radiating needles
SET 8	Exterior	S8-P8	2144	Laminar with spheres and needles
	Interior	S8-P8	2145	Laminar with radiating needles
SET 9	Exterior	S9-P8	2146	Laminar
	Interior	S9-P8	2147	Laminar with spheres and needles

Table 6.13 - SEM Morphology Summary

SEM Morphology Summary

Set	Treatment	30 Days	90 Days	240 Days
1	Control (No Treatment)	Packets of poorly formed spheres	Spheres, maps, rosettes, needles, laths, ettringite in matrix	Laminar, spheres, needles
2	Chimney Saver	Spheres, needles, ettringite in matrix and cavities	Packets of poorly formed spheres	Laminar, spheres, needles, clumps
3	Radcon Formula #7	Ettringite in matrix, laths, clumps, maps, rosettes, laminar	Spheres, rosettes, needles, laminar	Clumps and spheres
4	Dequest 2060S	Spheres in cavities, needles, laths	Clumps, spheres, needles, laminar	Maps, needles, spheres, clumps, laminar
5	Dequest 2060S & ChimneySaver	Spheres in cavities, needles in spheres, spheres in voids and pull outs	Clumps, maps, needles, spheres, laminar	Maps, needles, spheres, clumps, ettringite in matrix, laminar
6	Dequest 2060S & Radcon Formula #7	Spheres in cavities	Maps, laths, spheres, needles, laminar	Maps, needles, spheres, clumps, ettringite in matrix, laminar
7	Goodrite K752	Spheres in cavities	Maps, laths, spheres, needles, laminar	Maps, needles, spheres, laminar
8	Goodrite K752 & ChimneySaver	Spheres in cavities	Maps, laths, spheres, needles, laminar	Maps, needles, spheres, laminar
9	Goodrite K752 & Radcon Formula #7	Spheres in cavities	Maps, laths, spheres, needles, laminar	Maps, needles, spheres, clumps, ettringite in matrix, laminar

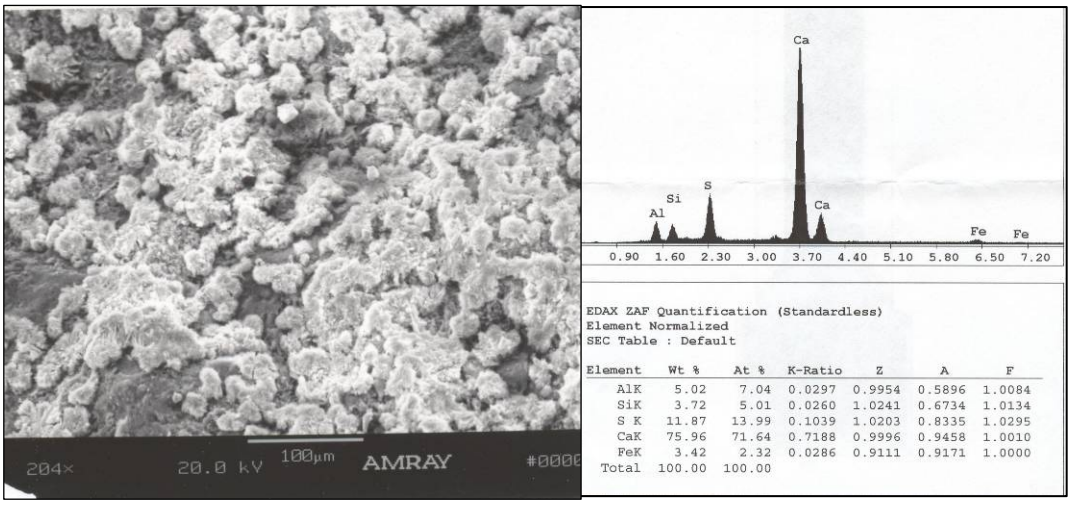

Figure 6.68 - Clumps of ettringite in Control prism (Set No. 1) at Day 30. SEM sample of exterior region of prism. (FHWA ID# - 1997) Ca-S-Al Ratio (Wt %) = 75.96 – 11.87 – 5.02

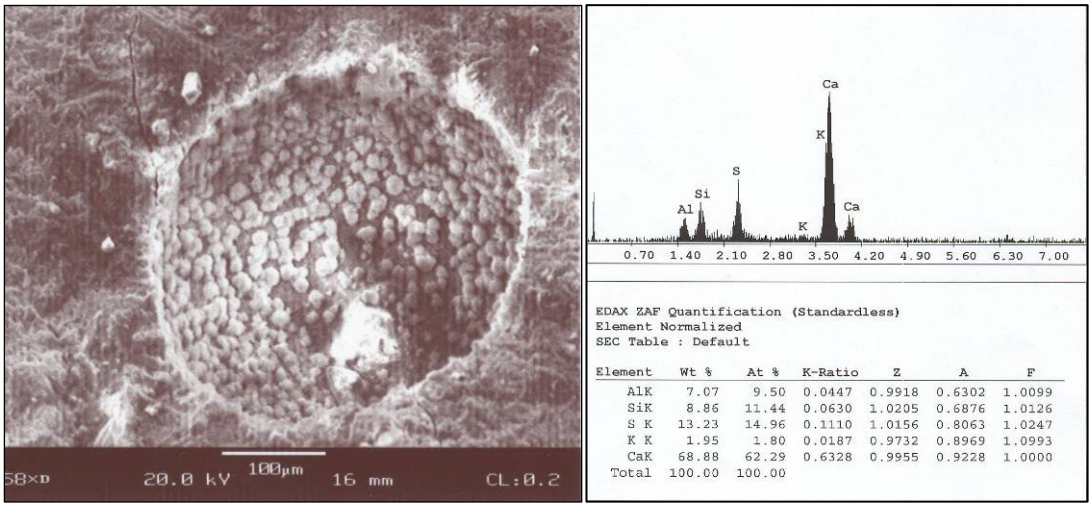

Figure 6.69 - Spheres of ettringite in cavities of prism treated with Dequest 2060S. (Set No. 4) at Day 30. SEM sample of exterior region of prism. (FHWA ID# - 2009) Ca-S-Al Ratio (Wt %) = 68.88 - 13.23 - 7.07

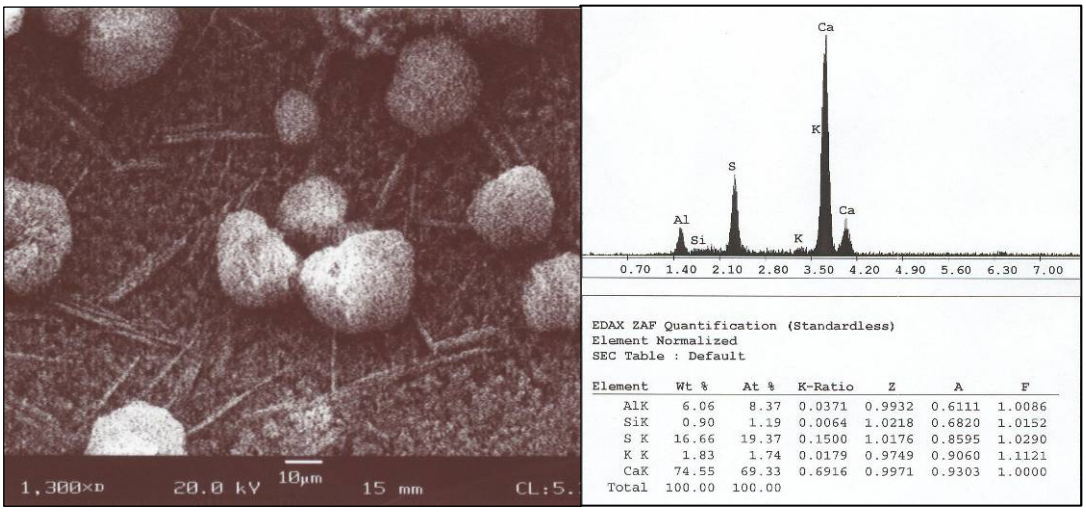

Figure 6.70 - Spheres with needles in prism treated with Dequest 2060S and ChimneySaver (Set No. 5) at Day 30. SEM sample of exterior region of prism. (FHWA ID# - 2011) Ca-S-Al Ratio (Wt %) = 74.55 – 16.66 – 6.06

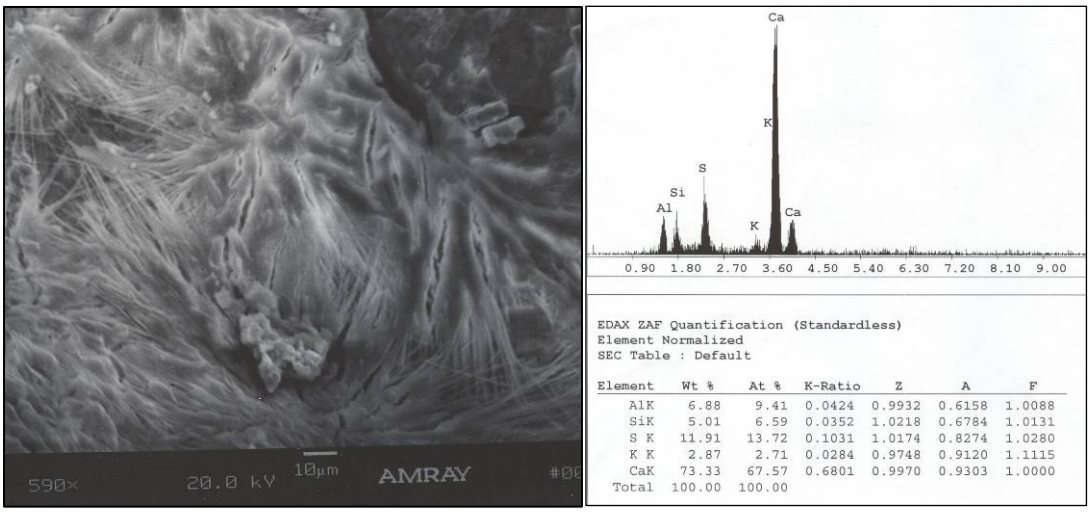

Figure 6.71 - Lamellar ettringite in prism treated with Radcon Formula #7 (Set No. 3) at Day 90. SEM sample of interior region of prism. (FHWA ID# - 2085) Ca-S-Al Ratio (Wt %) = 73.33 – 11.91 – 6.88

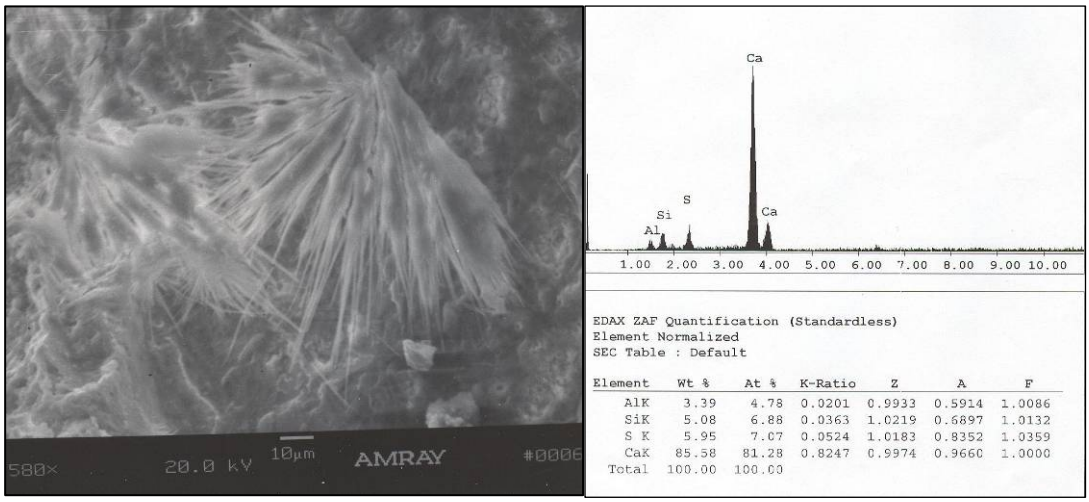

Figure 6.72 - Lamellar ettringite with radiating needles in Control prism (Set No. 1) at Day 90. SEM sample of exterior region of prism. (FHWA ID# - 2080) Ca-S-Al Ratio (Wt %) = 85.58 – 5.08 – 3.39

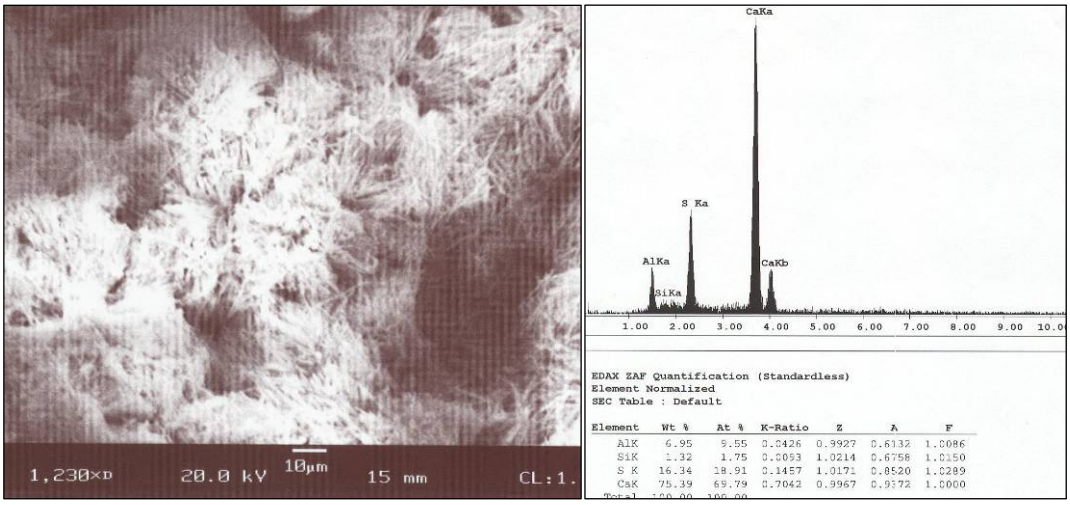

Figure 6.73 - Ettringite needles in prism treated with ChimneySaver (Set No. 2) at Day 240. SEM sample of interior region of prism. (FHWA ID# - 2132) Ca-S-Al Ratio (Wt %) = 75.39 – 16.34 – 6.95

Chapter 7: Summary and Conclusions

7.1 Summary

The objective of this ettringite mitigation project was to determine if the growth of delayed ettringite formation in existing concrete can be reduced or even prevented with commercial products. Additionally, the objective was to determine if externally treating concrete specimens with water repellents and crystal growth inhibitors will decrease DEF-related expansion and to identify any correlation between collected expansion and weight change data with mitigation effectiveness of a particular product. The project was conducted with concrete specimens prepared in the laboratory with a concrete mix specifically designed to accelerate the growth of ettringite. A total of nine sets with 13 cylinders and 9 prisms in each set were prepared. The mitigation products included two crystal growth inhibitors, Dequest 2060S and Good-Rite K752, and two water repellents, ChimneySaver and Radcon Formula #7. One of the nine sets was used as the control and was not treated with any products. Four sets were treated with single applications of the four individual products. The remaining four sets were treated with cross-combinations of water repellent and crystal inhibitor.

The products were applied to the concrete specimens after the existence of ettringite was confirmed through SEM testing which was approximately 45 days after the completion of the UMD/FHWA Modified Duggan Cycle. Four tests were conducted on the concrete prisms and cylinders to monitor the effectiveness of the mitigation products. Expansion and weight change measurements were collected for

300 days at 3 to 7 day intervals. Compression tests on cylinders and SEM analysis were performed at 30, 90, 240 days after the completion of the UMD/FHWA Modified Duggan Cycle.

7.2 Conclusions

The following conclusions were reached based on the analysis of the laboratory results:

1. A single treatment of ChimneySaver (Set No. 2), Dequest 2060S (Set No. 4), and Good-Rite K752 (Set No. 7) reduced concrete expansion when compared to the control set. Future research should be performed to substantiate this observation.
2. The cross combination of water repellent and crystal inhibitor treatment (Set Nos. 5, 6, 8 & 9) reduced concrete expansion and weight change however the results were not significantly different than single treatment.
3. A chemical reaction between the concrete and Radcon Formula #7 (Set No. 3) accelerated concrete expansion and weight change, eventually overtaking the Control set.
4. Weight change results are similar to expansion results. Single treatment of ChimneySaver (Set No. 2), Dequest 2060S (Set No. 4), and Good-Rite K752 (Set No. 7) experienced smaller weight gain than the control set. The weight change of the fourth product, Radcon Formula #7 (Set No. 3), was similar to the control.

5. A linear relationship was established between the concrete expansion and weight gain in all nine sets.
6. The concrete cylinders experienced up to 33% loss in strength at 90 days and 85% loss in strength at 240 days. A correlation between concrete strength and the mitigation products could not be developed due to the widespread loss in concrete strength across all nine sets.
7. The three of the four products reduced expansion in the concrete. However it is difficult to assess the products effectiveness in reducing growth of ettringite crystals. Further research is required in establishing methods to quantify and correlate SEM analysis with other parameters.
8. The study indicates that mitigation after some point in time may be unattainable and ettringite may have to be identified and mitigated early to prevent deleterious effects.

REFERENCES

Amde, A. M., Livingston, R. L. and Azzam, A. (2003), "Influence of Alkali Content and Development of Accelerated Test Method for Delayed Ettringite Formation," *Proceedings of the International Innovative world of Concrete Conference*, Pune, India, 2003.

Amde, A. M., Ceary, M., Livingston, R. A., and McMorris, N. (2004a), Pilot Field Survey of Maryland Bridges for Delayed Ettringite Formation Damage, Maryland State Highway Administration, Vol. 1, MD-04-SP107B4U.

Amde, A.M. and Livingston, R.A. (2004b), "UMD/FHWA Studies on Delayed Ettringite Formation," *International Conference on Advances in Concrete and Construction* (ICACC2004), Hyderabad, India, December 2004, 425-434 (***Keynote Paper***).

Amde, A. M., Williams, K., and Livingston, R. A. (2004c), Influence of Fine Aggregate Lithology on Delayed Ettringite Formation in High Early Strength Concrete, Maryland State Highway Administration, Vol. 2, MD-04-SP107B4U.

Amde, A.M., Azzam, A. and Livingston, R.L. (2005a), "Mitigation of DEF using Class F Fly Ash or Mix Water Conditioner," OWICS 05-Engaging the Future, Singapore, August 2005, 191-198, (**Bauchemie Award 2005 for Best Paper**).

Amde, A.M., Ceary, M. and Livingston, R. (2005b), "Correlation Between Map Cracking and DEF in Field Specimens," *The 11th Int. Conf. on Fracture*, Turin, Italy, Sec.15, #4526, Mar. 2005.

Amde, A.M., Ceary, M. and Livingston, R. A. (2005c), "Investigation of Maryland Bridges for DEF And ASR," ICACS 2005 Int. Conf., Chennai, India, January 2005, 809-816, (***Keynote Paper***).

Amde, A.M., Ceary, M. and Livingston, R.A. (2005d), "Investigation of Maryland Bridges for DEF and ASR," J of Structural Engineering, Vol. 32, No. 1, Apr.-May 2005, 33-36.

Amde, A.M., Williams, K. and Livingston, R.A. (2005e), "Influence of Fine Aggregate Lithology on DEF In High Early Strength Concrete," *Indo US workshop (sponsored by NSF) on High Performance Cement- based Concrete Composites, American Ceramic Society,* Chennai, India, January 2005, 199-209.

Amde, A.M., Azzam, A., Sabnis, G. and Livingston, R.A. (2006), "The Effects of Mix Water Conditioner on Internal Sulfate Attack in Concrete," Seventh International Congress on Advances in Civil Engineering (ACE 2006), Istanbul, Turkey, October 11-13.

American Concrete Institute (1998), "221.1R-98: Report on Alkali Aggregate Reactivity," ACI Committee 221.

Attiogbe, E. K., Wells, J. A., and Rizkalla, S. H. (1990), "Evaluation of Duggan Concrete Core Expansion Test," Research Report Sponsored by Canadian National Railways & Transport Institute, University of Manitoba, Winnipeg, Canada, Sept.

Azzam, A. (2002), "Delayed Ettringite Formation, the Influence of Aggregate Types, Curing Conditions, Exposure Conditions, Alkali Content, Fly Ash and Mix Water Conditioner (MWC)," Ph.D. Thesis, University of Maryland, College Park, USA.

Ceesay, J. (2004), "The Influence of Exposure Conditions on Delayed Ettringite Formation in Mortar Specimens," M.S. Thesis, University of Maryland, College Park, USA.

Cody, R. D. (1991), "Organo-Crystalline Interactions in Evaporate Systems: The Effects of Crystallization Inhibition," Journal of Sedimentary Petrology, Vol. 61, No. 5, 704-718.

Cody, R., Cody, A., Spry, P., and Hyomin, L. (2001), "Reduction of Concrete Deterioration by Ettringite Using Crystal Growth Inhibition Techniques," Iowa Department of Transportation, TR-431.

Collepardi, M. (1999), "Damage by Delayed Ettringite Formation," Concrete International, Vol. 21, No. 1, 69-74.

Day, R. L. (1992), "The Effect of Secondary Ettringite Formation on the Durability of Concrete: A Literature Analysis," Portland Cement Association.

Diamond, S. and Ong. S. (1994), "Combined Effects of Alkali Silica Reaction and Secondary Ettringite Deposition in Steam Cured Mortars," Cement Technology, The American Ceramic Society, Westerville, Ohio, 70-90.

Dow Corning Corporation (2006), "Dow Corning Construction Solutions: Brand Building Material Protection Brochure," Internet. http://www.dowcorning.com/content/publishedlit/63-1042-01.pdf?DCWS=Construction&DCWSS=, Accessed 05/01/06.

Duchesne, J., and Berube, M. A. (1994), "A Reply to a Discussion by S. Chatterji of the Paper: The Effectiveness of Supplementary Cementing Materials in Suppressing

Expansion Due to ASR. Part 1. Concrete Expansion and Portland Depletion," Cement and Concrete Research, Vol. 24, No. 8, 1574-1576.

Duggan, C. R. and Scott, J.F. (1987), "Proposed New Test for Alkali – Aggregate Reactivity," Canadian National Railways, Technical Research Report, Montreal, Canada, April 13th. (Revised October 31, 1989).

Duggan, C. R. and Scott, J.F. (1989), "Establishment of New Acceptance/Rejection Limits for Proposed Test Method for Detection of Potentially Deleterious Expansion of Concrete," Presented to ASTM Subcommittee C09.02.02, September.

Famy, C., Scrivener, K. L., and Brough, A. R. (2002), "Role of Microstructural Characterization in Understanding the Mechanism of Expansion Due to Delayed Ettringite Formation," Proceedings of the International RILEM TC 186-ISA Workshop in Internal Sulfate Attack and Delayed Ettringite Formation, Villars, Switzerland, September, 167-172.

Folliard, K., Bauer, S. et al. (2006), "Akali-Silica Reaction and Delayed Ettringite Formation in Concrete: A literature Review," University of Texas, Center for Transportation Research, CTR 4085-1.

Fu, Y. (1996), "Delayed Ettringite Formation in Portland Cement Products," Ph.D. Dissertation, University of Ottawa, Ontario, Canada.

Heinz, D., and Ludwig, U. (1986), "Mechanism of Subsquent Ettringite Formation in Mortars and Concretes after Heat Treatment," Proceedings, 8th International Congress on Chemistry of Cement, Rio de Janeiro, Brazil Vol. 5, 189-194.

Heinz, D., and Ludwig, U. (1987), "Mechanism of Subsquent Ettringite Formation in Mortars and Concretes after Heat Treatment," Concrete Durability, SP-100, Vol. 2, American Concrete Institute, Detroit MI. 2059-2071.

Heinz, D., and Ludwig, U. (1989), "Delayed Ettringite Formation in Heat Treated Mortars and Concretes," Concrete Precast Plant & Technology, Vol. 11, 56-61.

Johansen, V., Thaulow, N., and Skalny, J. (1993), "Simultaneous Presence of Alkali - Silica Gel and Ettringite in Concrete," Advances in Cement Research, Vol. 5, No. 17, 23-29.

Kennerely, R. A. (1965), "Ettringite Formation in Dam Gallery," Journ. Amer. Conc. Inst., Proc. V. 62, No. 5, May, 559-574.

Kelham, S. (1996), "The Effect of Cement Composition and Fineness on Expansion Associated with Delayed Ettringite Formation," Cement and Concrete Composites, Vol. 18, No. 3, 171-179.

Klingner, R.E., Fowler, T.J., et al. (2004a), "Mitigation Techniques for In-Service Structures with Premature Concrete Deterioration: A Literature Review," University of Texas, Center for Transportation Research, CTR 4069-1.

Klingner, R.E., Fowler, T.J., et al. (2004b), "Mitigation Techniques for In-Service Structures with Premature Concrete Deterioration: Development and Verification of New Test Methods," University of Texas, Center for Transportation Research, CTR 4069-2.

Klingner, R.E., Fowler, T.J., et al. (2004c), "Mitigation Techniques for In-Service Structures with Premature Concrete Deterioration: Synthesis Report," University of Texas, Center for Transportation Research, CTR 4069-3.

Lawrence, B. L. et al. (1999), "Evaluation and Mitigating Measures for Premature Concrete Distress in Texas Department of Transportation Concrete Elements," Cement, Concrete and Aggregates, 21 June, pp. 73-81.

Leming, M. L., and Nguyen, B. Q. (2000), "Limits on Alkali Content in Cement – Results from a Field Study," Cement, Concrete, and Aggregates, Vol. 22, No. 1, 41-47.

Livingston, R. A. & Amde, A. M. (2001a). "Nondestructive Test Field Survey for Assessing the Extent of Ettringite-related Damage in Concrete Bridges." in *Nondestructive Characterization of Materials X* (eds. Green, R. E., Kishi, T., Saito, T., Takeda, N. & Djordjevic, B. B.), Elsevier Science Ltd., Oxford: 167-174.

Livingston, R.A., Amde, A.M. and Ramadan, E. (2001b). "Characterization of Damage in Portland Cement Concrete Associated with DEF." *Proc. of the 6th Int. Conf. CONCREEP 6 @ MIT* (eds. Ulm, Bazant, and Wittmann), Elsevier, Cambridge: 463 – 468.

Livingston, R. A., H. H. Saleh, E. O. Ramadan and A. M. Amde (2001c). Characterization of Damage in Portland Cement Concrete Associated with Delayed Ettringite Formation. *Creep, Shrinkage and Durabiity Mechanics of Concrete and Other Quasi-Brittle Materials*, Amsterdam, Elseveier: 463-468.

Livingston, R. A., M. Ceary and A. M. Amde (2002). "Statistical Sampling Design for a Field Survey of Delayed-Ettringite-Formation Damage in Bridges." *Structural Materials Technology V: An NDT Conference*, Cincinnati, OH, ASNT: 411-420.

Livingston, R. A., H. H. Saleh, M. S. Ceary and A. M. Amde (2004), "Development of an Image Plate System for NDT Potassium Measurement in Concrete," *Structural Materials and Technology*, S. Alampalli and G. A. Washer. Columbus, OH, ASNT**,** 2004, 244-252.

Livingston, R., Sutin, A., Ceary, M., McMorris, N. and Amde, A. M (2005), "Characterization of Distributed Damage in Concrete Using Advanced Impact-echo Method," *The Eleventh International Conference on Fracture*, Turin, Italy, Section 15, Paper 4548, March 2005.

Livingston, R. A., (2006a), "Note on Analysis of Mitigation Study Prisms Expansion," Unpublished, June 4, Turner Fairbank Research Center, FHWA.

Livingston, R. A., C. Ormsby, A. M. Amde, M. Ceary, N. McMorris and P. Finnerty (2006b). "Field Survey of Delayed Ettringite Formation Related Damage in Concrete Bridges in the State of Maryland." *CANMET Conference on Durability of Concrete*, Montreal, CANADA: in press.

Livingston, R.A., Newman, J., Ceesay, J. and Amde, A.M. (2006c), "Laser Shearography for Detection of Fine Cracks in Concrete," ACI Spring 2006 Convention, Sponsored by ACI Committees 228 (Nondestructive Testing) and 201 (Durability), Charlotte, NC, March 26-30.

Livingston, R.A., Newman, J., Ceesay, J., Amde, A.M. and Wallace, D. (2006d), "Laser Shearography for Detection of Fine Cracks in Concrete and Masonry," Structural Faults and Repair, Edinburgh, Scotland, June 13-15.

Marusin, S. L. (1995), "Sample Preparation – The Key to SEM Studies of Failed Concrete," Cement Concrete Composites, Vol. 17, No. 4, 311-318.

McMorris, N., Amde, A.M. and Livingston, R.A. (2006), "Improved Impact-Echo Method Quantification of Distributed Damage in Concrete," Smart Material and Technology, St. Louis, Missouri, August.

Merrill, B. D. (2004) "Durability of Concrete in Highway Facilities," Internet. http//:gem1.cive.uh.edu/content/conf_exhib/00_present/9.htm Accessed 09/23/04.

Newman, J., Amde, A.M. and Livingston, R.A. (2006), "Development of a Portable Laser Shearography System for Crack Detection in Bridges," Smart Material and Technology, St. Louis, Missouri, August.

Noveon, Inc. (2005), "Good-rite K-752 Polyacrylate," Internet. http://www.noveoncoatings.com/products/americas/documents/goodrite/GRK-752tds.pdf, Accessed 05/28/05.

Pettifer, K., Nixon, P.J. (1980), "Alkali Metal Sulphate – A Factor Common to Both Alkali Aggregate Reaction and Sulphate Attack on Concrete," Cem. Concr. Res., V 10, 173-181.

Radcrete Pacific Pty. Ltd. (2005), "Radcon® Formula #7," Internet. http://www.radcrete.com.au/Downloads/02-Radcon%20Brochure.pdf, Accessed 05/28/05.

Ramadan, E. (2000), "Experimental and Theoretical Study of Delayed Ettringite Damage in Concrete," Ph.D. Dissertation, University of Maryland, College Park, USA.

Research Institute of the Cement Industry (1990), "Chemical Reactions in Concrete, Activity Report, 1981- 1984," Translated by TEX Associates Inc., Philadelphia.

Rogers, C. A. (1993), "Alkali-Aggregate Reactivity in Canada," Cement and Concrete Composites, Vol. 15, 13-19.

SaverSystems (2005), "ChimneySaver® Product Data," Internet. http://www.chimneysaver.com/ProductData/waterbase.pdf, Accessed 05/28/05.

Schlorholtz, S., (2002), "Determine Initial Cause for Current Premature Portland Cement Concrete Pavement Deterioration," Iowa Department of Transportation, TR-406.

Scrivener, K., and Taylor, H. F. W. (1993), "Delayed Ettringite Formation a Microstructural and Microanalytical Study," Advances in Cement Research, 139-145.

Shimada, Y. (2005), "Chemical Path of Ettringite Formation in Heat-Cured Mortar and Its Relationship to Expansion," Ph.D. Dissertation, Northwestern University, Evanston, Illinois, USA.

Solutia Inc. (2005), "Dequest 2060S Product Information," Internet. http://www.dequest.com/pages/products/product.asp?re=ap&id=134, Accessed 05/28/05.

Taylor, H. F. W. (1990), Cement Chemistry, Academic Press, London, England.

Tepponen, P. and Erickson, B. E. (1987), "Damages in Concrete Railway Sleepers in Finland," Nordic Concr. Res. Publication #6, 199-209.

United States Army Corps of Engineers (1994), "Engineering and Design – Standard Practice for Concrete Civil Works Structures," EM 1110-2-2000, Appendix A.

Volkwein, A. and Springenschmid, R. (1981), "Corrosion of Reinforcement in Concrete Bridges at Different Ages Due to Carbonation and Chloride Penetration," 2nd Intnl. Conf. on Durability of Building Materials and Components, Sept. 14-16, Publ. by NBS, Washington, D.C., 199-209.